In presenting this dissertation/thesis as a partial fulfillment of the requirements for an advanced degree from Emory University, I agree that the Library of the University shall make it available for inspection and circulation in accordance with its regulations, governing materials of this type. I agree that permission to copy from, or to publish, this thesis/dissertation may be granted by the professor under whose direction it was written, or, in his/her absence, by the Dean of the Graduate School when such copying or publication is solely for scholarly purposes and does not involve potential financial gain. It is understood that any copying from, or publication of, this thesis/dissertation which involves potential financial gain will not be allowed without written permission.

_____

Xiaojie Qi

Generation of Novel Yeast Prions through Domain Substitutions of *Saccharomyces cerevisiae* Sup35p

By

Xiaojie Qi
Doctor of Philosophy

Department of Chemistry

_____

Dr. Vincent P. Conticello
Adviser

_____

Dr. David G. Lynn
Committee Member

_____

Dr. Stefan Lutz
Committee Member

Accepted:

_____

Lisa A. Tedesco, Ph.D.
Dean of the Graduate School

_____

Date

Generation of Novel Yeast Prions through Domain Substitutions of *Saccharomyces cerevisiae* Sup35p

By

Xiaojie Qi
B.Engr., Heilongjiang University, 1998
M.S., Changchun Institute of Applied Chemistry,
Chinese Academy of Sciences, 2001

Adviser: Vincent P. Conticello, Ph.D.

An Abstract of
A dissertation submitted to the Faculty of the Graduate
School of Emory University in partial fulfillment
of the requirements for the degree of
Doctor of Philosophy

Department of Chemistry
2007

The yeast prion [*PSI*$^{+}$], formed by the component protein Sup35p in *Saccharomyces cerevisiae*, has been employed as a model to study prion formation and aggregation. The studies on yeast prions have revealed the mechanism of prion formation and propagation, which provides important clues for studying mammalian prions and other protein aggregates that are involved in protein misfolding diseases. It was recently suggested that the prion forming domain of Sup35p can be further divided into the Asn/Gln-rich domain (NQ) and the oligopeptide repeats domain (NR), which are responsible for protein aggregation and prion propagation, respectively.

In this study, aggregation-prone peptide sequences were selected as the candidates that could potentially replace the NQ domain and generate novel prions. The substitution of a fragment from alpha-synuclein for the NQ domain of Sup35p generated prion-like phenotypes. The substitution of a fragment of islet amyloid polypeptide (IAPP) for the NQ domain of Sup35p generated a novel prion. The novel prion formed by IAPP-substituted Sup35p exhibited similar characteristics as prion state of the wild-type protein. In addition, the substitution of a bacterial Asn/Gln-rich oligopeptide repeat for the NR domain of Sup35p generated prion-like phenotypes. These results demonstrated that novel prions could arise from domain substitution with Sup35p, and that the aggregation units were not restricted to Asn/Gln-rich proteins. As the characteristics of the prions were shown to depend on the properties of the aggregation units, yeast prions can potentially be used as model systems to study the aggregation of selected protein sequences. These models can be useful in the identification of factors that are critical for protein aggregation, such as amino acid composition, growth condition, and the presence of small molecules. Moreover, these models may provide a tool to screen for drugs that

can inhibit or counteract protein aggregation.

Generation of Novel Yeast Prions through Domain Substitutions of *Saccharomyces cerevisiae* Sup35p

By

Xiaojie Qi
B.Engr., Heilongjiang University, 1998
M.S., Changchun Institute of Applied Chemistry,
Chinese Academy of Sciences, 2001

Adviser: Vincent P. Conticello, Ph.D.

A dissertation submitted to the Faculty of the Graduate
School of Emory University in partial fulfillment
of the requirements for the degree of
Doctor of Philosophy

Department of Chemistry
2007

ACKNOWLEDGEMENTS

I would like to gratefully and sincerely thank Dr. Vincent P. Conticello for his guidance, understanding, patience, and most importantly, his friendship during my graduate studies at Emory University. His knowledge and wisdom greatly inspired and motivated me. Not only did he show me the correct path when I was in need of help, but he also encouraged me to think independently. I would also like to thank my committee members Dr. David Lynn and Dr. Stefan Lutz for their precious guidance and assistance in both my research and my life.

I would like to express my deep gratitude to Dr. Sonha Payne, Melissa Patterson, Yunyun Pei, Ying Yu, Christine Bassett, and Daniel Spollen, who put their valuable efforts into this research project. I also thank the members of Conticello's lab, Holly Carpenter, Wookhyun Kim, Weilin Peng, Steven Dublin, and Ye Tian, for their assistance and friendship.

I thank Dr. Yuri Chernoff and Dr. Susan Lindquist for providing experimental materials. I wish to thank Dr. Robert P. Apkarian, Jeannette Taylor, and Hong Yi for their assistance on electron microscopy. I thank Dr. Erik Weeks and Katherine Schaefer-Hales for their assistance on fluorescence microscopy. I also thank Dr. Anita Corbett and Sara Leung for their assistance on yeast tetrad dissection.

I would like to thank my wife Fang for the reasons that are too many to count; her love, understanding, and encouragement made me to succeed in completing my study as a graduate student. I thank my parents and Fang's parents for their unselfish help and support. I especially thank my son Jason for the happiness he brought to me.

TABLE OF CONTENTS

LIST OF TABLES

TABLE PAGE

LIST OF ILLUSTRATIONS

FIGURE PAGE

ABBREVIATIONS

aa	amino acid
Ab	antibody
Amp^R	ampicillin resistance gene
bp	base pair
CRBB	Congo red binding buffer
cyh	cycloheximide
DTT	dithiothreitol
x *g*	rcf or relative centrifugal force
G418	geneticin
GFP	green fluorescence protein
GuHCl	guanidine hydrochloride
hr	hour
IAPP	islet amyloid polypeptide
IPTG	isopropyl β-D-thiogalactopyranoside
KanMX	G418 resistance gene
kb	kilo bases
kDa	kilo Daltons
LB	Luria-Bertani broth
µg	micro gram
µl	micro liter
µM	micro molar

mg	milligram
mL	milliliter
mM	millimolar
min	minute
OD	optical density
PAGE	polyarylamide gel electrophoresis
PBS	phosphate buffered saline
PCR	polymerase chain reaction
[*psi*$^-$] (lower case)	non-prion state
[*PSI*$^+$] (upper case)	prion state
P_{SUP35}	wild type promoter for Sup35 gene
rpm	rotations per minute
SD medium	synthetic medium with dextrose
SDS	sodium dodecylsulfate
SUP35 (upper case)	wild type Sup35 gene
sup35 (lower case)	mutant Sup35 gene
Sup35p	protein product of Sup35 gene
sup35::KanMX (*::*)	mutation by insertion of *KanMX*
TBS	Tris buffered saline
Tris	tris-(hydroxyl-methyl) aminomethane

CHAPTER 1

Introduction

Protein folding and misfolding

Proteins must fold correctly to achieve functional structures that are both fundamental and essential for life. The correct folding not only provides proteins with biological functions by arranging certain residues at the active sites, such as in enzymes and structural proteins, but also prevents the exposure of certain residues on the surface which would otherwise cause a non-specific interaction among proteins. Anfinsen originally suggested that a protein could assemble spontaneously into its native conformation based only upon the information contained in its primary sequence (Anfinsen and Haber, 1961). By folding correctly, proteins almost always achieve the thermodynamically most stable structures under physiological conditions. Intracellularly, protein folding takes place either in the cytoplasm or within the secretory pathway, usually assisted by various molecular chaperones that make the folding process more efficient and reliable (Dobson, 2003b; Dobson et al., 1998).

In some circumstances, proteins fail to achieve their native structures and misfold into non-native conformations. Although thermodynamically less stable than the correctly folded proteins, they are usually kinetically trapped into relatively stable states.

Protein misfolding is a very common phenomenon in the overexpression of foreign proteins in bacteria or other expression hosts, while it is usually rare during the normal growth of cells (Clark, 2004). In contrast to correctly folded proteins, misfolded proteins either fail to exhibit correct amino acids at the active sites and lose the functions, or expose unwanted residues on the surface and cause nonspecific interactions among proteins. In addition, misfolded proteins can lead to the formation and deposition of large aggregates inside or outside the cell (Cohen and Kelly, 2003).

Cells have evolved exquisite quality control systems to manage the misfolded proteins. First, cells attempt to correct the misfolded proteins. Ring-shaped complex formed by Hsp104p, a molecular chaperone, is capable of mediating ATP-dependent disaggregation of aggregates of up to 600 kDa; additional chaperones of the Hsp70 family can assist the released components of such aggregates to refold into their native conformation (Glover and Lindquist, 1998b). Second, when chaperones are not sufficient for the correction, the misfolded proteins will be escorted to the proteasome for degradation (Goldberg, 2003).

Protein misfolding diseases

Protein misfolding diseases are the diseases caused by misfolding of proteins, which are either degraded or accumulated/aggregated in the cell (Gregersen et al., 2006). Alternatively, they are also known as “conformational diseases” because the difference between the native and aggregated structures is only at the conformational level (Carrell

and Lomas, 1997). There are mainly two types of protein misfolding diseases, loss-of-function diseases and toxic gain-of-function diseases. Several loss-of-function diseases are due to the degradation of the misfolded proteins by the proteasome, such as cystic fibrosis and α1-antitrypsin (α-AT) deficiency (Carrell and Lomas, 2002; Howard and Welch, 2002). Toxic gain-of-function diseases are sometimes caused by the aggregation of misfolded proteins associated with conformational changes and the deposition of the aggregates outside the cell. These latter diseases include such debilitating ones as Alzheimer's disease, Parkinson's disease, type II diabetes, and prion diseases such as bovine spongiform encephalopathy (BSE) and Creutzfeldt-Jakob disease (CJD). Insoluble protein plaques are often present in the brain or other organs of the patients, and they are found to consist of amyloid fibrils. Detailed study of the amyloid fibrils has revealed the same cross-ß structures, in which ß-strands, i.e. the hydrogen-bonding direction, were oriented perpendicularly to the long axis of the fibers (Dobson, 2003a). The proteins forming amyloid fibrils can be encoded within the host genome, although their normal functions are often unclear.

The reason that the misfolded proteins form insoluble plaques is believed to be the exposure of hydrophobic amino acids. In normal proteins, hydrophobic residues are buried inside the protein right from the start of folding. However, when the proteins misfold, these hydrophobic residues are exposed and can rapidly associate through interaction with exposed hydrophobic groups on other protein molecules, which leads to the formation of the plaques or insoluble aggregates.

Prion diseases

Prion diseases, such as mad cow disease (bovine spongiform encephalopathy; BSE) and Creutzfeldt-Jakob disease (CJD) in humans, are grouped together as transmissible spongiform encephalopathies (TSEs). Brains of the victims of TSEs often degenerate to a sponge-like structure, which has several neurological consequences. As examples of protein misfolding diseases, prion diseases are unique in that the prions that result from misfolding and aggregation of the parent proteins are transmissible and infectious (Weissmann, 2004).

Prions were first noticed as the infectious agents that exhibited unusual resistance to radiation, which led to the hypothesis that the agents might be devoid of nucleic acids. Prusiner showed later that the infectious agents consisted only of protein, and the protein, termed PrP^{Sc}, was just an insoluble isoform of the corresponding cellular protein PrP^{C}, which was completely soluble in normal conditions (Prusiner, 1982; Prusiner, 1991; Weissmann, 2004). These two forms of PrP protein have been characterized biochemically. PrP^{C} protein, as shown by NMR and X-ray crystallography, is rich in α-helical structure and contains little ß-sheet structure (James et al., 1997; Riek et al., 1996); however, the PrP^{Sc} form of the protein has a mainly ß-sheet structure (Post, 1998). Transgenic studies of mice further strengthened the essential role of PrP in prion disease, as PrP-knockout mice were resistant to scrapie and were incapable of prion propagation (Bueler, 1993).

The infectiousness of prion diseases is believed to be due to the ability of PrP^{Sc} to serve as a template to recruit soluble PrP^{C} and transform it to PrP^{Sc}. The spontaneous conversion to PrP^{Sc} is prevented because of the high activation energy barrier involved in the conformational change; however, the interaction with preformed PrP^{Sc} can cause PrP^{C} to undergo an induced conformational change to yield PrP^{Sc}. The conversion from PrP^{C} to PrP^{Sc} can be accelerated by certain mutations in PrP^{C}, which can explain some inheritable Creutzfeldt-Jakob diseases that can arise spontaneously in individuals carrying these mutations. The most direct evidence for the protein-only hypothesis of prion diseases is the observation that the fibrillary form of a recombinant truncated PrP^{C} (PrP 89-230), when injected into transgenic mice overexpressing the PrP^{C} 89-230 fragment, caused the development of BSE-like disease (Legname, 2004).

Yeast prions

In 1994, Wickner stated that the extra-chromosomal inheritance in yeast and other fungi could be caused by the same mechanism as in prion diseases, thus proposed the concept of yeast prions (Wickner, 1994). [*URE3*], the cytoplasmically inherited element that enables yeast to use ureidosuccinate in the presence of ammonium ion, was proposed to be a yeast prion formed by the conformational change of the native protein, Ure2p, a negative regulator of enzymes involved in nitrogen metabolism (Figure 1-1). In analogy to mammalian prions, [*URE3*] is an isoform of Ure2p that is functionally inactive and capable of converting normal Ure2p to the altered form. [PSI^{+}], another cytoplasmically

Figure 1-1. The yeast prions [*PSI*$^+$] and [*URE3*] are the result of self-propagating protein conformations (Chien et al., 2004).

(*A*) Sup35p is a modular protein involved in translation termination; self-propagating aggregation is responsible for the [*PSI*$^+$] phenotype. The amino-terminal prion-forming domain, N (*green*), is glutamine- and asparagine-rich. The middle domain, M (*blue*), is rich in charged residues. The carboxy-terminal domain, C (*orange*), contains the essential translation-termination function of the protein. (*B*) Sup35p is soluble in [*psi*$^-$] yeast and able to facilitate translation termination while in [*PSI*$^+$] yeast; Sup35p is aggregated, resulting in suppression of nonsense codons. Translation termination can be monitored using an *ADE1* reporter harboring a premature stop codon. [*PSI*$^+$] cells are white and capable of growth on media lacking adenine, whereas [*psi*$^-$] yeast accumulate a red pigment caused by lack of Ade1p and are incapable of growth on adenine-less media. (*C*) Ure2p is a modular protein involved in regulation of nitrogen catabolism; self-propagating aggregation of Ure2p is responsible for the [*URE3*] phenotype. In addition to the glutamine/asparagine-rich amino terminus (*green*), Ure2p also contains another region that facilitates prion behavor (*green*) and portions that antagonize prion formation (*black*). The remainder of the protein (*orange*) resembles glutathione S-transferase and is necessary for Ure2p signaling of the presence of high-quality nitrogen sources through Gln3p. (*D*) Normally Ure2p binds the transcription factor Gln3p, preventing the up-regulation of genes, such as *DAL5*, required for uptake of poor nitrogen sources. Serendipitously, Dal5p imports not only the poor nitrogen source

allantoate, but also USA (*n*-carbamyl aspartate), an intermediate in uracil biosynthesis. Thus [*ure-o*] yeast cannot grow on ureidosuccinate (USA) medium lacking uracil. In [*URE3*] yeast, Ure2p is aggregated and inactive, leading to constitutive activation of Dal5p and enabling growth on USA media lacking uracil.

A Sup35p

B [*psi*$^-$]

soluble Sup35p

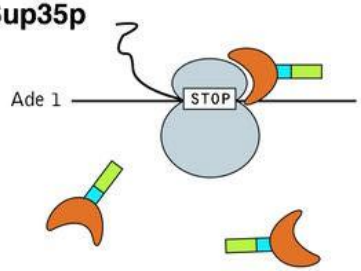

Growth on low ADE

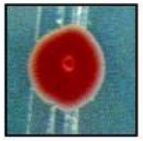

Growth on -ADE

No

[*PSI*$^+$]

Sup35p aggregates

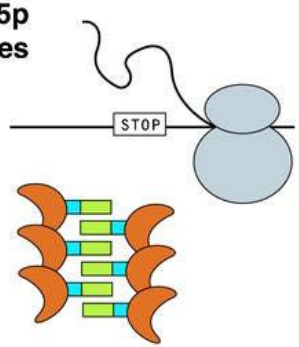

Growth on low ADE

Growth on -ADE

Yes

C Ure2p

D [*ure-o*]

soluble Ure2p

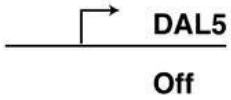

Growth on SD-URA +USA

No

[*URE3*]

Ure2p aggregates

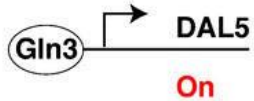

Growth on SD-URA +USA

Yes

inherited element that allows the yeast cell to generally suppress the nonsense codons, was also postulated as a yeast prion formed by the conformational change of the native protein, Sup35p, a termination factor for protein translation when in its native structure (Figure 1-1; Chien et al., 2004; Wickner, 1994). Through a directed search of yeast genome databases, an open-reading frame corresponding to a protein, Rnq1p (Rich in Asn, N and Gln, Q), was found because of its sequence similarity to Sup35p and Ure2p in the prion forming regions. Manipulation of Rnq1p showed that it was capable of forming a prion, [RNQ^{+}], which was coincident with an epigenetic element, [PIN^{+}] ([PSI^{+}] inducibility) that had been previously identified and demonstrated to affect [PSI^{+}] induction (Sondheimer and Lindquist, 2000). Other yeast prions include *P. anserina* mating-type incompatibility epigenetic factor [Het-s] (Coustou et al., 1997) and a newly found prion [NU^{+}] in *S. cerevisiae* (Osherovich and Weissman, 2002).

Wickner proposed three genetic criteria to identify the presence of a prion (Wickner et al., 2006). First, a prion should be reversibly curable by some growth condition or chemical treatment. The curing of a prion efficiently converts prion particles to the native form of the related proteins, which is still capable of becoming a prion under appropriate conditions. Second, overproduction of the protein should increase the rate of the *de novo* formation of the prion. Because the initial formation of a prion correlates with the nucleation resulting from the random encountering of the protein, increased concentration of the protein should generate prion more frequently. Third, the phenotype produced by a prion generally resembles that produced by mutation in the gene for the

related protein. This criterion is applicable only when a prion is in the inactive form, but not when the prion is in the active form.

Different from mammalian prions that cause diseases, yeast prions are not harmful, but are apparently benign and may indeed be beneficial to the host strains (Uptain and Lindquist, 2002). [*URE3*] cells, for example, are able to grow on uracil-deficient medium containing ureidosuccinate (USA), an intermediate in uracil biosynthesis. By comparing the growth characteristics of [PSI^+] and [psi^-] cells in more than 150 conditions, True and Lindquist demonstrated that [PSI^+] strains exhibited greater tolerance than their isogenic [psi^-] derivatives to many conditions, such as ethanol and heat stress. The switching of Sup35p activity, as a result of alternative prion and non-prion structures, may provide cells with an epigenetic tool to regulate translation of hidden genes, which is very flexible and evolutionarily advantageous (True and Lindquist, 2000). However, a study by Wickner's group suggested that [*URE3*] and [PSI^+] might have a net deleterious effect on its host, based on their finding that both prions were uniformly absent among over 70 wild *Saccharomyces* strains. In contrast, [PIN^+] was not thought to be deleterious because of its presence in 11 strains (Nakayashiki et al., 2005). The suggestion that yeast prions [*URE3*] and [PSI^+] are diseases does not contradict directly with the proposal that prions are beneficial, because normal and stressful growth conditions have been used in those studies, respectively.

[*PSI*$^+$] and Sup35p

As mentioned above, [*PSI*$^+$], first identified as a yeast non-Mendelian factor in 1965 (Cox, 1965), has been proposed to be the prion form of Sup35p. This remarkable hypothesis was proven by two independent research groups in 2004 (King and Diaz-Avalos, 2004; Tanaka et al., 2004). By showing that fibers formed by recombinant Sup35p *in vitro*, when transformed into yeast cells, can convert [*psi*$^-$] strains to [*PSI*$^+$], the researchers demonstrated that Sup35p, and only Sup35p, was the determinant of [*PSI*$^+$]. Furthermore, they also demonstrated that different prion variants, also known as strains, could arise from the assembly of the same protein, Sup35p.

Saccharomyces cerevisiae Sup35p is the GTP-dependent polypeptide chain release factor eRF3. Cooperating with Sup45p, the release factor eRF1, Sup35p functions to terminate protein translations at nonsense codons (Paushkin et al., 1997). Prion formation causes the aggregation of Sup35p, which limits its accessibility to Sup45p. Thus, the native termination complex cannot form, which leads to the read-through or the suppression of the stop codons. The detection of [*PSI*$^+$] is usually based on the suppression of nonsense-codon mutations in auxotrophic markers, and the most commonly used marker is the nonsense mutation in the *ADE1* gene, in which the UGG codon for Trp at position 244 is replaced by the termination codon UGA (Cox et al., 1988). Non-prion cells containing *ade1-14* gene are adenine auxotrophic and can not grow on adenine-deficient synthetic media (SD-Ade). In addition, a red pigment accumulates as a byproduct of adenine biosynthesis when the cells grow on rich media,

causing the formation of red colonies. In contrast, [*PSI*$^{+}$] cells are able to grow on SD-Ade media and are white on rich media as chain elongation through the internal termination codon can occur.

Domain dissection of Sup35p

Sup35p is a 685-amino acid protein composed of multiple domains (Figure 1-1). The evolutionarily conserved C domain (C-terminal 254-685 fragment) is homologous to eukaryotic translation elongation factors and indispensable for translation termination and cell viability, while the N-terminal 1-253 residues are not conserved and are not important for viability. The N-terminal region can be subdivided into N domain (1-123 fragment) which is critical for the prion formation, and M domain (124-253 fragment) which contains highly charged residues and shows no clear biological functions (Uptain and Lindquist, 2002).

N and M domains, also referred to as the prion forming domain (PrD), are sufficient for prion formation. When the C-terminal functional group was replaced by a steroid hormone-regulated transcription factor derived from the rat glucocorticoid receptor (GR), the new fusion protein could still undergo prion-like conformational change (Li and Lindquist, 2000). Other reporter proteins, such as green fluorescence protein (GFP), were also used in place of C domain to reflect the prion status. The GFP fusion proteins exhibited diffuse fluorescence throughout the cytoplasm in cells in the non-prion state, while in cells in the prion state, these GFP fusion proteins aggregated into cytoplasmic

foci (Patino et al., 1996). The critical elements for prion induction and propagation have been further narrowed to the N domain, and M domain appears to be dispensable. An M deletion mutant of Sup35p was able to exist in both the prion and the non-prion states, supporting that N domain was enough for prion formation (Liu et al., 2002). However, the M deletion mutant showed poor solubility in either case, and the substitution of other charged polypeptides for the M domain restored the solubility but generated unstable prions (Liu et al., 2002). Therefore, the M domain might play a crucial role in protein inheritance that has not been identified.

The N domain can be subdivided into NQ domain that correlates with a Asn/Gln-rich tract (residues 1–39) (DePace et al., 1998) and NR domain that consists of five and a half non-perfect repeats of the consensus sequence PQGGYQQ-YN (residues 40–112) (Crist et al., 2003; Liu and Lindquist, 1999; Parham et al., 2001). The NQ subdomain is required for the sequence-specific aggregation, while the NR subdomain is important for the replication and stable inheritance of these aggregates. Similarly, New1p, the protein component of prion [NU^{+}] (Santoso et al., 2000), contains both Asn/Gln-rich tract (Asn-Tyr-Asn (NYN) repeat, residues 70-100) and oligopeptide repeats (residues 50-69), although in a reversed order. The substitution the NYN repeat of New1p for the NQ domain in Sup35p generates a chimera protein F, which is capable of forming a prion state [F^{+}] (Osherovich et al., 2004). [F^{+}] and [NU^{+}] prion proteins interact with each other but not with [PSI^{+}]. When expanded polyglutamine, which underlies the formation of pathogenic aggregates associated with Huntington's disease, is utilized in place of the

NQ domain in Sup35p, the chimaeric protein forms a prion state [Q^+] (Osherovich et al., 2004). The interchangeability of the NQ domain with other aggregation-prone protein not only helps illuminate the mechanism by which protein forms prion, but also allows prion [PSI^+] to serve as a model to explore the aggregation of these proteins.

An increase of the numbers of oligopeptide repeat induces the spontaneous appearance of [PSI^+], while the truncation and deletion of the NR domain cause the destabilization and elimination of [PSI^+] (Liu and Lindquist, 1999). A systematic deletion analysis of the NR domain determined the minimum length required for stable [PSI^+] propagation as residues 1-93, which included 5 repeats (Osherovich et al., 2004; Parham et al., 2001). The requirement of NR region for the stable inheritance of prion aggregates is proposed to result from its capability of mediating their fragmentation by the chaperone Hsp104p, which helps explain why only a small portion of Q/N-rich proteins form heritable prions in yeast (Osherovich et al., 2004). The NR domain is also suggested to regulate the strain variation of [PSI^+] by the formation of conformational variants. Supporting evidence for this hypothesis includes the observation that different lengths of oligopeptide repeats are required for the maintenance of different prion strains (Shkundina et al., 2006).

[*RNQ*$^+$], or [*PIN*$^+$]

The *de novo* appearance of [PSI^+] was found to occur more frequently in some strains than in others, which led to the discovery of [PIN^+], the prion accounting for

[*PSI*$^+$] inducibility (Derkatch et al., 1997). The underlying mechanism was later shown to be that [*PIN*$^+$] was capable of "seeding" the formation of [*PSI*$^+$], by recruiting soluble Sup35p in the cell. The concept of [*PIN*$^+$] became ambiguous when both [*RNQ*$^+$] and [*URE3*] were shown to be able to induce [*PSI*$^+$] (Derkatch et al., 2001). Generally, [*PIN*$^+$] is now referred to as [*RNQ*$^+$], the prion formed by Rnq1p. The nature of [*RNQ*$^+$] as a prion was recently proven by the capability of *in vitro*-formed fibers by Rnq1p fragments, when transformed into the [*rnq*$^-$] strains, of inducing [*RNQ*$^+$] formation (Patel and Liebman, 2007).

Hsp104p chaperone and [*PSI*$^+$]

The molecular chaperone Hsp104p (Heat shock protein 104 kDa) is able to re-solubilize thermally denatured proteins (Glover and Lindquist, 1998; Parsell et al., 1994). In a genetic screen for factors that cure [*PSI*$^+$] at elevated expression level, Chernoff and coworkers found that overproduced Hsp104p cured [*PSI*$^+$] efficiently (Chernoff et al., 1995). Deletion of *HSP104* gene also cured [*PSI*$^+$] (Chernoff et al., 1995). Therefore, an intermediate level of Hsp104p is required for [*PSI*$^+$] propagation. Besides [*PSI*$^+$], other prions, such as [*URE3*] and [*RNQ*$^+$], can also be cured by *hsp104* gene deletion (Derkatch et al., 2001; Moriyama et al., 2000).

To explain why intermediate level of Hsp104p is required, the mechanism that Hsp104p mediate the prion propagation has been speculated from two points of view. One hypothesis is that Hsp104p promotes Sup35p conversion by stabilizing the

oligomeric intermediate state formed by Sup35p, and overproduced Hsp104p completely disaggregates Sup35p prion aggregates (Chernoff et al., 1995; Uptain and Lindquist, 2002). In consequences, the unstable intermediate state returns to the non-prion state in the absence of Hsp104p. The reason why transient overproduction of Sup35p induces [*PSI*$^+$] *de novo* is the increased propensity of Hsp104p and the Sup35p intermediate to interact. This hypothesis was supported by the indirect evidence for a transient interaction between Sup35p and Hsp104p (Schirmer and Lindquist, 1997). Also consistent with this hypothesis, *in vitro* Sup35p amyloid formation was found to associate through an oligomeric state that formed without the assistance of Hsp104p (Serio et al., 2000)

The other hypothesis is that Hsp104p simply functions by disaggregating Sup35p prion aggregates and generating more and smaller ones that can be passed during cell division (Kushnirov and Ter-Avanesyan, 1998). Without Hsp104p, Sup35p prion aggregates become fewer and larger, thus they can not be passed to daughter cells. Overproduced Hsp104p cures [*PSI*$^+$] simply because all prion aggregates are re-solubilized. This hypothesis was supported by the observations that, first, Sup35NM-GFP foci became fewer and larger when Hsp104p levels were reduced (Wegrzyn et al., 2001); second, [*PSI*$^+$] was unstable in a *sup35* mutant strain due to the inefficient disaggregation by Hsp104p, and moderately overproducing Hsp104p increased the stability of [*PSI*$^+$] in the mutant strain (Borchsenius et al., 2001).

Guanidine hydrochloride (GuHCl), through its inhibition of Hsp104p, is capable of

curing yeast prions including [*PSI*$^{+}$] (Ferreira et al., 2001). A lag of four to five cell generations follows the addition of GuHCl to a growing culture of [*PSI*$^{+}$] cells, before the appearance of [*psi*$^{-}$] cells. The population of [*PSI*$^{+}$] cells then declines exponentially, which matches the exponential cell multiplication. The kinetics of [*PSI*$^{+}$] decline suggests that GuHCl inhibits the generation of new "propagons", or “seeds”, that need to be transmitted to daughter cells in order for stable propagation to occur (Cox et al., 2003; Ness et al., 2002). Consequently, Sup35p prion aggregates become larger, on the basis of the electrophoresis analysis, after the addition of GuHCl (Kryndushkin et al., 2003). Cell division, based on the observations, was proposed be a requirement for elimination of [*PSI*$^{+}$] by GuHCl (Ness et al., 2002). Although this proposal was challenged (Wu et al., 2005), it has received further support and remains plausible (Byrne et al., 2007).

Despite the importance of Hsp104p in prion propagation, it is not the only chaperone that mediates the prion propagation. Other chaperones, including Hsp70p and Hsp40p, also play important role in the process of disaggregation (Glover and Lindquist, 1998a). On the other hand, although Hsp104 has been shown to interact with mammalian PrP in vitro (Schirmer & Lindquist 1997), a direct orthologue for Hsp104 has not been identified in humans (Gottesman et al. 1997).

The structure of Sup35p prion aggregates

Purified Sup35p forms highly ordered fibers *in vitro* that exhibit the characteristics of amyloids, such as binding to the dye Congo red and displaying conformations that are

rich in ß sheet structure (Glover, 1997). The detailed structure of the aggregates remains unavailable because the amyloid fibers formed by Sup35p are insoluble (solution NMR-incompatible) and not amenable to crystallization (X-ray-incompatible). Remarkably, Eisenberg's group resolved the crystal structures of the fibers formed by N-terminal Sup35 peptides, e.g. ^{7}GNNQQNY^{13} (Balbirnie et al., 2001; Nelson et al., 2005). The crystal analysis shows a double beta-sheet structure, with each sheet formed from parallel in-register stacking of peptide segments. The two sheets are held together by a dry, tightly self-complementing 'steric zipper' formed by the side chains protruding from the two sheets, which is a van der Waals forces interaction without hydrogen bonds. Outside the double-layer beta-sheet, they interact with neighboring double-layer beta-sheet through wet, hydrogen bonding between side chains (Figure 1-2). This structure is proposed to be a fundamental feature of amyloid-like fibrils, which helps explain the stability of amyloid fibrils, their self-seeding characteristic, and their tendency to form polymorphic structures (Liebman, 2005; Nelson et al., 2005).

Krishnan and Lindquist investigated the structure and formation of fibers formed by the Sup35pNM in another approach (Krishnan and Lindquist, 2005). The creation of 37 individual cysteine-substitution mutations throughout NM allows the attachment of fluorophores and crosslinkers to the protein at different sites, which makes it feasible to characterize the architecture of Sup35NM fibers. It is proposed that the amyloid core consists of head, central, and tail regions. The central regions collapse through intramolecular interaction to initiate fiber formation, and fibers grow by head-to-head

Figure 1-2. Structure of Sup35p peptide (Nelson et al., 2005).

Unless otherwise noted, carbon atoms are colored in purple or grey/white, oxygen in red, nitrogen in blue. a, The pair-of-sheets structure, showing the backbone of each beta-strand as an arrow, with side chains protruding. The dry interface is between the two sheets, with the wet interfaces on the outside surfaces. Side chains Asn 2, Gln 4 and Asn 6 point inwards, forming the dry interface. The 21 screw axis of the crystal is shown as the vertical line. It rotates one of the strands of the near sheet 180° about the axis and moves it up 4.87 Å/2 so that it is superimposed on one of the strands of the far sheet. b, The steric zipper viewed edge on (down the a axis). Note the vertical shift of one sheet relative to the other, allowing interdigitation of the side chains emanating from each sheet. The amide stacks of the dry interface are shaded in grey at the centre, and those of the wet interface are shaded in pale red on either side. c, The GNNQQNY crystal viewed down the sheets (from the top of panel a, along the b axis). Six rows of beta-sheets run horizontally. Peptide molecules are shown in black and water molecules are red plus signs. The atoms in the lower left unit cell are shown as spheres representing van der Waals radii. d, The steric zipper. This is a close-up view of a pair of GNNQQNY molecules from the same view as panel c, showing the remarkable shape complementarity of the Asn and Gln side chains protruding into the dry interface. 2Fo - Fc electron density is shown, and the position of the central screw axis is indicated.

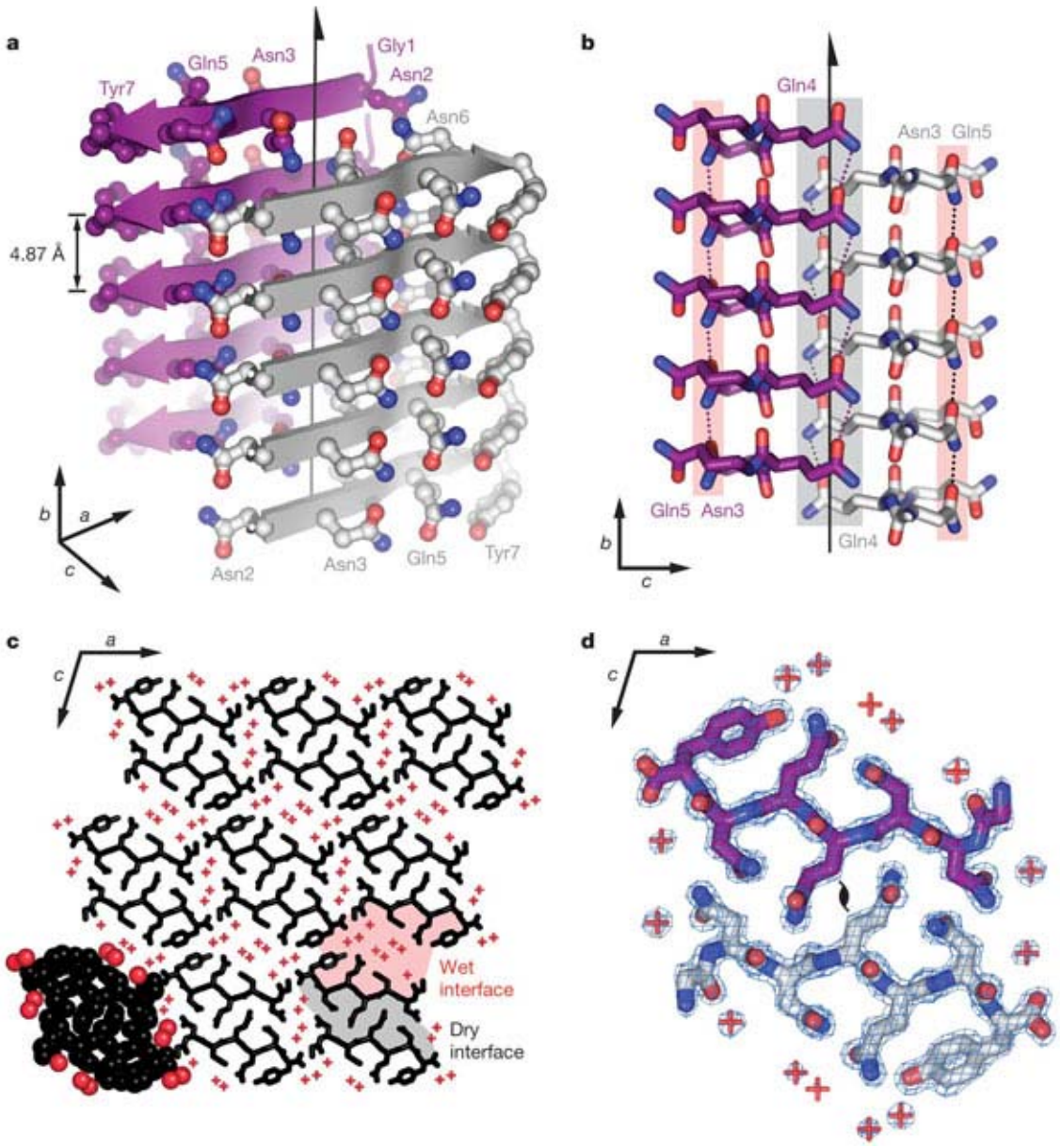
a
Tyr7
Gln5
Asn3
Gly1
Asn2
Asn6
4.87 Å
b
a
c
Asn2
Asn3
Gln5
Tyr7
b
Gln4
Asn3
Gln5
Gln5
Asn3
Gln4
b
c
c
a
c
Wet
interface
Dry
interface
d
a
c

and tail-to-tail additions (Figure 1-3). Interestingly, the length of the amyloid core varies, causing the formation of different structures, which is believed to the structural basis of the distinct prion strains. The "variable core length" model is also able to explain the observation that different Sup35NM fibers, when transformed into cells, caused the appearance of different prion phenotypes, with fibers formed at 4 °C causing the appearance of stronger prion than fibers formed at 37 °C (Tanaka et al., 2004). The structure predicts that fibers formed at 4 °C should be more fragile due to their shorter central core; therefore, more prion aggregates can be generated from the breakage of fibers and be passed to daughter cells during cell division (Krishnan and Lindquist, 2005). The "head-to-head, tail-to-tail" model explains the bidirectional growth of Sup35NM fibers and predicts that growth should be same at both ends; however, some fibers turn out to be asymmetric (DePace and Weissman, 2002), which awaits an explanation other than this model. Meanwhile, Tycko performed a solid state NMR of labeled NM domain that indicated a parallel in-register structure (Shewmaker et al., 2006).

Exploring protein aggregation in yeast prions

Yeast prions are excellent models to study protein aggregation for many reasons. First, yeast prions are generally not harmful to their host cells, so they can be monitored both in real time and for multiple generations. Second, the yeast *S. cerevisiae* provides powerful genetic tools for gene manipulations, such as gene deletion, replacement, and recombination, which can be conducted easily and efficiently. In addition, the genome of

Figure 1-3. Proposed structure of Sup35NM fibers (Krishnan and Lindquist, 2005).

a–d, One model for NM assembly is provided to illustrate the constraints that our data place on the nature of NM fibre structures. In the cooperatively folded amyloid core, Head residues (red) in one NM molecule are in close proximity to Head residues of their neighbours; the same is true for the Tail residues (green) (c). Central Core residues (blue) are sequestered from intermolecular interactions. M (dashed line) is largely unstructured, but the segment of M proximal to N becomes structured when amyloid forms. In the initial stages, NM molecules rapidly acquire a collapsed state (a) that retains a molten character until the Head regions of two molecules (b) come into proximity with each other and nucleate assembly. It is unclear how fibrils are arranged within fibres (d).

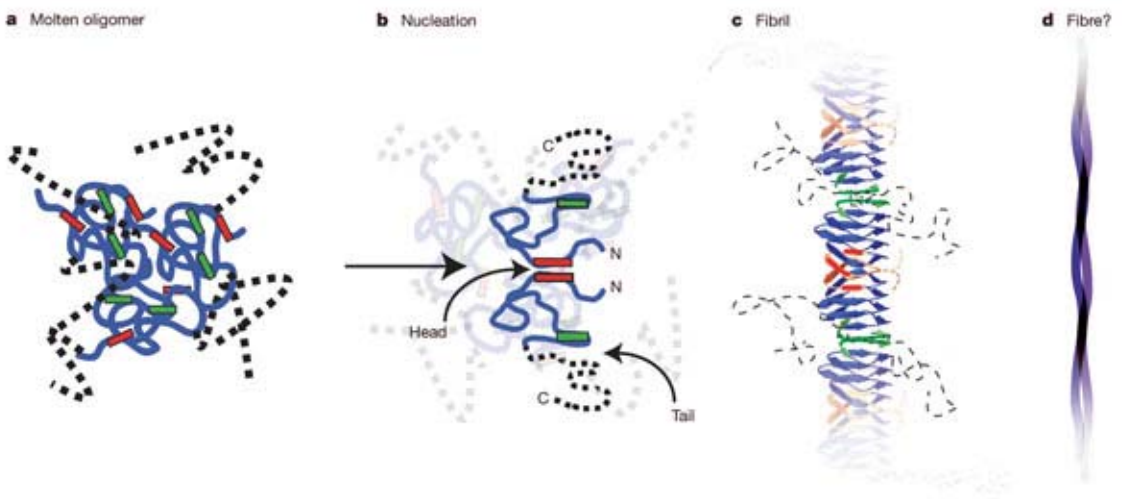

S. cerevisiae has been sequenced, and gene knockout libraries in *S. cerevisiae* are generally available. Last, prion-containing yeast cells can be used for drug screening *in vivo*, as will be discussed below (Bach et al., 2003; Tribouillard et al., 2006).

Inhibition assays have been conducted in *S. cerevisiae* prion strains, which have led to the identification of several compounds as anti-prion drugs (Bach et al., 2003; Tribouillard et al., 2006). The compounds were selected based on their ability to cure the prion phenotype, and, interestingly, they were also able to clear mammalian prions in cell free conditions. The detailed mechanism by which yeast prions are cured by these compounds is unclear. The compounds are believed to be involved in certain biological pathways indirectly, instead of interacting directly with the prions. If they interacted with prions directly, like the compound Congo red does, the curing process would have started at the addition of the compounds. However, there is actually a lag phase for the prion to be cured after the compounds are added. Although still in its early stage, the future of yeast prions serving as models for drug screening is promising. If customized prions can be made through the incorporation of general aggregation-prone proteins into the component proteins of prions, it will be feasible to select the compounds that can cure the novel prions specifically.

As illustrated by the experimental dissection of Sup35p, the NQ domain is the main driving force for aggregation, while the NR domain is related to prion propagation, possibly through Hsp104 interaction. In this study, the NQ and the NR domains are replaced with other peptides to generate novel prions derived from [*PSI*$^{+}$].

Amyloid-forming peptides from both natural and artificial sources were chosen as replacement for the NQ domain. In Chapter 2, the methodology of NQ domain replacement and the selection of the candidate proteins are described in detail. In Chapter 3, a fragment of α-synuclein, the protein whose aggregation is responsible for Parkinson's disease, is studied for the its potential to drive aggregation of this Sup35 variant into a prion state. In Chapter 4, a fragment of islet amyloid polypeptide (IAPP), the protein whose aggregation is associated with type II diabetes, is explored as a structural alternative for the NQ domain of Sup35p to generate novel prions. As described in Chapter 5, the NR domain is replaced by a bacterial Asn/Gln-rich oligopeptide repeats fragment to further study the requirement of the NR domain for prion propagation.

CHAPTER 2

Selection of Aggregation-Prone Protein Candidates and Their Substitutions for the NQ Domain of Sup35p

Introduction

The N-terminal domain of Sup35p, essential for prion formation and propagation, consists of an NQ domain that is rich in Asn/Gln residues, and an NR domain that comprises five and a half oligopeptide repeats. The NQ domain, which is responsible for the aggregation, can be replaced by other aggregation-prone sequences such as expanded polyglutamine and NYN repeats from yeast New1p (Osherovich et al., 2004). The polar Asn/Gln residues, which appear frequently in expanded polyglutamine, the NQ domain of Sup35p, and NYN repeats of New1p, can form "polar zippers" that stabilize protein aggregates (Perutz et al., 1993). It remains an open question as to whether the polar zippers formed by Asn/Gln residues are essential for the aggregation and the prion propagation. In other words, it is unclear whether the Asn/Gln-rich NQ domain is replaceable by other aggregation-prone peptides that have low or no Asn/Gln content.

Various component proteins of misfolding diseases contain non-Asn/Gln-rich fragments that can aggregate both *in vivo* and *in vitro*. Substitution of these naturally

existing fragments for the NQ domain of Sup35p will produce chimera proteins that can be tested for their capability of forming prions. In addition, many artificial peptides are capable of undergoing a transition from a soluble, unassociated state to an aggregated form. The substitution of these sequences for the NQ domain might enable the generation of more diversified prions.

In this chapter, different fragments from both natural sequences and artificial design are substituted for the NQ domain. The general methodology for the construction of variant sequences in yeast-based expression plasmids and the replacement of mutant genes is described. The results from some substitutions are briefly described and discussed.

Experimental Procedures

Sources of reagents

Chemicals were purchased from Sigma-Aldrich (St Louis, MO) and Fisher Scientific Co. (Fair Lawn, NJ) unless specified. Restriction endonuclease enzymes, unless specified, were purchased from New England Biolabs (Beverly, MA). Plasmids preparation kits were purchased from Qiagen (Valencia, CA). High fidelity DNA polymerase Pfx-50 was purchased from Invitrogen (Carlsbad, CA). Yeast transformation kits were purchased from either Invitrogen (Carlsbad, CA) or Zymo Research (Orange, CA).

Media and growth conditions

YPD (1%, w/v, yeast extract; 2%, w/v, peptone; 2%, w/v, glucose) and 1/4YPD (0.25%, w/v, yeast extract; 2%, w/v, peptone; 4%, w/v, glucose) media were prepared in ddH_2O and autoclaved for sterilization. To prepare solid media, agar (1.5%) was added to the media before sterilization. Synthetic minimal media were prepared using standard protocols, and minimal drop-out media lacking appropriate amino acids were prepared as needed. LB media containing appropriate antibiotics were prepared using standard protocols. Normally, *S. cerevisiae* strains were grown at 30 °C and *E. coli* strains were grown at 37 °C with sufficient aeration.

Plasmids and strains

The plasmids, as listed in Table 2-1, were constructed using standard molecular cloning methods. The oligonucleotides used for PCR amplification and DNA construction are listed in Table 2-2. The strains used in this study are listed in Table 2-3.

The plasmid pJET101 contains the native P_{SUP35} promoter together with *SUP35* gene in a *HIS3*-marked centromeric plasmid backbone. The backbone of pJET101 was from the shuttle vector pRS313. The promoter, which contains an engineered *Bam*H I restriction site at its 3' end to facilitate the subsequent cloning, was cloned from the plasmid p316-Sp-Sup35 (DePace et al., 1998). The *SUP35* gene was amplified from yeast genomic DNA and cloned into the vector plasmid at the *Bam*H I/*Sac* I restriction sites.

Table 2-1. Plasmids used in Chapter 2.

Plasmids	Characteristics	References
pZErO-1	*E. coli* cloning vector, Zeocin^R	Invitrogen
pRS313	Yeast shuttle vector, *CEN, HIS3,* Amp^R	(Sikorski and Hieter, 1989)
pRS316	Yeast shuttle vector, *CEN, URA3,* Amp^R	(Sikorski and Hieter, 1989)
p316-Sp-Sup35	pRS316, P_{SUP35}, *SUP35*	(DePace et al., 1998)
pJET101	pRS313, P_{SUP35}, *SUP35*	this study
pZErO-1+NM	pZErO-1, *sup35-NM* pZErO-1 ← Sup35-NM PCR (*Bam*H I/*Xho* I)	this study
pZErO-1+NM .AEAK	pZErO-1, *sup35-NM(Δ3-39::AEAK)* pZErO-1+NM ← AEAK (*Bam*H I/*Pst* I)	this study
pJET101.AEAK	pRS313, P_{SUP35}, *sup35(Δ3-39::AEAK)* pJET101 ← pZErO-1+NM.AEAK (*Bam*H I/*Pfl*M I)	this study
pZErO-1+NM .IAPP	pZErO-1, *sup35-NM(Δ3-39::IAPP)* pZErO-1+NM ← IAPP (*Bam*H I/*Pst* I)	this study
pJET101.IAPP	pRS313, P_{SUP35}, *sup35(Δ3-39::IAPP)* pJET101 ← pZErO-1+NM.IAPP (*Bam*H I/*Pfl*M I)	this study
pZErO-1+NM .Aß	pZErO-1, *sup35-NM(Δ3-39::Aß)* pZErO-1+NM ← Aß (*Bam*H I/*Pst* I)	this study
pJET101.Aß	pRS313, P_{SUP35}, *sup35(Δ3-39::Aß)* pJET101 ← pZErO-1+NM.Aß (*Bam*H I/*Pfl*M I)	this study
pZErO-1+NM .syn1	pZErO-1, *sup35-NM(Δ3-39::syn1)* pZErO-1+NM ← syn1 (*Bam*H I/*Pst* I)	this study
pJET101.syn1	pRS313, P_{SUP35}, *sup35(Δ3-39::syn1)* pJET101 ← pZErO-1+NM.syn1 (*Bam*H I/*Pfl*M I)	this study
pZErO-1+NM .TTR	pZErO-1, *sup35-NM(Δ3-39::TTR)* pZErO-1+NM ← TTR (*Bam*H I/*Pst* I)	this study
pJET101.TTR	pRS313, P_{SUP35}, *sup35(Δ3-39::TTR)* pJET101 ← pZErO-1+NM.TTR (*Bam*H I/*Pfl*M I)	this study

Plasmids	**Characteristics**	**References**
pJET102.T20	pZErO-1, *(Thr)$_{20}$* pZErO-1 ← polyT (*Hin*d III/*Bam*H I)	this study
pJET102.T40	pZErO-1, *(Thr)$_{40}$* pJET102.T20 (*Xba* I/*Bsm*B I) ← pJET102.T20 (*Bbs* I/*Xba* I)	this study
pJET102.T60	pZErO-1, *(Thr)$_{60}$* pJET102.T40 (*Xba* I/*Bsm*B I) ← pJET102.T20 (*Bbs* I/*Xba* I)	this study
pJET103	pZErO-1, *sup35-NM(Δ3-39::polyT adaptor)* pZErO-1+NM ← polyT adaptor (*Bam*H I/*Pst* I)	this study
pJET104.T20	pZErO-1, *sup35-NM(Δ3-39::(Thr)$_{20}$)* pJET103 (*Bsm*B I) ← pJET102.T20 (*Bbs* I/*Bsm*B I)	this study
pJET104.T40	pZErO-1, *sup35-NM(Δ3-39::(Thr)$_{40}$)* pJET103 (*Bsm*B I) ← pJET102.T40 (*Bbs* I/*Bsm*B I)	this study
pJET104.T60	pZErO-1, *sup35-NM(Δ3-39::(Thr)$_{60}$)* pJET103 (*Bsm*B I) ← pJET102.T60 (*Bbs* I/*Bsm*B I)	this study
pJET105.T20	pRS313, P_{SUP35}, *sup35(Δ3-39::(Thr)$_{20}$)* pJET101 ← pJET104.T20 (*Bam*H I/*Pfl*M I)	this study
pJET105.T40	pRS313, P_{SUP35}, *sup35(Δ3-39::(Thr)$_{40}$)* pJET101 ← pJET104.T40 (*Bam*H I/*Pfl*M I)	this study
pJET105.T60	pRS313, P_{SUP35}, *sup35(Δ3-39::(Thr)$_{60}$)* pJET101 ← pJET104.T60 (*Bam*H I/*Pfl*M I)	this study
pJET106.SW1	pZErO-1, *sup35-NM(Δ3-39::SW1)* pZErO-1+NM ← SW1 (*Bam*H I/*Pst* I)	this study
pJET106.SW2N Asn m=a	pZErO-1, *sup35-NM(Δ3-39::SW2N)* pZErO-1+NM ← SW2 (*Bam*H I/*Pst* I)	this study
pJET106.SW2T Thr m=c	pZErO-1, *sup35-NM(Δ3-39::SW2T)* pZErO-1+NM ← SW2 (*Bam*H I/*Pst* I)	this study
pJET109.SW1	pRS313, P_{SUP35}, *sup35(Δ3-39::SW1)* pJET101 ← pJET106.SW1 (*Bam*H I/*Pfl*M I)	this study
pJET109.SW2N	pRS313, P_{SUP35}, *sup35(Δ3-39::SW2N)* pJET101 ← pJET106.SW2N (*Bam*H I/*Pfl*M I)	this study
pJET109.SW2T	pRS313, P_{SUP35}, *sup35(Δ3-39::SW2T)* pJET101 ← pJET106.SW2T (*Bam*H I/*Pfl*M I)	this study
pJET112	pZErO-1, *sup35-NM(Δ3-39)* pJET103 (*Bsm*B I) self-ligate	this study
pJET113	pRS313, P_{SUP35}, *sup35(Δ3-39)* pJET101 ← pJET112 (*Bam*H I/*Pfl*M I)	this study

Plasmids	**Characteristics**	**References**
pJET125	pZErO-1, *(Gln)$_{20}$* pZErO-1 ← polyQ (*Hin*d III/*Bam*H I)	this study
pJET126	pZErO-1, *sup35-NM(Δ3-39::polyQ adaptor)* pZErO-1+NM ← adaptor (*Bam*H I/*Pst* I)	this study
pJET127.Q20	pZErO-1, *sup35-NM(Δ3-39::(Gln)$_{20}$)* pJET126 (*Bsm*B I) ← pJET125.Q20 (*Bbs* I/*Bsm*B I) (single)	this study
pJET127.Q40	pZErO-1, *sup35-NM(Δ3-39::(Gln)$_{40}$)* pJET126 (*Bsm*B I) ← pJET125.Q20 (*Bbs* I/*Bsm*B I) (double)	this study
pJET127.Q60	pZErO-1, *sup35-NM(Δ3-39::(Gln)$_{60}$)* pJET126 (*Bsm*B I) ← pJET125.Q20 (*Bbs* I/*Bsm*B I) (triple)	this study
pJET128.Q20	pRS313, P_{SUP35}, *sup35(Δ3-39::(Gln)$_{20}$)* pJET101 ← pJET127.Q20 (*Bam*H I/*Pfl*M I)	this study
pJET128.Q40	pRS313, P_{SUP35}, *sup35(Δ3-39::(Gln)$_{40}$)* pJET101 ← pJET127.Q20 (*Bam*H I/*Pfl*M I)	this study
pJET128.Q60	pRS313, P_{SUP35}, *sup35(Δ3-39::(Gln)$_{60}$)* pJET101 ← pJET127.Q20 (*Bam*H I/*Pfl*M I)	this study

Table 2-2. The oligonucleotides used for PCR amplification and DNA construction.

PCR primers (restriction sites are underlined)	
NM-F	5’-GCTTA*GGATCC*AACAATGTCGGATTCAAACCAAGGC-3’
NM-R	5’-GGAC*CTCGAG*GTAATTTCCACGGCCACCTTGTGG-3’
MC-F	5’-GCTTA*GGATCC*AACAATGTCTCCACAAGGTGGCCGTGGAAATTAC-3’
MC-R	5’-GGA*CTCGAG*TTATTACTCGGCAATTTTAACAATTTTACCAATTGC-3’
sup35-up45	5’-CGACTTGCTCGGAATAACATCTATATCTGCCCACTAGCAACAATG-3’
sup35-down45	5’-TCGGTATTATTGTGTTTGCATTTACTTATGTTTGCAAGAAATTTA-3’
SupN-F	5’-CAGCAACTCGACAAGATATCCATCATATTACC-3’
KanB	5’-CTGCAGCGAGGAGCCGTAAT-3’
KanC	5’-TGATTTTGATGACGAGCGTAAT-3’
SupC-R	5’-TCCCGCGGTGAAAAGAGTCAGTGAGACGACGACTTCA-3’
Oligonucleotides for DNA annealing	
polyT-F	5’-*AGCTT*GAAGACAAACTACWACSACSACWACWACSACWACWACSACS ACWACWACWACSACSACWACWACSACWACTACGAGACGG-3’
polyT-R	5’-*GATCC*CGTCTCGTAGTWGTSGTWGTWGTSGTSGTWGTWGTWGTSGT SGTWGTWGTSGTWGTWGTSGTSGTWGTAGTTTGTCTTCA-3’
polyT-adaptor-F	5’-*GATCC*AACAATGTCTACTATGAGACGAATTCCGTCTCAACTACCCAAC *CTGCA*-3’
polyT-adaptor-R	5’-GGTTGGGTAGTTGAGACGGAATTCGTCTCATAGTAGACATTGTTG-3’
AEAK-F	5’-*GATCC*AACAATGTCTCCAGCTGAAGCAGAAGCCAAGGCAAAGGCTG AGGCTGAAGCCAAAGCTAAGGCAGGTGGTCAAC*CTGCA*-3’
AEAK-R	5’-GGTTGACCACCTGCCTTAGCTTTGGCTTCAGCCTCAGCCTTTGCCTTG GCTTCTGCTTCAGCTGGAGACATTGTTG-3’ (AEAK aa’s AEAEAKAKAEAEAKAK)
SWITCH1-F	5’-GCTTA*GGATCC*AACAATGTCTAAGGTTGCTGCATTGGAAACTAAGATT GCAGCTTTAGAAACTAAGAAGGCTGCTTTGGAGA-3’
SWITCH1-R	5’-GGAC*CTGCAG*GTTGACCACCTTCCAATGCAGCAATCTTAGTCTCCAAA GCAGCCTTCTTAGTTTCTAAAGCTGCAATCTTA-3’ (Switch1 aa’s KVAALETKIAALETKKAALETKIAALEGG)

SWITCH2-F	5’-GCTTA*GGATCC*AACAATGTCTGTTGAAATTGCTCAATTGAAGACTGAA ATACAAGCTTTAAAGAMTGAGAAGGCTCAATTGAA-3’
SWITCH2-R	5’-GGAC*CTGCAG*GTTGACCACCCTTCAATGCCTGAATTTCAGTCTTCAAT TGAGCCTTCTCAKTCTTTAAAGCTTGTATTTCAG-3’ (Switch2N aa’s VEIAQLKTEIQALKNEKAQLKTEIQALKGG) (Switch2T aa’s VEIAQLKTEIQALKTEKAQLKTEIQALKGG)
polyQ-F	5’-*AGCTT*GAAGACAACAGCAACAGCAACAGCAACAACAGCAGCAACAA CAGCAGCAACAGCAGCAACAGCAACAACAGCCGAGACGG-3’
polyQ-R	5’-*GATCC*CGTCTCGGCTGTTGTTGCTGTTGCTGCTGTTGCTGCTGTTGTT GCTGCTGTTGTTGCTGTTGCTGTTGCTGTTGTCTTCA-3’
polyQ-adaptor-F	5’-*GATCC*AACAATGTCTCAGCTGAGACGAATTCCGTCTCACAGCAACAA C*CTGCA*-3’
polyQ-adaptor-R	5’-GGTTGTTGCTGTGAGACGGAATTCGTCTCAGCTGAGACATTGTTG-3’
TTR-F	5’-*GATCC*AACAATGTCTTATACTATTGCAGCTTTGTTATCTCCATATTCTC*C TGCA*-3’
TTR-R	5’-GGAGAATATGGAGATAACAAAGCTGCAATAGTATAAGACATTGTTG-3’ (TTR aa’s YTIAALLSPYS)
syn1-F	5’-*GATCC*AACAATGTCTAACGTTGGTGGTGCTGTTGTTACTGGTGTTACT GCTGTTGCTCAAC*CTGCA*-3’
syn1-R	5’-GGTTGAGCAACAGCAGTAACACCAGTAACAACAGCACCACCAACGT TAGACATTGTTG-3’ (syn1 aa’s NVGGAVVTGVTAVA)
Aß-F	5’-GCTTA*GGATCC*AACAATGTCTGGTTACGAAGTTCACCACCAAAAGTTA GTTTTCTTCGCTGAAGATGTT-3’
Aß-R	5’-GGAC*CTGCAG*GTTGAGCCAAACCAATAATAGCACCCTTGTTAGAACC AACATCTTCAGCGAAGAAAACT-3’ (Aß aa’s YEVHHQKLVFFAEDVGSNKGAIIGL)
IAPP-F	5’-GCTTA*GGATCC*AACAATGTCTGCTACTCAAAGATTGGCTAACTTCTTG GTTCACTCTTCTAACAACTTCGGTGCTAT-3’
IAPP-R	5’-GGAC*CTGCAG*GTTGAGCGTTGTAAGTGTTAGAACCAACGTTAGTAGA AGACAAAATAGCACCGAAGTTGTTAGAAG-3’ (IAPP aa’s ATQRLANFLVHSSNNFGAILSSTNVGSNTY)

Key to symbols: B=C+G+T, D=A+G+T, H=A+C+T, K=T+G, M=A+C, N=A+C+G+T, R=A+G, S=G+C, W=A+T, V=A+C+G, Y=C+T

Table 2-3. Strains used in Chapter 2.

Strain	Genotype	Reference
TOP10F'	*rec*A1 *ara*D139 *end*A1 (Str^R) F'{*lac*I^q, Tn*10*(Tet^R)}	Invitrogen
OT56 ([PSI^+] 7-74-D694)	*MAT***a** *ade1-14*$_{UGA}$ *his3 leu2 trp1-289*$_{UAG}$ *ura3* [PSI^+]	(Derkatch et al., 1996)
OT60 ([psi^-] 74-D694)	*MAT***a** *ade1-14*$_{UGA}$ *his3 leu2 trp1-289*$_{UAG}$ *ura3* [psi^- PIN^+]	(Chernoff et al., 1995)
GT17	*MAT***a** *ade1-14*$_{UGA}$ *his3 leu2 trp1-289*$_{UAG}$ *ura3* [psi^- pin^-]	(Derkatch et al., 1997)
YPR172W	BY4743, *sup35::KanMX*	(Giaever et al., 2002)
OT56k	OT56, *sup35::KanMX*	this study
OT60k	OT60, *sup35::KanMX*	this study
GT17k	GT17, *sup35::KanMX*	this study

Two-step substitution was used to construct the plasmids with the substitutions of AEAK peptide, switch peptide, Aß(10-35), IAPP(8-37), α-synuclein(65-78), and transthyretin(105-115), for the NQ domain. Oligonucleotides encoding the respective peptides were designed, synthesized, and annealed to generate double-strand DNAs, which were then cloned into pZErO-1+NM to replace the NQ domain at *Bam*H I/*Pst* I sites. The resulted plasmids were digested at *Bam*H I/*Pfl*M I restriction sites, and the inserts were ligated into pJET101 to produce full-length *sup35* mutants (Figure 2-1).

Oligonucleotides encoding 20 Thr residues were annealed and inserted into pZErO-1, generating the plasmid encoding polythreonine peptides (polyT). The DNA cassette encoding polyT was multimerized into dimer (40 Thr residues) and trimer (60 Thr residues) by taking advantage of the type IIs restriction sites flanking the cassette, *Bbs* I and *Bsm*B I. Adaptor plasmid pJET103 was utilized to embrace the DNAs encoding polyTs of different lengths at its two *Bsm*B I sites, generating plasmids pJET104.XX (XX=T20, T40, or T60). The DNA fragments were cut out from pJET104.XX and inserted into pJET101 at *Bam*H I/*Pfl*M I sites to generate pJET105.XX, the *sup35* mutants containing polyT peptides in place of the NQ domain (Figure 2-2).

Plasmids containing polyglutamine peptides (polyQ) substitution were constructed using a slightly different method. After the construction of the polyQ monomer plasmid pJET125 and the adaptor plasmid pJET126, the insert and the vector were prepared directly from the digestion of the plasmids with *Bbs* I/*Bsm*B I and *Bsm*B I respectively. The ligation was then set up by mixing the vector with excess amount of insert. Due to

Figure 2-1. Construction of pJET101.syn1 as an example of the substitutions for the NQ domain of Sup35. Oligonucleotides encoding the syn1 peptide were designed, synthesized, and annealed to generate the double-strand DNA, which was subsequently cloned into pZErO-1+NM to replace the NQ domain at *Bam*H I/*Pst* I sites. The resulted plasmid was digested at *Bam*H I/*Pfl*M I restriction sites, and the insert was ligated into pJET101 to produce pJET101.syn1.

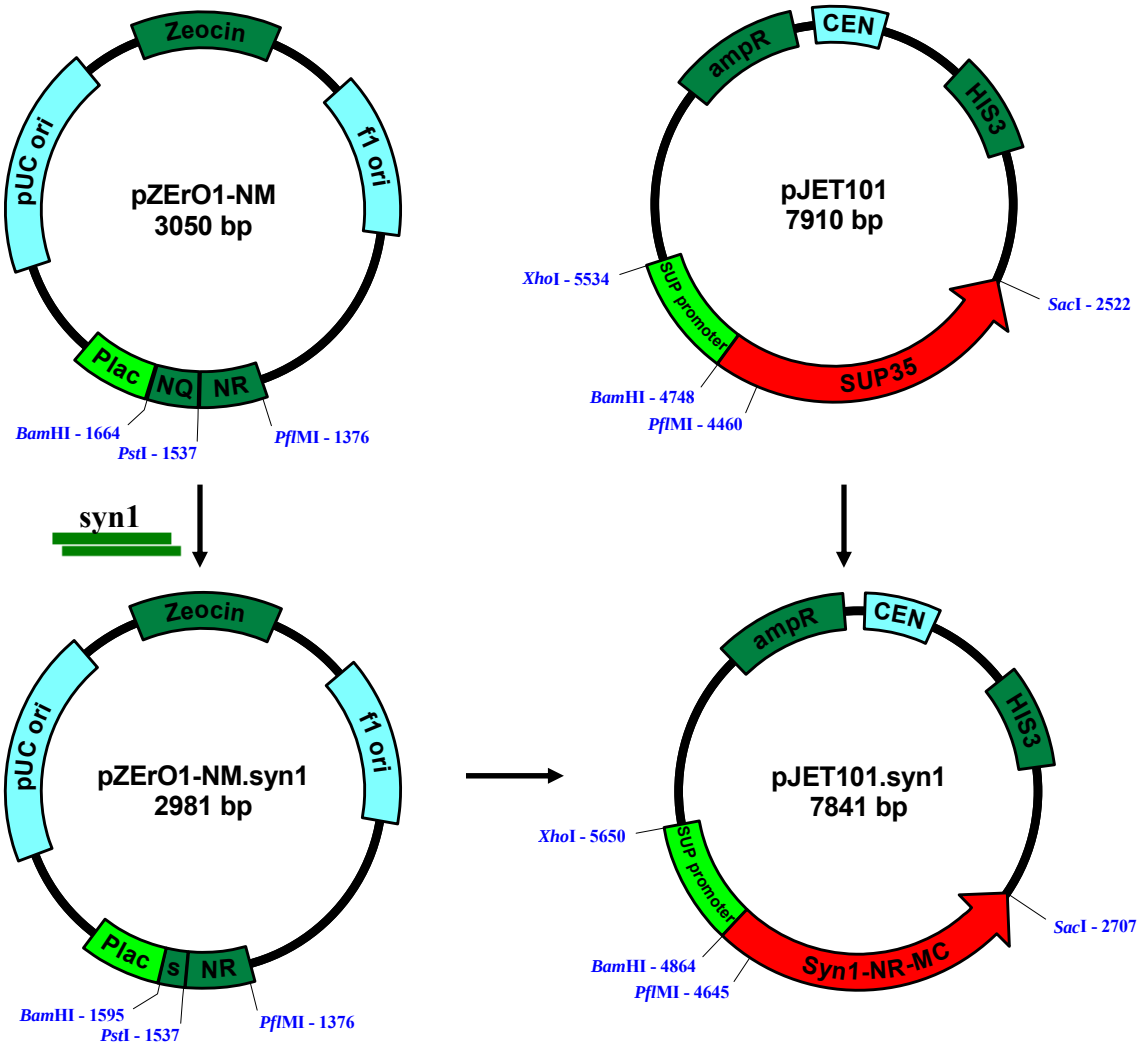

Figure 2-2. Plasmids that contain polyT DNA cassette and cloning adaptor.

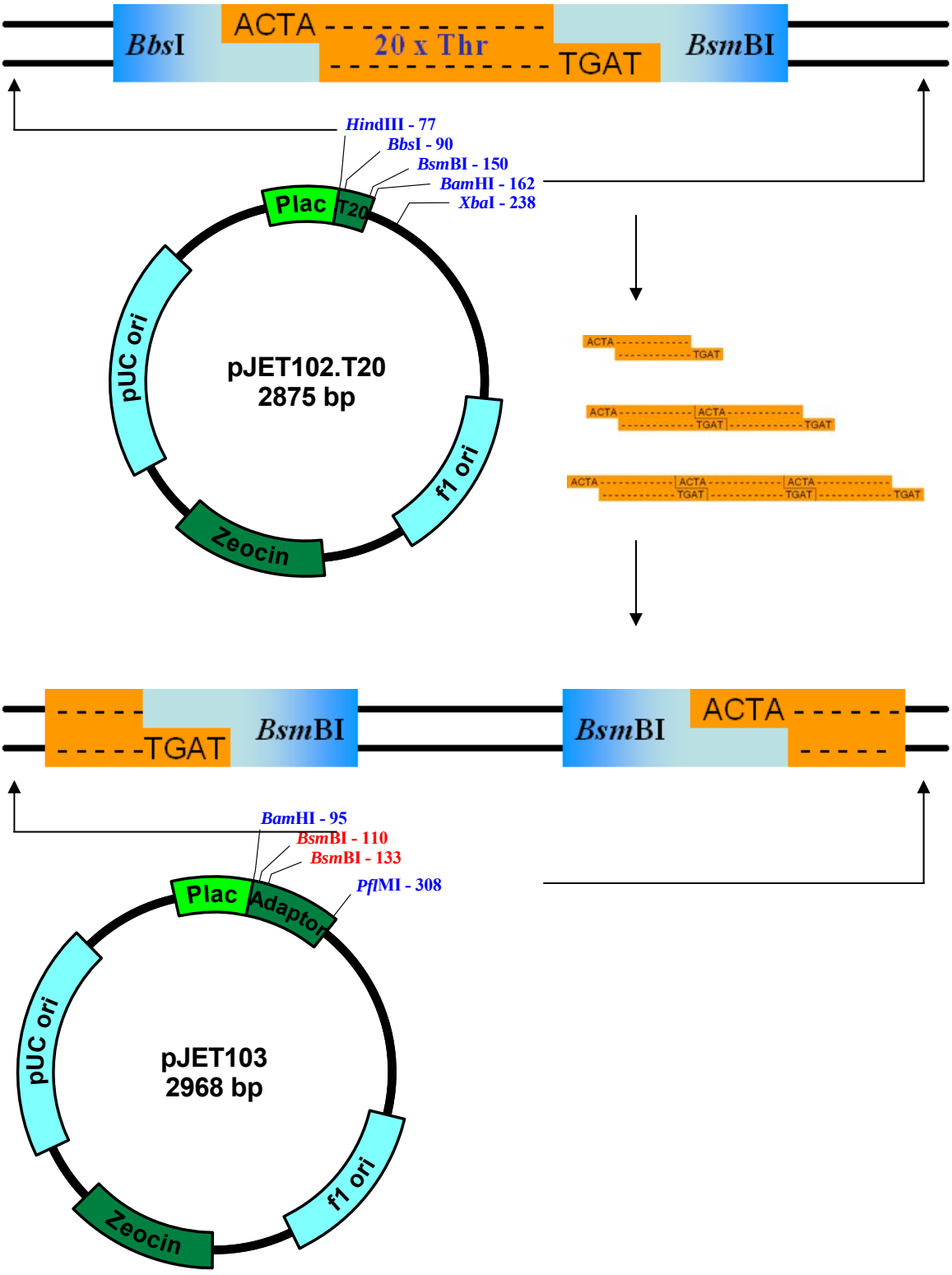

the double- or triple- insertion of the insert DNA, polyQs of different lengths were obtained, which were subsequently subcloned into pJET101 to replace the NQ domain.

The yeast *Saccharomyces cerevisiae* strains OT56 ([PSI^+], [PIN^+]), OT60 ([psi^-], [PIN^+]), and GT17 ([psi^-], [pin^-]), which are the prion variants of 74-D694 with the initial genotypes (*MAT***a** *ade1-14*$_{UGA}$ *his3 leu2 trp1-289*$_{UAG}$ *ura3)*, were kindly provided by Yuri Chernoff at GaTech. The strains were modified to disrupt the native *SUP35* gene located on the chromosome, using the method previously reported (Giaever et al., 2002). The maintenance plasmid p316-Sp-Sup35 was transformed into the strains before the chromosomal gene disruption, as the presence of *SUP35* gene or Sup35p activity is essential for cells to survive. For gene disruption, *sup35::KanMX* was amplified from *S. cerevisiae* strain YPR172W using PCR primers Sup35-up45 and Sup35-down45, and the PCR product was used to transform OT56 harboring p316SpSup35 to replace the chromosomal *SUP35* gene. Transformants were then selected for the successful gene replacement, resulting from the spontaneous DNA recombination in yeast, on YPD medium containing 200 μg/mL geneticin (G418). The correct gene replacement was verified in mutant cells that grew on YPD+G418 by the appearance of PCR products of the expected size using primer sets SupN-F/KanB and KanC/SupC-R, which span the left and right junctions of the deletion module within the genome. The mutant strain was named as OT56k to represent OT56 with *sup35::KanMX* mutation. OT60 was similarly modified to generate OT60k. GT17k was generated by curing OT60k harboring p316SpSup35 after passing the strain on YPD medium containing 5 mM GuHCl for 3

times.

Gene replacement by plasmids shuffling

A plasmid shuffling procedure was used to exchange *SUP35* alleles in the *sup35::KanMX* mutation strains, including OT56k, OT60k, and GT17k. For example, recombinant *SUP35* genes were transformed into OT56k harboring p316-Sp-Sup35. Transformants were selected on SD-His medium and then plated to SD-His medium containing 5-fluoroorotic acid (5-FOA) to select for cells that had lost the *URA3*-based plasmid p316-Sp-Sup35. Single colonies were then picked from the 5-FOA-containing medium and further characterized.

Results

Selection of peptides and their substitutions for the NQ domain

One class of aggregation-prone peptides chosen for this study are the proteins related with the misfolding diseases. Human α-synuclein, the component protein of Parkinson's disease, contains a stretch in the middle of its hydrophobic domain that can assemble into filaments (Giasson et al., 2001). Therefore, an overlapping stretch (residues 65-78) was selected as a candidate peptide and substituted for the NQ domain. Human islet amyloid polypeptide (hIAPP, IAPP), a 37-residue polypeptide that causes type II diabetes while accumulating as pancreatic amyloid, can form fibrils *in vitro* (Jaikaran et al., 2001). The

aggregation core fragment (residues 8-37) was thus selected for this study. Other peptides in this class include Aß(10-35), a truncation of Aß peptides related to Alzheimer's disease (Benzinger et al., 1998), TTR(105-115) from the amyloidosis-related transthyretin (Jaroniec et al., 2002), and expanded polyglutamine that are related to Huntington's disease (Poirier et al., 2002).

The other peptide candidates were artificially designed. Polythreonine, like polyglutamine, can form aggregates, although it is rarely found in natural sources (Oma et al., 2004). AEAK peptide, with the sequence of $(AEAEAKAK)_2$, can spontaneously aggregate into stable macroscopic membrane based upon ß-sheet fibrils (Zhang et al., 1993). Switch peptide sequences were designed to be potentially capable of switching between coiled-coil and β-sheet structures. All plasmids were constructed as designed, and the mutations were verified by DNA sequencing.

Viability of *sup35* mutant strains

Cells transformed with HIS3-marked mutant *sup35* plasmids were selected for those losing the original wild type *SUP35* plasmid on 5-FOA-containing medium. All transformants except for the one containing AEAK-substituted *sup35* were able to grow on the minimal medium containing 5-FOA, suggesting that the *URA3*-marked wild type *SUP35* gene had already been eliminated from these strains. The strains were further tested for the loss of *SUP35* by whole-cell PCR using a forward primer NM-F that can bind to wild type *SUP35* only, and the absence of the PCR product suggested the loss of

wild type *SUP35*. Viability of *S. cerevisiae* strains on 5-FOA-containing medium indicated that the *sup35* mutant genes in these strains were able to maintain the functional activity as a translation termination factor. The viability was not affected by the existence of prion [PSI^+] or [PIN^+], as no difference was observed when parental strains with different prion backgrounds were used in the plasmid shuffling experiments.

Phenotypes of *sup35* mutant strains

The chromosomal *ade1-14* mutant gene allows the host strains to be tested for their phenotypes. [PSI^+] strain OT56 grows on SD-Ade medium and appears white on YPD medium, due to the partial read-through of the *ade1-14*, while [psi^-] strains OT60 and GT17 do not grow on SD-Ade medium and appear red on YPD medium. 1/4YPD was used in place of YPD to enhance color development of the red/white phenotypic screen. The *sup35::KanMX* strains (OT56k, OT60k, and GT17k) containing the NQ-replaced *sup35* mutant genes were tested for their phenotypes on SD-Ade and 1/4YPD media. When the plasmid pJET101 containing wild type *SUP35* gene was used as positive control, both prion and non-prion phenotypes were generated by the inheritance from the parent strains, with OT56k[pJET101] being white and OT60k[pJET101] being red on 1/4YPD. However, no prion-like phenotype was detected when the negative control plasmid pJET113, in which the NQ domain was deleted, was used.

Based on the phenotype assay, the substitutions can be divided into two classes (Table 2-4). The first class of substitutions resulted in strains showing only a single

Table 2-4. Phenotype characterization of *sup35* mutants.

Substitution	Viability	Phenotype(s)
AEAK	No	N/A
Aß(10-35)	Yes	Single
Switch 1	Yes	Single
Switch 2	Yes	Single
T20	Yes	Single
T40	Yes	Single
T60	Yes	Single
Q20	Yes	Single
Q40	Yes	Single
Q60	Yes	Multiple
TTR	Yes	Multiple
syn-1	Yes	Multiple
IAPP	Yes	Multiple
Switch 3	Yes	Multiple

phenotype, with the colonies usually showing light pink color on 1/4YPD medium. These substituions include T20, T40, T60, Q20, Q40, Aß(10-35), switch peptide 1, and switch peptide 2. The other class of substitutions caused more than one phenotype, with the colonies showing different colors on 1/4YPD medium. This class includes Q60, syn1, IAPP, TTR, and switch 3. The prion states of the parent strains had no effect on the phenotypes after plasmids shuffling, except for the substitution of Q60, where the prion-like phenotypes were inherited by Q60-containing strains.

Discussion

To substitute aggregation-prone peptide for the NQ domain of Sup35p, mutant genes were designed and the plasmids were constructed. These constructs not only allow evaluation of the effect of the substitutions, but they also serve as starting points to generate more substitution by simply designing and cloning the DNA at the appropriate sites, e.g. *Bam*H I/*Pst* I and *Bam*H I/*Pfl*M I sites. It might also be feasible to study a peptide library, for example, the structural permutations at specific sites within the switch peptides.

The AEAK peptide has been reported as a very potent aggregating peptide, and it possibly tends to aggregate in vivo. The aggregate itself should not be toxic enough to inhibit growth, as the strain expressing AEAK-Sup35 fusion protein can still survive. However, the aggregation might have abolished the terminator factor activity completely,

such that AEAK-Sup35 fusion protein cannot support the growth in the absence of native Sup35p. Therefore, cells would die if the aggregation tendency is too strong, although moderate aggregation tendency is essential for prion formation and propagation. Furthermore, some substitutions exhibited single phenotype, but it doesn't mean that they cannot be used. Some other cellular parameters, such as the expression level of Sup35 variants, might play critical roles and these would need to be modified. The yeast strains that exhibit multiple phenotypes suggested the possibility that they might exist in distinct prion and non-prion states. The first criterion, i.e., the spontaneous formation of phenotypes associated with these states, has been satisfied; however, this phenomenon cannot be assumed as conclusive for prion formation. Among these substitutions, the Syn1 and IAPP variants appeared to be the best candidates and were subjected to further characterization as described in more detail in Chapter 3 and 4, respectively.

CHAPTER 3

The Substitution of Alpha-Synuclein Fragment for the NQ Domain of Sup35p Generated Prion-Like Phenotypes

Introduction

Parkinson's disease is a progressive neurodegenerative disease that mainly affects elderly people, and its clinical characteristics include impaired movement and speech of the patients. The major disabling symptoms of Parkinson's disease are mainly due to the profound loss of neurons involved in dopamine release, a process essential for stimulating and coordinating the body's motor movements. Levodopa, the precursor of dopamine, has been used to ameliorate some symptoms. In addition to extensive loss of dopaminergic neurons, intracytoplasmic protein-containing inclusions called Lewy bodies are found in the patients (Giasson, 2004). Researchers have demonstrated that α-synuclein molecules are the major building blocks of the ~10-nm fibrils that form Lewy bodies (Goedert, 2001). Although its biological function has not been fully characterized, recent evidence suggests that α-synuclein may function as a molecular chaperone in the formation of SNARE complexes (Chandra et al., 2005). Normally a soluble monomeric protein, α-synuclein can be triggered to polymerize into insoluble

fibrils. Result from transgenic *Drosophila* and mouse models shows that the polymerization of α-synuclein into filaments, which eventually form large intracytoplasmic inclusions, can lead to the dysfunction of neurons and/or oligodendrocytes, the cells that help insulate neurons (Goedert, 2001).

In rare cases of familial forms of Parkinson's disease there is a mutation in the gene coding for α-synuclein. Three such point mutations, A53T, A30P, and E46K, have been identified in families with autosomal dominant Parkinson's disease thus far (Kruger et al., 1998; Polymeropoulos et al., 1997; Zarranz et al., 2004). In addition, triplication of α-synuclein gene has been found to cause Parkinson's disease in another lineage (Singleton et al., 2003). Both the wild type α-synuclein and the variants are able to form amyloid fibrils *in vitro*. Compared to the wild type α-synuclein, the mutants carrying the point mutations form amyloid fibrils more quickly (Greenbaum et al., 2005), which is consistent with the early onset of Parkinson’s disease.

A hydrophobic stretch of 12 amino acid residues in the middle of α-synuclein has been suggested to be essential for filament assembly (Giasson et al., 2001). It was noticed initially that α-synuclein was homologous in primary sequence to ß-synuclein. The intracellular concentration and localization of both proteins are very similar; however, ß-synuclein is absent in fibrillar pathological lesions while α-synuclein is abundant. Detailed analysis revealed that a hydrophobic stretch of amino acids (residues 71-82) in the middle of α-synuclein was lacking in ß-synuclein. Deletion of the hydrophobic fragment abolished the ability of α-synuclein to polymerize, whereas the

introduction of charged residues within the region (A76E, or A76R) significantly reduced the rate of filament formation. The synthetic peptide ^{71}*VTGVTAVAQKTV*^{82} was capable of polymerizing into filaments and inducing the assembly of full-length α-synuclein. Therefore, the hydrophobic fragment plays a very important role in the polymerization of α-synuclein (Giasson et al., 2001).

Because the α-synuclein fragment can polymerize and subsequently induce the assembly of the full-length protein, it would be potentially capable of replacing the NQ domain in Sup35p and serving as the aggregation unit. In this study, the fragment ^{65}*NVGGAVVTGVTAVA*^{78}, a larger peptide located in the middle of α-synuclein that encompasses the main fibrillogenic sequence ^{71}*VTGVTAVAQKTV*^{82}, is substituted for the NQ domain (Figure 3-1). The substitution leads to the appearance of two different phenotypes, suggesting the presence of prion formed by the Sup35 mutant. The charged residues are introduced at the position equivalent to Ala76 in wild-type α-synuclein to study the effect of such mutations on the formation of prion-like phenotypes *in vivo*.

Experimental Procedures

Plasmids and strains

The oligonucleotides, syn1-F and syn1-R, were designed such that (1) DNA generated by oligonucleotides annealing encoded for ^{65}*NVGGAVVTGVT***A***VA*^{78} (named as syn1 or syn1 peptide); (2) the annealing of the oligonucleotides would generate

Figure 3-1. Sequences of α-synuclein and Syn1-Sup35 mutant. The sequence of syn1 peptide is underlined.

α-synuclein:

1 MDVFMKGLSK AKEGVVAAAE KTKQGVAEAA GKTKEGVLYV

41 GSKTKEGVVH GVATVAEKTK EQVTNVGGAV VTGVTAVAQK

81 TVEGAGSIAA ATGFVKKDQL GKNEEGAPQE GILEDMPVDP

121 DNEAYEMPSE EGYQDYEPEA

Syn1-Sup35p:

Met-Ser-[syn1 peptide]-[NR domain]-[Sup35MC domain]

(syn1 peptide = NVGGAVVTGVTAVA)

overhangs at both ends of the DNA that were compatible with the *Bam*H I/*Pst* I digestion product; (3) for expression in yeast, the sequence encoding syn1 was optimized based on the codon usage. To anneal the DNA, the mixture of syn1-F and syn1-R was cooled down by 1 °C per 5 minutes from 99 °C to 30 °C. The annealed DNA was desalted by ethanol precipitation, phosphorylated with T4 kinase in the presence of ATP, and ligated into the *Bam*H I/*Pst* I-digested vector plasmid pZErO-1+NM. The generated plasmid pZErO-1+NM-syn1, which was confirmed by DNA sequencing, was subsequently used for subcloning syn1-NR fragment into pJET101 at *Bam*H I/*Pfl*M I sites, generating plasmid pJET101.syn1.

The charged residues were introduced at the Ala76 position by using site-directed mutagenesis via PCR. Forward primer M13R and reverse primer syn1-A76E (or syn1-A76R) were used to amplify the region flanking syn1 from the pZErO-1+NM.syn1 template. Because M13R primer binds to pZErO-1+NM.syn1 at the upstream of the *Bam*H I site, there is one *Bam*H I site within the PCR products. The PCR products also contain a *Pst* I site because of the inclusion of *Pst* I recognition sequence in the reverse primers. The PCR products were digested by *Bam*H I/*Pst* I and ligated into pZErO-1+NM at the *Bam*H I/*Pst* I sites, generating plasmids pJET117E and pJET117R. The mutations A76E and A76R were confirmed by DNA sequencing. The plasmids were then subcloned into pJET101 to make pJET101.syn1E and pJET101.syn1R, which put syn1A76E and syn1A76R in place of the NQ domain of Sup35, respectively.

Primers NM-GF and NM-GR were used to amplify the Sup35-NM gene, and the

PCR product was inserted into plasmids p316CUP1sGFP at *Bam*H I/*Sac* II sites, making the single-copy plasmid pJET84. The gene encoding for NM-GFP fusion protein, together with the promoter P_{CUP1}, was subcloned into the high-copy number plasmid pRS426 at *Xho* I/*Sac* I sites to make pJET108.WT. Subsequently, pJET108.WT was used to construct pJET108.syn1, pJET108.syn1E, and pJET108.syn1R by replacing the *Bam*H I/*Pfl*M I region flanking the NQ domain with syn1, syn1E, and syn1R, respectively.

Hsp104 gene was amplified from yeast genomic DNA using primers hsp2F and hsp2R, and the PCR product was digested with *Bam*H I/*Sac* I and cloned into p426CUP1 and p426ADH to generate pJET114 and pJET119, respectively. The gene encoding SsaI, a member of yeast Hsp70p family, was amplified from plasmid pJ120 using primers SsaI-F and SsaI-R. The PCR product was digested with *Bam*H I/*Sac* I and cloned into p426CUP1 and p426ADH to generate pJET122 and pJET123, respectively. The sequence of pJET114 was confirmed by terminal and internal DNA sequencing, using oligonucleotides CUP-F, his-1, his-2, his-3, and esp-r as the sequencing primers.

The expression plasmid for Sup35-NM protein, pJET154.WT, was made on the backbone of pET21a (Novagen). The gene encoding Sup35-NM protein was amplified using primers Colin-F and NM-GR. The PCR product was digested with *Sac* II, blunt-ended with Klenow, and digested with *Nde* I. Meanwhile, the vector pET21a was prepared by being digested with *Not* I, blunted-ended with Klenow, and digested with *Nde* I. These two compatible fragments were then ligated together to construct pJET154.WT, which was subsequently used to construct pJET154.syn1, pJET154.syn1E,

and pJET154.syn1R. After syn1, syn1E, and syn1R were amplified using primers syn1-NdeI-F and ColiN-R, they were cloned into pJET154.WT at *Nde* I/*Acc*65 I sites.

Unless specified, TOP10F' was used routinely as the host strain to carry out the molecular cloning. BL21[DE3] was used for the expression of the recombinant proteins in *E. coli*. Yeast strains GT17k, OT60, and OT56k were described in Chapter 2. Additional information is listed in Table 3-1 and 3-2.

Hsp104 gene knockout construction

Hsp104 gene knockout was conducted by transforming *hsp104::URA3*, amplified from the genomic DNA of strain 74-D694-Δsup35-Δhsp104 (74-D694, *sup35::TRP1* [*HIS3, SUP35*] *hsp104::URA3*) (Hara et al., 2003), into the desired prion strains and selecting the knockout strains on minimal medium lacking uracil. Firstly, the gene was amplified using primers hsp-F and hsp-R, and purified on an agarose gel. The linear DNA was then transformed into the competent cells of the desired yeast strains. The transformants were incubated in rich medium for 2 hours or overnight to allow the DNA recombination, and then spread on minimal medium without uracil for knockout selection. Colonies of cells with *hsp104::URA3* integration appeared in about 3 days, and they were further tested for *hsp104* deletion. PCR amplification of the chromosome containing wild type *HSP104* generates a ~3-kb product, whereas that of *hsp104::URA3* generates a ~4-kb product. In addition, the PCR product of *hsp104::URA3,* but not of *hsp104*, can be cut into two fragments by *Nco* I.

Table 3-1. Plasmids used in Chapter 3.

Plasmids	Characteristics	References
pZErO-1+NM	pZErO-1, *sup35-NM* pZErO-1 ← Sup35-NM PCR (*Bam*H I/*Xho* I)	Chapter 2
pZErO-1+NM .syn1	pZErO-1, *sup35-NM(Δ3-39::syn1)* pZErO-1+NM ← syn1 (*Bam*H I/*Pst* I)	Chapter 2
pJET101	pRS313, P_{SUP35}, *SUP35*	Chapter 2
pJET101.syn1	pRS313, P_{SUP35}, *sup35(Δ3-39::syn1)* pJET101 ← pZErO-1+NM.syn1 (*Bam*H I/*Pfl*M I)	Chapter 2
pJET117.E	pZErO-1+NM.syn1, A76E pZErO-1+NM ← syn1A76E (*Bam*H I/*Pst* I)	this study
pJET117.R	pZErO-1+NM.syn1, A76R pZErO-1+NM ← syn1A76R (*Bam*H I/*Pst* I)	this study
pJET101.syn1E	pRS313, P_{SUP35}, *sup35(Δ3-39::syn1A76E)* pJET101 ← pJET117.E (*Bam*H I/*Pfl*M I)	this study
pJET101.syn1R	pRS313, P_{SUP35}, *sup35(Δ3-39::syn1A76R)* pJET101 ← pJET117.R (*Bam*H I/*Pfl*M I)	this study
p316CUP1sGFP	pRS316, P_{CUP1}, sGFP	(Liu and Lindquist, 1999)
pJET84	pRS316, P_{CUP1}, sup35NM-GFP p316CUP1sGFP ← sup35NM PCR (*Bam*H I/*Sac* II)	this study
pJET108.WT	pRS426, P_{CUP1}, sup35NM-GFP pRS426 ← pJET84 (*Xho* I/*Sac* I)	this study
pJET108.syn1	pRS426, P_{CUP1}, sup35NM*(Δ3-39::syn1)*-GFP pJET108.WT ← pJET101.syn1 (*Bam*H I/*Pfl*M I)	this study
pJET108.syn1E	pRS426, P_{CUP1}, sup35NM*(Δ3-39::syn1E)*-GFP pJET108.WT ← pJET101.syn1E (*Bam*H I/*Pfl*M I)	this study
pJET108.syn1R	pRS426, P_{CUP1}, sup35NM*(Δ3-39::syn1R)*-GFP pJET108.WT ← pJET101.syn1R (*Bam*H I/*Pfl*M I)	this study
pJET114	pRS426, P_{CUP1}, *HSP104* p426-P_{CUP1}-Sup35NM-GFP ← Hsp104 PCR (*Bam*H I/*Sac* I)	this study

Plasmids	**Characteristics**	**References**
pJET119	pRS426, P_{ADH}, *HSP104* p426ADH ← pJET114 (*Bam*H I/*Sac* I)	this study
pJ120	pRS315, *SSAI*	(Jones and Masison, 2003)
pJET122	pRS426, P_{CUP1}, *SSAI* p426-P_{CUP1}-Sup35NM-GFP ← pJ120 PCR (*Bam*H I/*Sac* I)	this study
pJET123	pRS426, P_{ADH}, *SSAI* p426ADH ← pJ120 PCR (*Bam*H I/*Sac* I)	this study
pET21a	*E. coli* expression vector, C-terminal 6xHis tag	Novagen
pJET154.WT	pET21a, *sup35-NM-(His)$_6$* pET21a ← Sup35 PCR	this study
pJET154.syn1	pET21a, *sup35-NM(Δ3-39::syn1)-(His)$_6$* pJET154.WT ← syn1 PCR (*Nde* I/*Acc*65 I)	this study
pJET154.syn1E	pET21a, *sup35-NM(Δ3-39::syn1E)-(His)$_6$* pJET154.WT ← syn1E PCR (*Nde* I/*Acc*65 I)	this study
pJET154.syn1R	pET21a, *sup35-NM(Δ3-39::syn1R)-(His)$_6$* pJET154.WT ← syn1R PCR (*Nde* I/*Acc*65 I)	this study
p306-α-syn (WT)-GFP	pRS306, P_{GAL1}, α-synuclein-GFP	(Outeiro and Lindquist, 2003)
p306-α-syn (A30P)-GFP	pRS306, P_{GAL1}, α-synuclein(A30P)-GFP	(Outeiro and Lindquist, 2003)
p306-α-syn (A53T)-GFP	pRS306, P_{GAL1}, α-synuclein(A53T)-GFP	(Outeiro and Lindquist, 2003)

Table 3-2. The oligonucleotides used in Chapter 3.

Name	Sequence
syn1-F	5’-*GATCC*AACAATGTCTAACGTTGGTGGTGCTGTTGTTACTGGTGTTACT GCTGTTGCTCAAC*CTGCA*-3’
syn1-R	5’-GGTTGAGCAACAGCAGTAACACCAGTAACAACAGCACCACCAACGT TAGACATTGTTG-3’
M13R	5’-GGCAGGAAACAGCTATGACC-3’
syn1-A76E	5’-C*CTGCAG*GTTGAGCAACTTCAGTAA-3’
syn1-A76R	5’-C*CTGCAG*GTTGAGCAACTCTAGTAA-3’
hsp2F	5’-TCA*GGATCC*AACAATGAACGACCAAACGCA-3’
hsp2R	5’-TG*GAGCTC*TTAATCTAGGTCATCATC-3’
SsaI-F	5’-TCAGGATCCAACAATGTCAAAAGCTGTCGG-3’
SsaI-R	5’-TGGAGCTCTTAATCAACTTCTTCAAC-3’
CUP-F	5’-GCGTCTTTTCCGCTGAACCG-3’
his-1	5’-CTGTCATCGGCCGTGAAGAA-3’
his-2	5’-TTGAGAGGTCTGCAACCAAA-3’
his-3	5’-GCTTGAAGATCAGGTTGCTG-3’
esp-r	5’-GCTTAATGCGCCGCTACAGG-3’
hsp-F	5'-GGGGTCGACATGAACGACCAAACGCAATTT-3'
hsp-R	5'-GGGGTCGACTTTTAGATTATTCACAGC-3'
Gal-F	5’-AATATACCTCTATACTTTAACGTC-3’
Cyc-R	5’-CACCGCTGGTAGCGGTGGT-3’

Synuclein-GFP integration

The genes encoding for the full length α-synuclein-GFP fusion protein were integrated into the chromosome of desired yeast strains. The integrative plasmids containing α-synuclein-GFP, α-synuclein(A30P)-GFP, and α-synuclein(A53T)-GFP genes under the P_{GAL1} promoter have been described previously (Outeiro and Lindquist, 2003). They were transformed into [*syn1*$^{-}$] and [*SYN1*$^{+}$], the syn1-substituted sup35 strains without and with syn1 prions, respectively. OT56k/pJET101 was transformed as the negative control. Cells were allowed to grow in rich medium overnight after the transformation to enhance the chromosomal integration. Colonies that grew on SD-Ura medium were then used to extract the genomic DNA, and the correct integration was confirmed by the presence of the 1.5-kb product when the genomic DNA was used as the PCR template and Gal-F and Cyc-R were used as PCR primers.

Fluorescence microscopy

Depending on the promoters, GFP fusion proteins were induced in the presence of copper or galactose, and the cells was inspected under the fluorescence microscopy. For P_{CUP1}-promoted genes, 50 μM $CuSO_4$ was added in the medium when the cell density reached about 1 OD_{600}. For P_{GAL1}-promoted genes, cells were grown in medium containing 2% glucose to mid-log phase, and switched into the medium containing 2% raffinose and 2% galactose to induce the expression. The culture was incubated to stationary phase and subject to the observation under the fluorescence microscopy.

Culture in minimal medium was spotted on slides directly; however, cells grown in YPD medium were washed and resuspended in distilled water or PBS buffer, because YPD medium showed a high fluorescence background.

In vitro study of syn1-NM aggregation

The expression and purification of syn1-NM and its variant proteins were conducted according to the procedure described previously (Chernoff et al., 2002). *E. coli* strain BL21[DE3] was used as the expression host strain because contains a [DE3] lysogen for a high-level expression of T7 polymerase following induction with IPTG. To induce expression, cells were grown until an OD600 of 0.8 was reached. IPTG was added to a final concentration of 0.8 mM, and cells were incubated for an additional 3 hr at 37 °C. Culture was harvested by centrifugation (3000 x g, 10 min, 4 °C). Proteins were purified by affinity column because of the C-terminal 6xHis tag under denatured condition. After washing, proteins were eluted from Ni-NTA column and purified again using DEAE column. Protein was then methanol precipitated and resuspended in 6 M GuHCl overnight to disaggregate preformed polymers. To initiate the fiber formation, protein was diluted by at least 100 times to the Congo red binding buffer (CRBB) to a final concentration of 2.5 μM. Fibers formed by the protein was negatively stained with uranyl acetate and observed using transmission electron microscopy (TEM).

Results

Cells containing the *syn1-sup35* mutant gene showed two prion-like phenotypes

The plasmid pJET101.syn1 was constructed such that syn1, a peptide fragment from α-synuclein, was substituted for the NQ domain of Sup35. Furthermore, the *syn1-sup35* mutant gene was placed under P_{SUP35}, the native promoter for Sup35p, on a single-copy plasmid to ensure that the protein would be expressed in a similar level as Sup35p in wild type strains. Wild type *SUP35* gene has been replaced by the *syn1-sup35* fusion gene through plasmid shuffling in yeast cells. OT60k ([*psi*$^-$], [*PIN*$^+$]) containing wild type *SUP35* gene on plasmid p316SpSup35 was transformed with pJET101.syn1, and the transformants that had lost the wild type SUP35 gene were counter-selected with 5-FOA. The correct gene replacement was confirmed by the inability of the cells to grow on SD-Ura. Additionally, plasmids prepared from the cells with gene replacement were confirmed by PCR and DNA sequencing.

After the plasmid shuffling, almost all the yeast cells containing *syn1-sup35* gene (OT60k[pJET101.syn1]) were white on YPD medium plate. Under careful visual inspection, some tiny red sectors were observed on the edge of the white cell streaks. By restreaking the cells from the red edge to a new YPD plate repeatedly, red cells were enriched from the red-and-white mixture to pure red single colonies. The white cells, but not the red cells, were able to grow on the minimal medium lacking adenine (SD-Ade) (Figure 3-2). These two phenotypes resembled those exhibited by [*psi*$^-$] and [*PSI*$^+$]

Figure 3-2. Phenotypes exhibited by [*syn1*$^-$] and [*SYN1*$^+$] strains. [*syn1*$^-$] and [*SYN1*$^+$] strains (top and bottom sector) growing on (A) 1/4YPD medium plate and (B) SD-Ade medium plate.

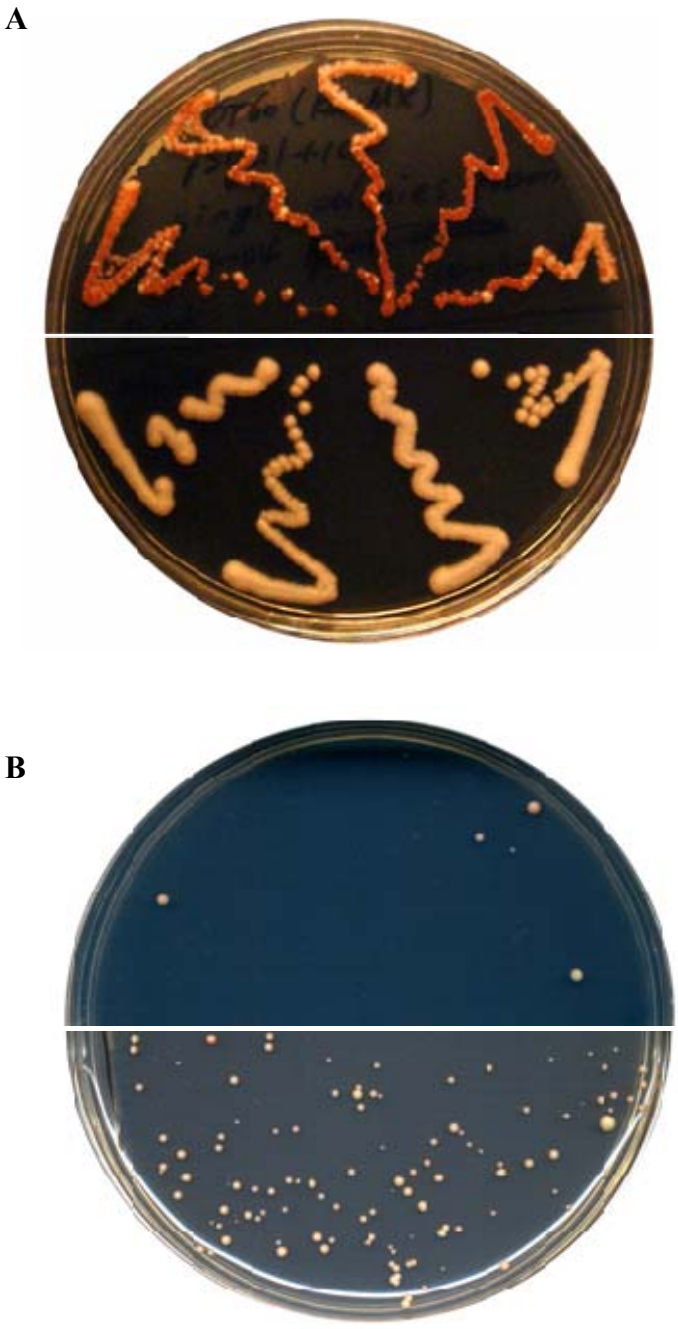

strains, which suggested that they might be the non-prion and prion forms of the strain OT60k[pJET101.syn1]. Following the nomenclature of native prions, the red and white cells containing *syn1-sup35* have been named as [*syn1*$^{-}$] and [*SYN1*$^{+}$], respectively.

Unlike [*psi*$^{-}$] cells, which are stable and only convert to [*PSI*$^{+}$] spontaneously at a low rate of 10^{-6}, [*syn1*$^{-}$] cells converted to [*SYN1*$^{+}$] at a uncommonly high rate that was estimated to be about 13% (Figure 3-3). Similarly, although [*syn1*$^{-}$] cells grew poorly on SD-Ade compared to the [*SYN1*$^{+}$] counterparts, they grew much better than [*psi*$^{-}$] cells. On the other hand, [*SYN1*$^{+}$] cells, like [*PSI*$^{+}$] cells, are very stable, and the rate of their conversion to [*syn1*$^{-}$] is too low to be measured.

GT17k ([*psi*$^{-}$], [*pin*$^{-}$]) and OT56k ([*PSI*$^{+}$], [*PIN*$^{+}$]) were used as to study the effect of [*PSI*$^{+}$] and [*PIN*$^{+}$] prions on the formation of the possible Syn1-Sup35 prion. Similarly as above, GT17k and OT56k strains harboring pJET101.syn1 were constructed through plasmids shuffling. The subsequent strains were similar, indicating that the formation of Syn1-Sup35 prion was not affected by heterologous prions [*PSI*$^{+}$] and [*PIN*$^{+}$].

The mutations A76E and A76R stabilized the non-prion state of Syn1-sup35p

Based on the finding that the mutations A76E and A76R decreased the rate of aggregation of the α-synuclein ^{71}*VTGVT***A**̲*VAQKTV*^{82} peptide, the mutations were introduced in the syn1-sup35 gene at the position related to Ala76 in α-synuclein. Through plasmid shuffling, syn1A76E-sup35 and syn1A76R-sup35 were substituted for SUP35 in OT60k. Like syn1-sup35, both A76E and A76R showed two phenotypes, red

Figure 3-3. Estimation of the frequency in the conversion from [*syn1*$^-$] to [*SYN1*$^+$] cells. Among ~135 total [*syn1*$^-$] cells spread on 1/4YPD medium, ~17 colonies became white, suggesting a conversion rate of ~13%.

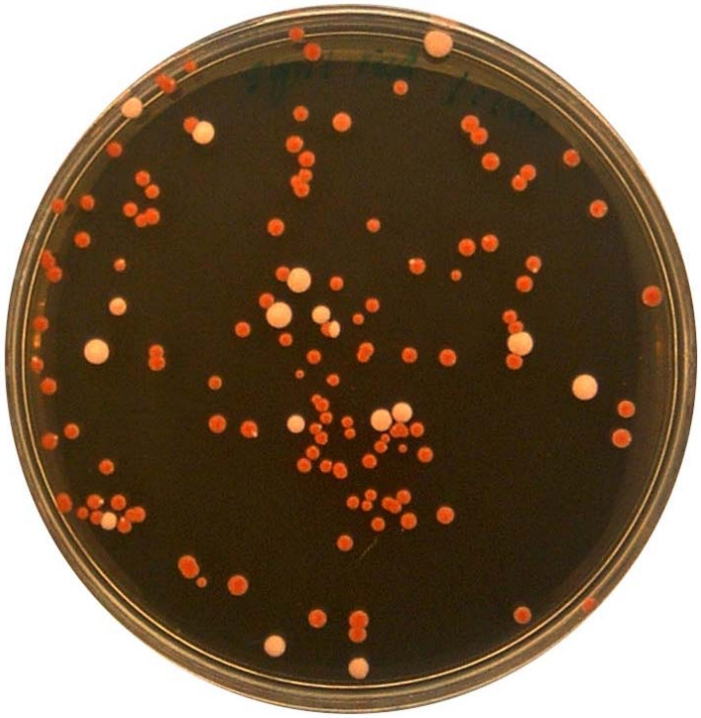

and white on YPD medium. They have been similarly named as [*syn1e*$^-$], [*SYN1E*$^+$], [*syn1r*$^-$], and [*SYN1R*$^+$] to represent the different phenotypes. Compared to [*syn1*$^-$] that was very unstable, [*syn1e*$^-$] and [*syn1r*$^-$] were stable as no spontaneous conversion to the prion phenotype were observed. The prion form [*SYN1E*$^+$] and [*SYN1R*$^+$] were also stable; however, the color of [*syn1e*$^-$] and [*syn1r*$^-$] cells were lighter than [*syn1*$^-$] ones, for reasons that are still unknown (Figure 3-4).

Wild type SUP35 restored the red phenotype when reintroduced into [*SYN1*$^+$]

As described previously, [*psi*$^-$] cells with *ade1* mutations are red on YPD medium because a pigment accumulates during growth without active Ade1p protein. To exclude the possibility that [*syn1*$^-$] cells turn white on YPD due to the reversion of the *ade1-14* mutation, [*SYN1*$^+$] was assayed for the integrity of *ade1*. Plasmid p316SpSup35 was transformed back into [*SYN1*$^+$], and the transformants that contain p316SpSup35, but has lost pJET101.syn1 spontaneously, were identified by their inability to grow on SD-His medium. The cells, when growing on YPD medium, showed the red color that was indistinguishable from the original OT60k/p316SpSup35. The red phenotype was restored by the reintroduction of wild type SUP35, which suggests that the white phenotype was not due to the reversion of *ade1*, and supports the explanation that it was due to the formation of Syn1-Sup35 prion aggregates.

Figure 3-4. Different phenotypes exhibited by Syn1-Sup35 proteins with A76E and A76R mutations. Compared to Syn1-Sup35p, the non-prion state of the mutant proteins are more stable, as no significant conversion to white colonies is observed.

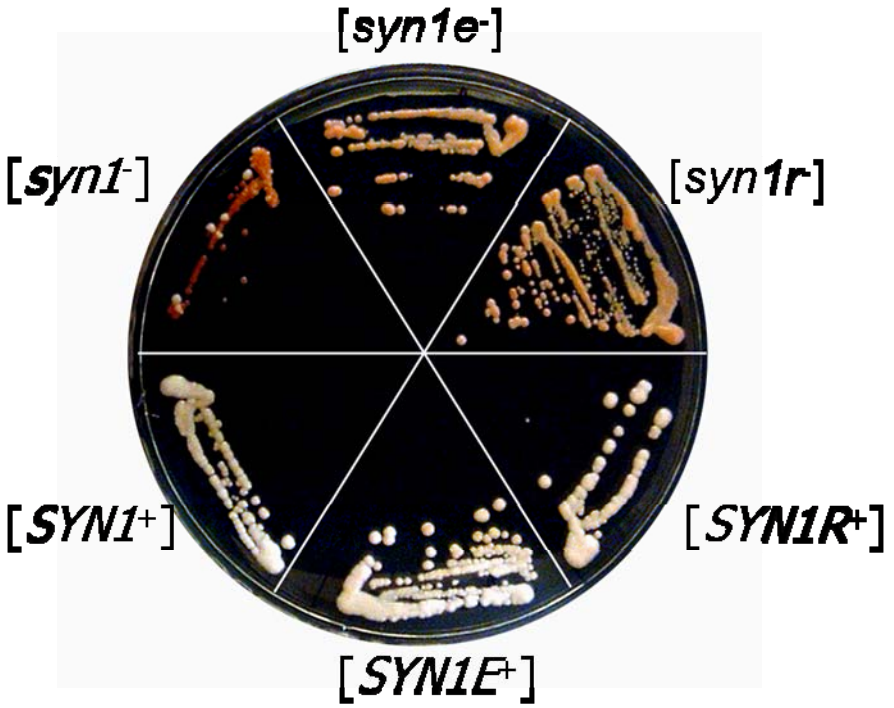

The effect of molecular chaperones on [*SYN1*$^+$]

GuHCl has been commonly used as a reagent to cure prions in yeast. [*SYN1*$^+$] was cultured on YPD medium plates containing 5 mM GuHCl for 3 consecutive times, and cells were streaked on YPD to assay for their phenotypes. No curing was observed, as all the cells remained white on YPD medium plates. As it has been suggested that GuHCl cures prions by inhibiting Hsp104p, the deletion of *hsp104* can be a further step to GuHCl. The *hsp104* gene was knocked out from [*SYN1*$^+$]. The cells still remained white. As a control, [*PSI*$^+$] was cured completely by *hsp104* deletion. The overexpression of Hsp104p, which is usually able to cure yeast prions, showed barely an effect on the curing of [*SYN1*$^+$]. Like [*SYN1*$^+$], [*SYN1E*$^+$] and [*SYN1R*$^+$] were hardly affected by GuHCl treatment, *hsp104* deletion, or Hsp104p overexpression.

The effect of SsaI, a member of Hsp70p family, on the prion-like strains expressing Syn1-substituted Sup35p or its A76E and A76R derivatives was studied. *SSAI* gene was cloned on the expression plasmids under P_{CUP1} or P_{ADH} promoters for inducible or constitutive overexpression, respectively. No significant effect were observed when SsaI protein was overexpressed in [*SYN1*$^+$], [*SYN1E*$^+$] and [*SYN1R*$^+$] strains.

Overexpression of Syn1-M-GFP caused diffuse fluorescence.

As a reporter protein, GFP was constructed as a fusion protein, following the Sup35 M domain and replacing the Sup35 C domain. When overexpressed under the $CuSO_4$ induction in [*SYN1*$^+$] cells, Syn1-NR-M-GFP showed diffuse fluorescence (Figure 3-5).

Figure 3-5. Fluorescence images of [*SYN1*$^{+}$] cells expressing Syn1-M-GFP. The fusion protein of the prion-forming domain and GFP were induced with the addition of $CuSO_4$ (50 μM).

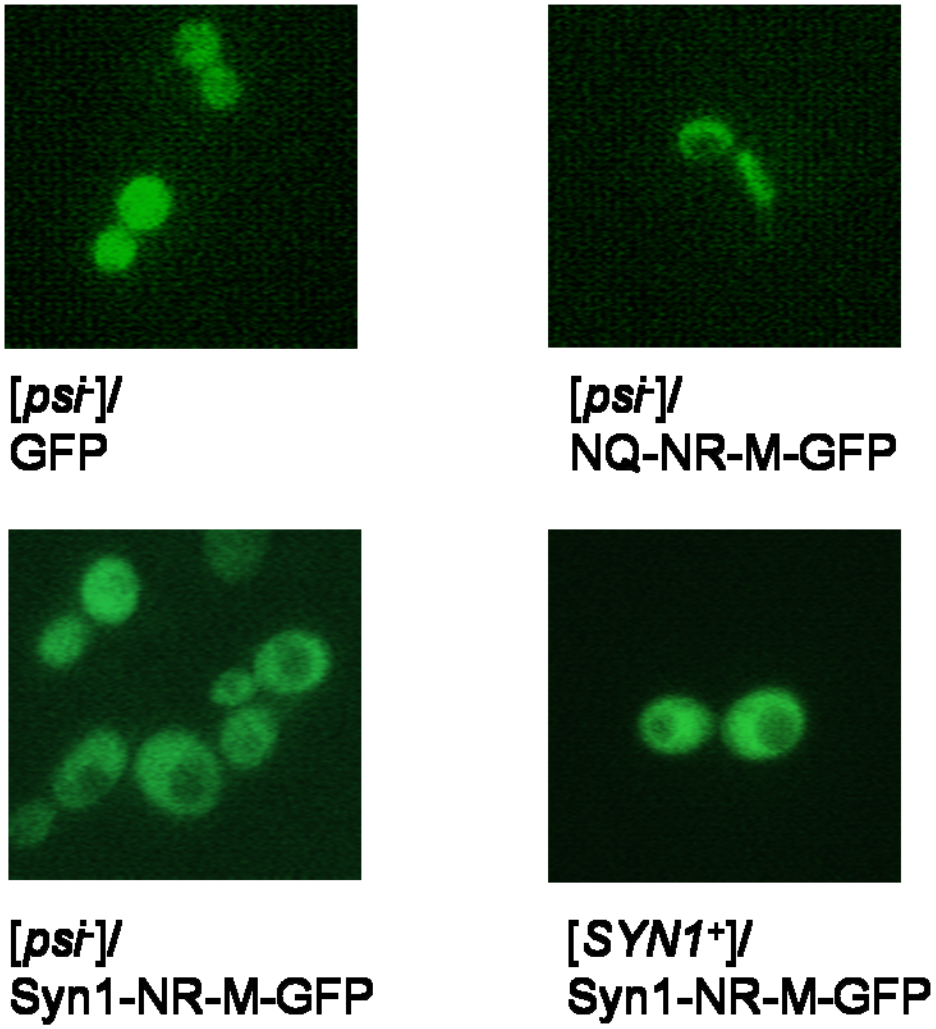

Similar results were observed when it was expressed in [*psi*$^-$] control strain. The assay in [*syn1*$^-$] strain could not be conducted because [*syn1*$^-$] cells turned to [*SYN1*$^+$] too frequently. The fluorescence of Syn1-NR-M-GFP proteins with A76E or A76R mutations was also diffuse, regardless of the genetic background of the host strains.

To test whether the formation of [*SYN1*$^+$] prion can be induced by overproducing Syn1-NR-M-GFP, which contains the prion forming domain, the fusion protein was overexpressed in [*syn1*$^-$] cells. However, due to the high frequency of the spontaneous conversion, it could not be determined whether the conversion rate was affected. Prion induction through overexpression of A76E and A76R mutated Syn1-NR-M-GFP was conducted in [*syn1e*$^-$] and [*syn1r*$^-$] cells, respectively, and no induction effects were observed. Furthermore, Syn1-NR-M-GFP and its derivatives did not induce prion formation from [*psi*$^-$] strain when overexpressed.

Syn1 prions caused the aggregation of full-length α-synuclein.

The plasmids encoding α-synuclein-GFP fusion proteins (wild type α-synuclein and its A30P and A53T mutants) were integrated into the genome of [*syn1*$^-$] and [*SYN1*$^+$] strains. OT56k[pJET101.WT] strain (*SUP35*, [*PSI*$^+$]) was used as a control without *syn1-sup35* gene. The expression of α-synuclein-GFP fusion was induced by switching the culture from glucose to galactose. In the control strain, diffuse fluorescence was observed in the cytoplasm and more concentrated fluorescence within the cell membrane. However, in both [*syn1*$^-$] and [*SYN1*$^+$] strains that contain *syn1-sup35* gene, punctate

Figure 3-6. Fluorescence image of cells expressing α-synuclein-GFP fusion proteins.

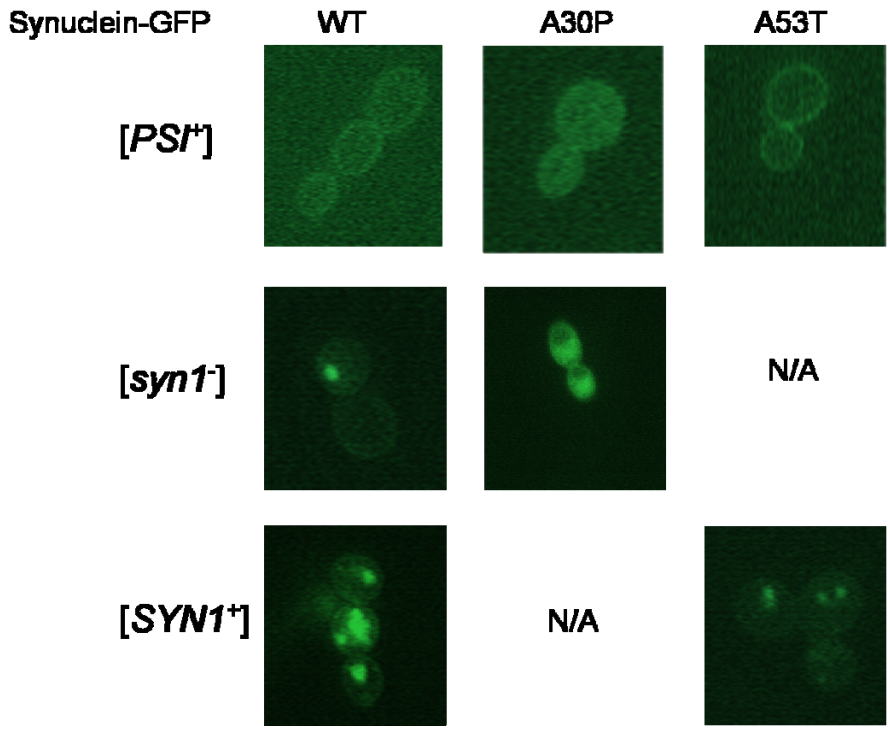

fluorescence were observed, indicating that α-synuclein-GFP formed aggregates (Figure 3-6). This observation suggests that Syn1 peptide aggregates can serve as the template for the aggregation of full-length α-synuclein *in vivo*, a process that has been observed in previous *in vitro* studies (Giasson et al., 2001).

Syn1-substituted Sup35NM protein formed amyloid fibers *in vitro*

To test whether syn1-substituted Sup35NM (syn1-NM) can form amyloid fibers *in vitro*, the recombinant proteins were expressed in *E. coli*. Purified proteins formed two bands on SDS-PAGE gel (Figure 3-7). The major band was located at a size (36kD) higher than the calculated molecular weight of Syn1-NM (27kD) because the protein consists of many positively charged residues. The appearance of the lower band (16kD) was unlikely due to contamination or degradation, because only the peaks representing the correct product were present when protein was checked by MALDI mass spectrometry (Figure 3-8). Purified protein was able to form amyloid fibers, as observed in transmission electron microscope (TEM) (Figure 3-9).

Discussion

According to the domain analysis of Sup35p, the NQ domain is rich in Asn/Gln residues and acts mainly as the aggregation unit (Osherovich et al., 2004). The modular domain structure of Sup35p makes it possible to construct fusion proteins that can

Figure 3-7. Purification of Syn1-NM expressed in *E. coli*. Syn1-NM was purified on Ni-NTA column and fractions were loaded on SDS-PAGE gel. Lane M, Protein marker; 1, total protein; 2, cell debris; 3, flow through; 4 and 5, washing; 6, elution.

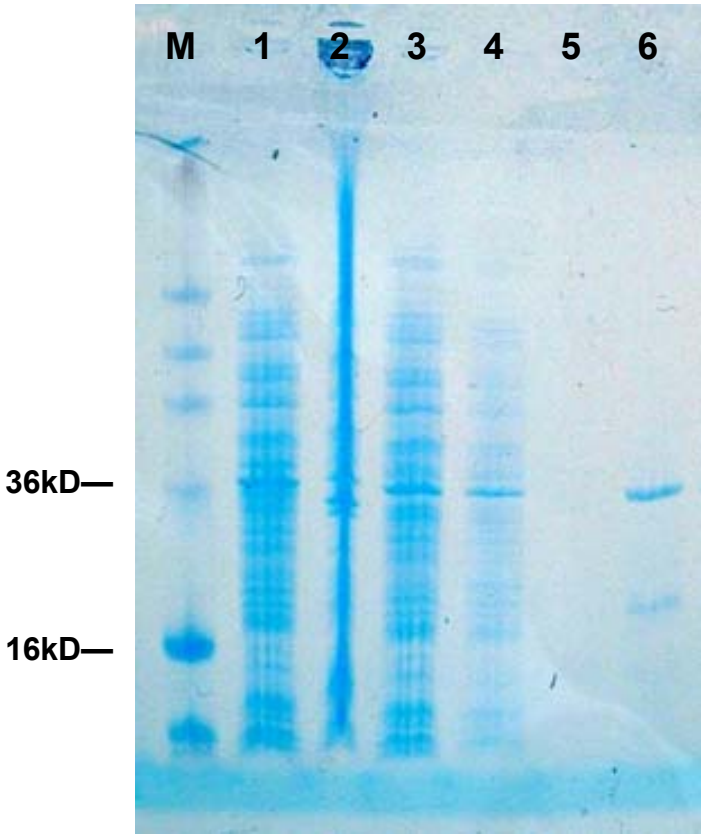

Figure 3-8. MALDI-TOF mass spectrum of purified Syn1-NM protein. Cal. MW. of Syn1-NM, 26941.

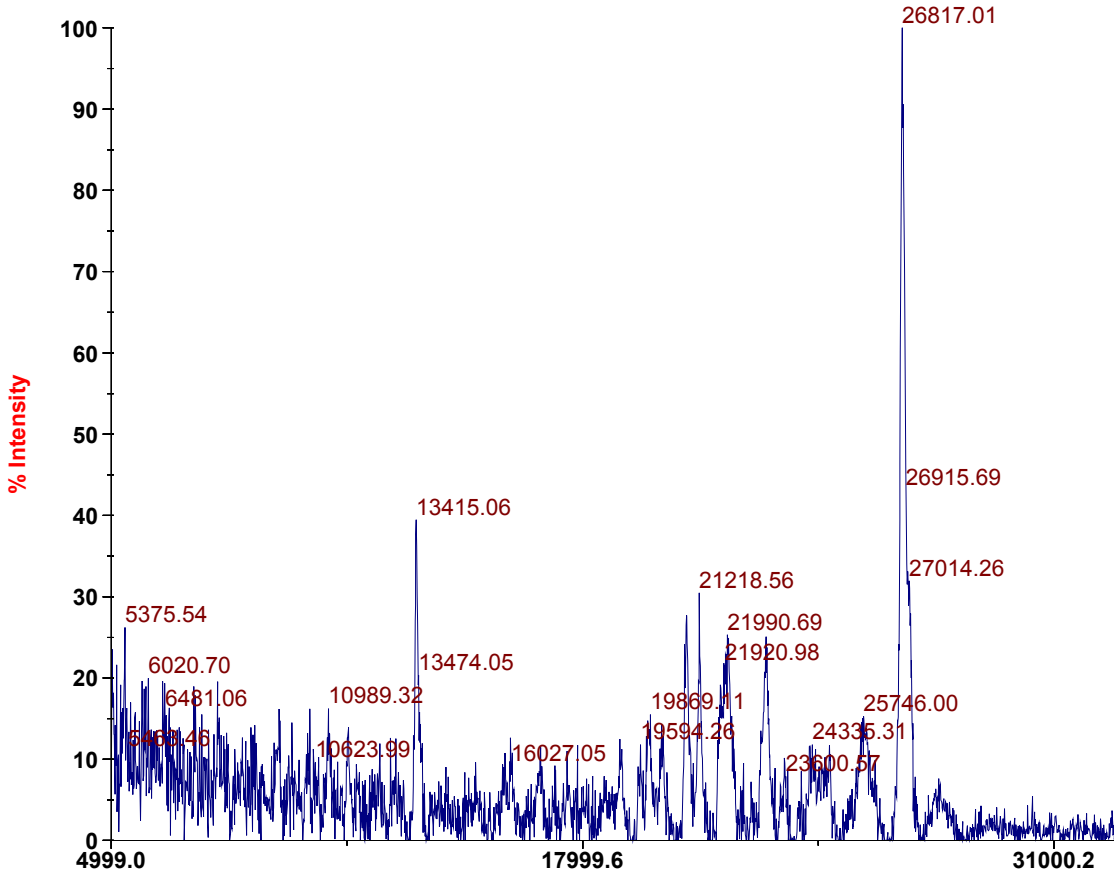

Figure 3-9. Electron microscopy of fibers formed by Syn1-NM.

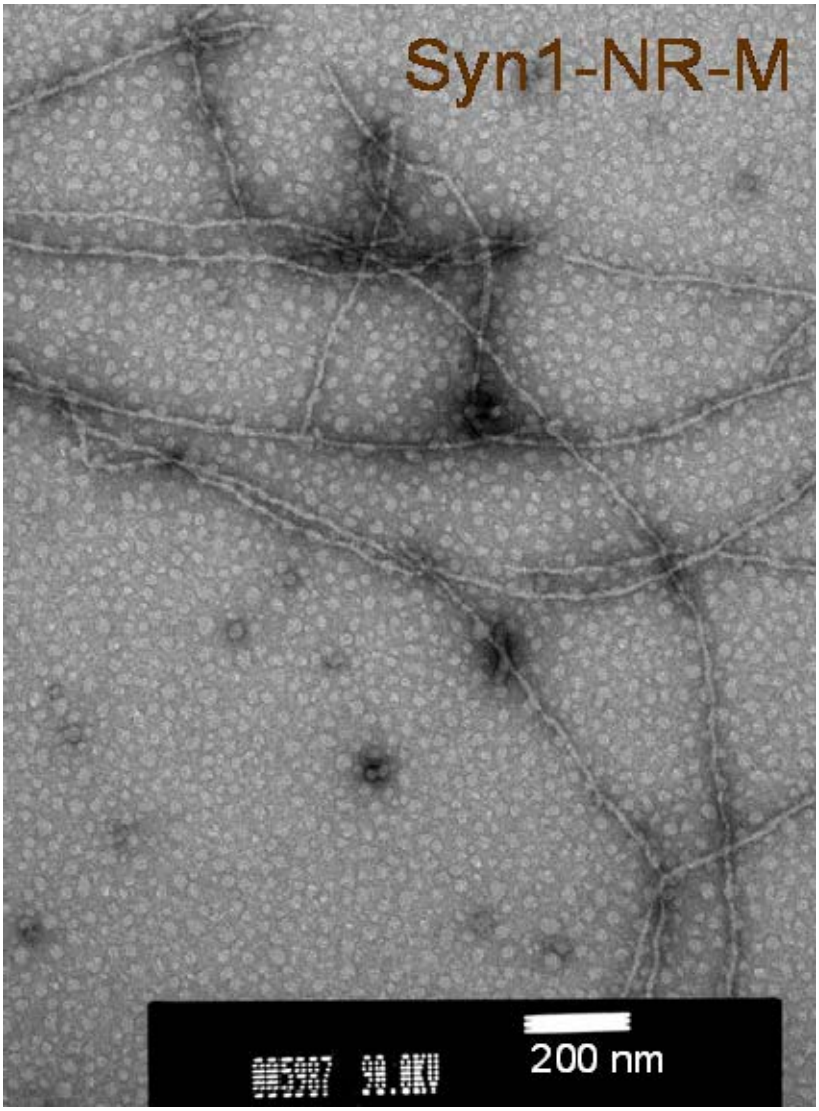

potentially form novel prions by replacing the NQ domain with other aggregation-prone proteins. α-synuclein, the component protein of Parkinson's disease, aggregates into fibrils that form Lewy body in the patients (Goedert, 2001). Instead of the entire α-synuclein coding sequence, which is 140-residue in length, the ^{65}*NVGGAVVTGVT***A**^{78} peptide stretch was substituted for the NQ domain to construct the Sup35 mutants. The selection of the fragment was mainly based on its proximity to ^{71}*VTGVT***A**^{82}, a peptide stretch that was shown to be capable of forming amyloid fibrils and assisting the aggregation of the full-length α-synuclein (Giasson et al., 2001).

The strains containing the *syn1-sup35* mutant gene are able to exhibit two distinct phenotypes, as monitored by the color assay on YPD medium and the growing assay on SD-Ade minimal medium. Because two phenotypes are shown by the cells in the same genotype, it is very likely that the different phenotypes result from the different conformation of the same protein, Syn1-Sup35p. Although alternative mechanisms may also be plausible, such as the spontaneous change in genotype and the fluctuation of protein expression level, no mechanism can better explain the result than the occurrence of prion phenomenon. For example, one can argue that the change in the phenotype is due to the reversion mutation in *ade1-14* gene that recovers the ability of cells to synthesize the full-length Ade1p protein. However, the very high rate (~13%) in the spontaneous conversion from [*syn1*$^-$] to [*SYN1*$^+$] can hardly be explained by a reversion mutation that usually happens at a low frequency. In addition, it has been shown that the [*SYN1*$^+$] cells can be restored to the red colonies on YPD when the wild type Sup35 is

transformed back. These results suggest that the reporter system, including *ade1-14* and related proteins, has remained the same during the phenotype change. Furthermore, there are no mutations in the gene encoding for the Syn1 fragment either, as shown by the DNA sequencing of the plasmids prepared from [*syn1*$^-$] and [*SYN1*$^+$] cells subsequent to transformation into yeast (data not shown). On the other hand, the fluctuation of the protein expression could have caused the phenotype change not only from [*syn1*$^-$] to [*SYN1*$^+$], but in both directions. Experimentally, the semi-quantification of Syn1-Sup35p showed that their concentration is similar in [*syn1*$^-$] and [*SYN1*$^+$] cells (Figure 3-10). Therefore, it is most likely that the phenotypes are caused by prion formation.

A76E and A76R are the mutations that have been shown to slow the aggregation of the peptide stretch from α-synuclein. It was proposed that the hydrophobic residue Ala76 was important for the aggregation. When Syn1-Sup35 containing A76E or A76R mutation was substituted for wild type Sup35, cells showed prion-like phenotypes like Syn1-Sup35 did. Interestingly, the non-prion cells were very stable as no substantial spontaneous conversion to prion was found. The effect of the mutations on the stability of the non-prion phenotypes is in consistence to the previously reported aggregating propensity of the peptides. Because the syn1 peptide, in place of the NQ domain, is acting as the aggregation unit for prion propagation, it is reasonable to suggest that mutations that hinder the aggregation *in vitro* are able to decrease the rate of spontaneous formation of prions *in vivo*. *In vitro*, the mutations increase the lag phase of the fibril formation possibly because of the increased energy barrier in the initial formation of

Figure 3-10. Sedimentation assay of proteins from [*syn1*$^-$] and [*SYN1*$^+$] cells.

Proteins were assayed using dot blotting and were detected by anti-Sup35 antibody. Proteins were serial diluted and spotted on the membrane, with the first row representing the samples with the original concentrations. 1, [*syn1*$^-$] supernatant; 2, [*syn1*$^-$] pellet; 3, Sup35NM control; 4, [*SYN1*$^+$] supernatant; 5, [*SYN1*$^+$] pellet; 6, [*syn1*$^-$] total; 7, [*SYN1*$^+$] total.

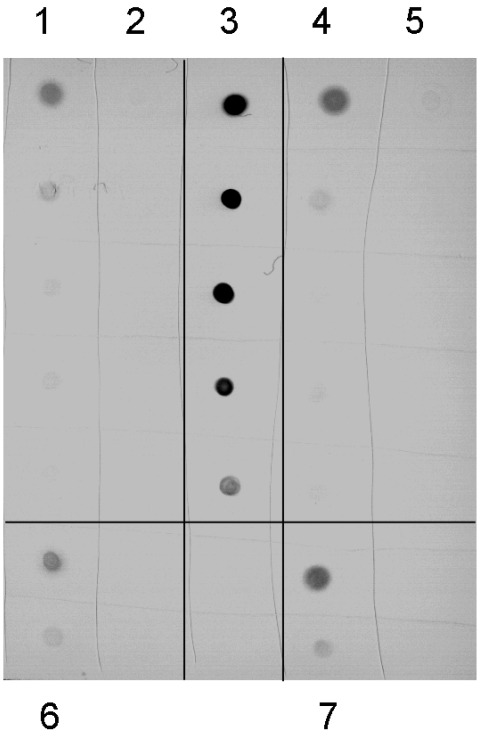

protein aggregates. *In vivo,* the *de novo* formation of prion also involves the formation of the prion particles from the soluble proteins. The result shows the potential of yeast prions to be useful in exploring the tendency of different proteins to aggregate.

GuHCl, a potent inhibitor of the molecular chaperone Hsp104p, did not cure [*SYN1*$^{+}$], consistent with the finding that [*SYN1*$^{+}$] was not be cured when *hsp104* was deleted. Hsp104p overexpression also had no effect on [*SYN1*$^{+}$] strains. Although all naturally formed yeast prions require Hsp104p for propagation, a yeast prion that was independent on Hsp104 has been reported previously (Crist et al., 2003). The independence of [*SYN1*$^{+}$] on Hsp104, together with the diffuse fluorescence seen when Syn1-M-GFP was overexpressed, also combined with the distribution of all the Syn1-Sup35 protein into the supernatant portion in the sedimentation assay, lead to a model that attempts to explain the mechanism involved in the unusual inheritance of [*SYN1*$^{+}$] prion (Figure 3-11). The model is based on the proposal that large aggregates are dead-end products (Ripaud et al., 2003), and it hypothesizes that the prion particles formed by Syn1-Sup35p can not form large aggregates *in vivo*. When Syn1-M-GFP fusion proteins are incorporated into preformed Syn1-Sup35 prion particles, or when they form prion particles alone, the prion particles do not apparently aggregate into higher order assemblies. Therefore, no fluorescence foci can be observed by fluorescence microscopy. As another consequence of this inability to form larger aggregates, Syn1 prion particles can be easily disaggregated into smaller ones that can template the prion growth. Therefore, there might be more prion particles in [*SYN1*$^{+}$] strain than in [*PSI*$^{+}$] or

Figure 3-11. A model attempting to explain the mechanism involved in the unusual inheritance of [*SYN1*$^+$] prion. In [*PSI*$^+$] prion cells, prion particles further aggregate into large complexes that cannot incorporate soluble proteins as templates. The larger complexes appear as the fluorescence foci under microscope. In [*SYN1*$^+$] prion cells, prion particles do not form larger aggregates, as suggested by the diffuse fluorescence, and they can be disaggregated to generate more seeds, which makes [*SYN1*$^+$] prion not curable by GuHCl.

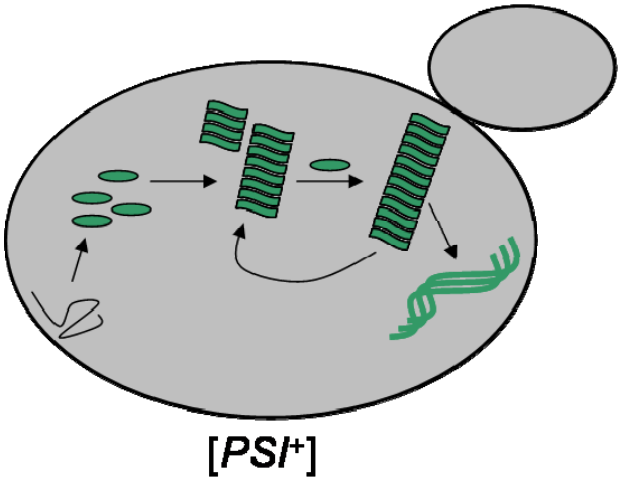

other prion strains. The number of the prion particles might be so high that they can propagate efficiently without the assistance of Hsp104 chaperone, which explains why *hsp104* deletion or GuHCl treatment do not cure [*SYN1*$^{+}$]. The reason why Hsp104 overexpression can not cure [*SYN1*$^{+}$] might just be the high tendency of prion formation by Syn1-Sup35. Even if [*SYN1*$^{+}$] prion particles were disaggregated completely to the monomeric proteins by Hsp104 chaperone, they would be able to form prions again promptly.

CHAPTER 4

The Substitution of Islet Amyloid Polypeptide (IAPP) Fragment for the NQ Domain of Sup35p Generated a Novel Prion

Introduction

Type II (non-insulin-dependent) diabetes is the most common form of diabetes and affects a great number of people in the world. In Type II diabetes, the cells do not respond appropriately to insulin, which causes accumulation of glucose in the blood instead of entry into cells. Type II diabetes is a chronic, progressive disease that has no medical cure, and it is often associated with obesity, hypertension, and elevated cholesterol. Islet amyloid polypeptide (IAPP), or amylin, was originally discovered as amyloid occurring in human insulinomas and pancreases from Type II diabetic patients in the 1980s. The normal expression of IAPP in beta cells has been suggested to be beneficial for beta-cell function and survival (Gebre-Medhin et al., 2000); however, an aggregated but not necessarily fibrillar form of IAPP is toxic in cell culture, suggesting that prefibrillar oligomeric (protofibrillar) IAPP may be pathogenic. The toxicity of protofibrillar IAPP was proposed as the ability to permeabilize cell membranes. Protofibrillar IAPP was able to permeabilize synthetic vesicles by a pore-like mechanism

(Anguiano et al., 2002). The protofibrillar IAPP oligomers that form *in vitro* can grow into fibrils that are rich in ß-sheet structure.

Human IAPP is a short peptide consisted of 37 residues (Figure 4-1). Interestingly, despite the sequence homology among the IAPPs in different mammals, only a few animal species are known to develop Type II diabetes spontaneously. Besides humans, these include non-human primates, cats, raccoons, and the degu (*Octodon degus*). The reason that other species do not develop spontaneous Type II diabetes is believed to be the substitution of proline residues at positions that are proposed to reside within the core region of aggregation (Westermark et al., 1990). In contrast, an S20G mutation in IAPP has been found to be associated with the early onset of Type 2 diabetes in Japanese, Chinese, and some other ethnic groups (Lee et al., 2001). The occurrence of these natural substitutions has assisted in the identification of the residues that are important for the aggregation of the peptide.

Similar to the full-length IAPP, the amylin (8-37) fragment can form aggregates and has been successfully used as a model to study the amyloid formation by IAPP (Abedini and Raleigh, 2006). The aggregation of IAPP(8-37) displayed a nucleation mechanism for fibril formation, as the presence of nucleating seeds shortens the lag phase of fibril formation. Structural analysis of the IAPP(8-37) aggregates revealed a cross beta-sheet structure that was possibly parallel (Abedini and Raleigh, 2006).

In this study, a yeast prion was utilized in an attempt to establish a model that may be useful to study the aggregation of IAPP *in vivo*. IAPP(8-37) was substituted for the

Figure 4-1. Sequences of IAPP and IAPP-NR-GFP-MC fusion protein. The (8-37) fragment of IAPP is underlined.

IAPP:

KCNTATCATQ RLANFLVHSS NNFGAILSST NVGSNTY

IAPP-NR-GFP-MC:

Met-Ser-[IAPP 8-37]-Asn-Ala-[NR domain]-[GFP]-[Sup35MC domain]

NQ domain of Sup35p in a Sup35-N-GFP-MC (NGMC) construct. *S. cerevisiae* cells expressing the fusion protein showed prion-like phenotypes, and the detailed characterization confirmed the formation of a novel prion. This study represents the first instance in which a non-Asn/Gln-rich sequence has been demonstrated to serve as the aggregation domain in the formation of yeast prion. Version of Sup35p may be employed to create synthetic yeast prions that may be used as models to study protein aggregation *in vivo*. The IAPP-containing prion might be particularly useful in exploring the factors, such as the residue substitutions, that affect the aggregation of IAPP.

Experimental Procedures

Plasmids construction

The plasmids and oligonucleotides used in this study are listed in Table 4-1 and 4-2. The oligonucleotides IAPP-F and IAPP-R were designed such that (1) DNA generated by oligonucleotides annealing and extension encoded for IAPP(8-37) peptide; (2) *Bam*H I and *Pst* I recognition sequences were included at the ends of the oligonucleotides; (3) for expression in yeast, the sequence encoding IAPP was optimized based on the preferred codon usage in yeast. To anneal the DNA, the mixture of IAPP-F and IAPP-R was cooled down by 1 °C per 5 minutes from 99 °C to 30 °C. The annealed DNA was consisted of the double-stranded DNA in the middle region and two long 5'-overhangs at both ends. The overhangs were filled in with Klenow fragment to generate the full length DNA,

Table 4-1. Plasmids used in this study.

Plasmids	Characteristics	References
pRS313	Yeast shuttle vector, *CEN, HIS3,* Amp^R	(Sikorski and Hieter, 1989)
pRS316	Yeast shuttle vector, *CEN, URA3,* Amp^R	(Sikorski and Hieter, 1989)
pRS423	Yeast shuttle vector, 2μ, *HIS3,* Amp^R	(Sikorski and Hieter, 1989)
pRS424	Yeast shuttle vector, 2μ, *TRP1,* Amp^R	(Sikorski and Hieter, 1989)
pRS426	Yeast shuttle vector, 2μ, *URA3,* Amp^R	(Sikorski and Hieter, 1989)
p316-Sp-Sup35	pRS316, P_{SUP35}, *SUP35*	(DePace et al., 1998)
pJET101	pRS313, P_{SUP35}, *SUP35*	Chapter 2
pJET101.IAPP	pRS313, P_{SUP35}, *sup35(Δ3-39::IAPP)* pJET101 ← pZErO-1+NM.IAPP (*Bam*H I/*Pfl*M I)	Chapter 2
pJET101. IAPP(S20G)	pRS313, P_{SUP35}, *sup35(Δ3-39::IAPP)* pJET101 ← S20G PCR (*Bam*H I/*Pfl*M I)	this study
pJET149.WT	pRS313, P_{SUP35}, *sup35-N-GFP-MC* pJET101 ← NGMC PCR (*Bam*H I/*Sac* I)	this study
pJET149.IAPP	pRS313, P_{SUP35}, *sup35-N(Δ3-39::IAPP)-GFP-MC* pJET149.WT ← pJET101.IAPP (*Bam*H I/ *Pfl*M I)	this study
pJET150.WT	pRS423, P_{SUP35}, *sup35-N-GFP-MC* p423GPD ← pJET149.WT (*Xho* I/*Sac* I)	this study
pJET150.IAPP	pRS423, P_{SUP35}, *sup35-N(Δ3-39::IAPP)-GFP-MC* pJET150.WT ← pJET101.IAPP (*Bam*H I/ *Pfl*M I)	this study
pJET150. IAPP(S20G)	pRS423, P_{SUP35}, *sup35-N(Δ3-39::IAPP(S20G))-GFP-MC* pJET150.WT ← pJET101.IAPP (*Bam*H I/ *Pfl*M I)	this study
pJET113	pRS313, P_{SUP35}, *sup35(Δ3-39)* pJET101 ← pJET112 (*Bam*H I/*Pfl*M I)	Chapter 2
pJET150. ΔNQ	pRS423, P_{SUP35}, *sup35-N(Δ3-39::IAPP)-GFP-MC* pJET150.WT ← pJET113 (*Bam*H I/ *Pfl*M I)	this study

Plasmids	**Characteristics**	**References**
pJET114	pRS426, P_{CUP1}, *HSP104* p426-P_{CUP1}-Sup35NM-GFP ← Hsp104 PCR (*Bam*H I/*Sac* I)	Chapter 3
pJET108.WT	pRS426, P_{CUP1}, sup35NM-GFP pRS426 ← pJET84 (*Xho* I/*Sac* I)	Chapter 3
pJET108.IAPP	pRS426, P_{CUP1}, sup35NM*(Δ3-39::IAPP)*-GFP pJET108.WT ← pJET101.IAPP (*Bam*H I/*Pfl*M I)	this study
pJET159.IAPP	pRS426, P_{SUP35}, *sup35N(Δ3-39::IAPP)-GFP-MC* pRS426 ← pJET150.IAPP (*Xho* I/*Sac* I)	this study
pJET162.IAPP	pRS424, P_{SUP35}, *sup35N(Δ3-39::IAPP)-GFP-MC* pRS424 ← pJET150.IAPP (*Xho* I/*Sac* I)	this study
pET21a	*E. coli* expression vector, C-terminal 6xHis tag	Novagen
pJET154.WT	pET21a, *sup35-NM-(His)$_6$* pET21a ← Sup35 PCR	Chapter 3
pJET154.IAPP	pET21a, *sup35-NM(Δ3-39::IAPP)-(His)$_6$* pET21a ← IAPP PCR (*Nde* I/*Bam*H I)	this study
pJET154. IAPP(S20G)	pET21a, *sup35-NM(Δ3-39::IAPP(S20G))-(His)$_6$* pET21a ← IAPP(S20G) PCR (*Nde* I/*Bam*H I)	this study
pJET154.ΔNQ	pET21a, *sup35-NM(Δ3-39)-(His)$_6$* pET21a ← ΔNQ PCR (*Nde* I/*Bam*H I)	this study

Table 4-2. The oligonucleotides used in this study.

Name	Sequence
IAPP-F	5’-GCTTA*GGATCC*AACAATGTCTGCTACTCAAAGATTGGCTAACTTCTTG GTTCACTCTTCTAACAACTTCGGTGCTAT-3’
IAPP-R	5’-GGAC*CTGCAG*GTTGAGCGTTGTAAGTGTTAGAACCAACGTTAGTAGA AGACAAAATAGCACCGAAGTTGTTAGAAG-3’
SUP-PROM	5’-CCGGGTATTATATCTTACAT-3’
1025NR	5’-TCCGCGGCATACCTTGAGACTGTGGTTG-3’
1025GF	5’-GTCTCAAGGTATGCCGCGGATGGCTAGC-3’
1025GR	5’-TCAAAGACATTTTGTATAGTTCATCCAT-3’
1025MF	5’-ACTATACAAAATGTCTTTGAACGACTTT-3’
M13F	5’-GTAAAACGACGGCCAGT-3’
IAPP-S20G	5’-CTTCTTGGTTCACTCTGGTAACAAC-3’
colinF	5’-GCTTA*CATATG*TCGGATTCAAACCAAGGCAAC-3’
IAPP-NdeI-F	5’-TA*CATATG*TCTGCTACTCAAAGATT-3’
0313F	5’-GCTTA*CATATG*TCTACTACCCAACCTGC-3’
0313R	5’-ACT*GGATCC*ATATCGTTAACAACTTCGTC-3’
MATa	5’-AAATAAACGTATGAGATCTA-3’
MATalpha	5’-GCAGCACGGAATATGGGACT-3’
MATdistal	5’-ATGTGAACCGCATGGGCAGT-3’

which was then cloned into the *Bam*H I/*Pst* I-digested vector plasmid pZErO-1+NM. The generated plasmid pZErO-1+NM-IAPP, with the sequence confirmed by DNA sequencing, was subsequently used to subclone the fragment IAPP-NR into pJET101 at the *Bam*H I/*Pfl*M I sites, generating plasmid pJET101.IAPP.

The GFP insertion in between the N and M domains of Sup35 was accomplished by multi-step via PCR. Primers 1025NR and 1025GF were designed such that the C-terminus of Sup35-N is homologous to the N-terminus of GFP. Similarly, 1025GR and 1025MF were designed such that the C-terminus of GFP is homologous to the N-terminus of Sup35-MC. In the first round, individual PCR reactions were conducted to amplify Sup35-N, GFP, and Sup35-MC. Sup35-N was amplified using SUP-PROM/1025NR as the primers and p316SpSup35 as the template, and Sup35-MC was amplified using 1025-MF/M13F as the primers and also p316SpSup35 as the template. GFP was amplified using 1025GF/1025GR as the primers and p426CUPsGFP as the template. Product from each PCR was purified and confirmed appropriately. In the second round, the PCR products of Sup35-N and GFP were fused together through another PCR to generate Sup35-N-GFP DNA. Terminal primers SUP-PROM and 1025GR were used to set up the PCR, with the mixture of Sup35-N and GFP as the new template. The PCR product showed the same size as the sum of the lengths of two fragments, which indicated that the gene fusion succeeded. In the final round, Sup35-N-GFP from the second-round PCR and Sup35-MC from the first round PCR were fused together through a new PCR reaction. SUP-PROM and M13F were used as

the primers, and the mixture of Sup35-N-GFP and Sup35-MC was used as the new template. The full-length PCR product, Sup35-N-GFP-MC (NGMC), was verified by DNA electrophoresis, which showed the correct size, and DNA sequencing. Subsequently, NGMC was cloned into pJET101 at *Bam*H I/*Sac* I sites to generate pJET149.WT.

The high-copy number plasmid pJET150.WT was generated by subcloning the P_{SUP35}-NGMC gene into pRS423 at *Xho* I/*Sac* I sites. The *Xho* I/*Sac* I fragments were also inserted into pRS424 and pRS426 to make the plasmids with *TRP1* and *URA3* markers, respectively. The substitution of IAPP was accomplished by replacing NQ with IAPP at *Bam*H I/*Pfl*M I sites. Similarly, the plasmid pJET150.ΔNQ was constructed by subcloning the *Bam*H I/*Pfl*M I fragment of pJET113 into pJET150.

The S20G mutation was achieved through a site-directed mutagenesis PCR. First, IAPP-S20G and NM-R were used as the primers, and pJET101.IAPP was used as the template to conduct the PCR, generating the TCT-to-GGT mutation. Second, the product from the first PCR and the primer SUP-PROM were mixed together, and pJET101.IAPP was added to the mixture as the template to generate the full-length DNA containing the TCT-to-GGT mutation. The IAPP(S20G)-flanking region was subsequently cloned into pJET101 or pJET150 at *Bam*H I/*Pfl*M I sites.

To construct the plasmids for the expression in *E. coli*, 0313R was designed as the reverse primer. Sup35-NM, IAPP-NR-M, IAPP(S20G)-NR-M, and ΔNQ-NR-M were amplified using colinF, IAPP-NdeI-F, IAPP-NdeI-F, and 0313F as the forward primer, respectively. The PCR products were cloned into pET21a at *Nde* I/*Bam*H I sites.

Yeast strains

Yeast strains OT56k, OT60k, and GT17k have been described in Chapter 2. GT247-1C, GT247-1D, and GT388 have been described previously (Table 4-3) (Borchsenius et al., 2001). GT247-1C and GT247-1D are identical in their genotypes except for the mating type. The knockout of chromosomal *sup35* gene in GT388 was conducted in the same method as the one described in the construction of OT60k previously (Chapter 2). The PCR product of *sup35::KanMX* was transformed into GT388, and the transformants growing on YPD+G418 medium plates were verified for *sup35* knockout through genomic PCR.

Prion assays *in vivo*

The suppression of *ade1-14* gene was monitored by color assay on 1/4YPD medium or growth assay on SD-Ade as described previously. The GuHCl curing of prions was conducted by passage of the cells on YPD medium containing 5 mM GuHCl for three successive rounds. Hsp104p overexpression was achieved by the addition of 50 μM $CuSO_4$, which induced the P_{CUP1}:*HSP104* expression in plasmid pJET114. Cells were incubated in the induction medium for 1 day and then subjected to the color assay on 1/4YPD medium. The deletion of chromosomal *hsp104* gene was generated by transforming cells with *hsp104::URA3* that was amplified from 74-D694-Δsup35-Δhsp104 (Hara et al., 2003). The transformants were grown in rich medium overnight to

Table 4-3. Strains used in this study.

Strain	Genotype	Reference
TOP10F'	*rec*A1 *ara*D139 *end*A1 (Str^R) F'{*lac*I^q, Tn*10*(Tet^R)}	Invitrogen
OT56 ([PSI^+] 7-74-D694)	*MAT***a** *ade1-14*$_{UGA}$ *his3 leu2 trp1-289*$_{UAG}$ *ura3* [PSI^+]	(Derkatch et al., 1996)
OT60 ([psi^-] 74-D694)	*MAT***a** *ade1-14*$_{UGA}$ *his3 leu2 trp1-289*$_{UAG}$ *ura3* [psi^- PIN^+]	(Chernoff et al., 1995)
GT17	*MAT***a** *ade1-14*$_{UGA}$ *his3 leu2 trp1-289*$_{UAG}$ *ura3* [psi^- pin^-]	(Derkatch et al., 1997)
YPR172W	BY4743, *sup35::KanMX*	(Giaever et al., 2002)
OT56k	OT56, *sup35::KanMX*	Chapter 2
OT60k	OT60, *sup35::KanMX*	Chapter 2
GT17k	GT17, *sup35::KanMX*	Chapter 2
74-D694-Δsup35 -Δhsp104	74-D694, *sup35::TRP1* [*HIS3, SUP35*] *hsp104::URA3*	(Hara et al., 2003)
GT17k IAPP--Δhsp104	GT17, *sup35::KanMX* [*HIS3, IAPP-sup35*] *hsp104::URA3*	this study
GT247-1C	*MAT*a *ade1-14 his3 leu2 lys2 ura3 trp1 sup35::HIS3* [*LEU2 sup35-*Δ*22/69*] [psi^- PIN^+]	(Borchsenius et al., 2001)
GT247-1D	the same as GT247-1C but *MAT*α	(Borchsenius et al., 2001)
GT388	*MAT*α *lys1-1 his3 leu1 ura3 ade2-1 SUQ5 kar1-1* cyh^R [psi^- rho^-]	(Borchsenius et al., 2001)
GT388k	GT388, *sup35::KanMX*	this study

allow the DNA recombination before they were selected on SD-Ura.

For prion induction experiments, yeast strains harboring P_{CUP1}-promoted IAPPA-NR-M-GFP fusion protein were incubated in the minimal medium SD-Ura-His containing 50 μM $CuSO_4$ for 1 day and then spread on 1/4YPD for the color assay. The culture was diluted such that around 100 cells were spread on each plate for the convenience in counting the colonies. The induction rate was calculated by dividing the number of the white colonies by that of the total colonies. Some white colonies were randomly picked and tested for their GuHCl curability.

GFP images were scanned using a Zeiss LSM510 UV confocal laser scanning microscope (Carl Zeiss Inc., New York, NY) at wavelength 488 nm, and image analysis was conducted using a Zeiss LSM image browser (Carl Zeiss). Flow cytometry of yeast cells expressing the GFP-fusion proteins were conducted on a FACsort flow cytometer (Becton Dickinson) at the flow cytometry core facility at Emory University.

Differential centrifugation analysis of yeast extract

Total cellular proteins were extracted from yeast as previously described (Chernoff et al., 2002). Yeast cells were grown to midlog phase (~2 OD_{600}) in YPD medium at 30 °C with constant shaking. After cooling to 0 °C for 15 min, cells were harvested at 2000 x *g* for 5 min at 4 °C. The pellet was washed and resuspended with yeast lysis buffer (50 mM Tris-HCl, pH7.5, 5 mM $MgCl_2$, 10 mM KCl, 0.1 mM EDTA, 1mM DTT) at a concentration of ~3 x 10^6 cells/μl, and the protease inhibitor cocktail for yeast

(Sigma) was added at a concentration suggested by the supplier. An equal volume of 425- to 600-μm acid-washed glass beads were added to the cell resuspension, and then cells were lysed by vigorous agitation. After the lysate was centrifuged at 2000 x *g* for 10 mins at 4 °C to pellet unbroken cells and cellular debris, the supernatant was carefully transferred to a new tube as the total protein sample. The protein concentration was determined using the Bio-Rad protein assay kit (Bio-Rad) with BSA as a standard. Subsequently, protein was centrifuged at 16000 x *g* for 10 minutes at 4 °C to separate the soluble and pellet portions of the whole-cell protein obtained at 2000 x *g*. The soluble portion was removed to a new tube, and the pellet was resuspended in an equal volume of yeast lysis buffer. Proteins of different portions were prepared with the addition of SDS loading buffer and loaded on SDS-PAGE gel for the separation by electrophoresis. The target proteins were visualized by Western blot with the anti-Sup35 antibody (Ab0327, a gift kindly provided by Lindquist) or the anti-GFP antibody (BD Bioscience).

Cytoduction, mating, sporulation and tetrad dissection

GT388k[pJET150.IAPP], the recipient strain of cytoduction, was constructed through the plasmid shuffling between p316SpSup35 and pJET150.IAPP. For cytoduction experiments, the donor strains GT17k[pJET150.IAPP] ([*I-PSI*$^{+}$] or [*i-psi*$^{-}$]), OT56k[pJET149.WT] and OT60k[pJET149.WT] were mated to the recipient strain described above, which is karyogamy-defective *kar1* (Conde and Fink, 1976). The recipient lacks functional mitochondrial DNA and bears the recessive *cyh*^{R} mutation.

After 1 day mating on YPD medium, cell mixtures were replica plated to synthetic medium containing glycerol and ethanol as the sole carbon sources and cycloheximide (5 mg/l) to select for cytoductants receiving the mitochondria from the donor strain. Cells were then characterized on 1/4YPD medium plates.

GT247-1C[pJET159.IAPP] and GT247-1D[pJET162.IAPP] cells were mixed on YPD medium for the mating experiment. Following the overnight growth on YPD, cells were velveteen replica plated to synthetic medium lacking uracil and tryptophan (SD-Ura-Trp) to select the cells that contained both plasmids of different markers, which possibly formed as a result of mating. The cells were verified as diploids by their ability to sporulate under defined conditions. Additionally, genomic DNA was extracted and used as the template in subsequent PCR reactions that were designed to identify the mating type of cells. The forward primers MATa and MATalpha bind specifically to the genomic DNA from cells that are *MAT***a** and *MATα*, respectively, and the reverse primer MATdistal binds to the genomic DNA from both mating types. Therefore, the mating types can be reflected by the appearance of amplification products using different primers, and cells were verified as **a**/*α* diploids when products from both reactions were present (Aylon et al., 2004).

Diploid cells generated from the mating experiments were sporulated after they were incubated in the sporulation medium for 5 to 7 days. Tetrads were observed and dissected on YPD medium under a dissecting microscope. Following tetrad dissection, viable spores were grown on 1/4YPD for the color assay, and the genomic DNA was extracted

and used in mating-type PCR to determine their mating types.

The expression and characterization of IAPP-substituted Sup35NM proteins

As described in Chapter 3, Sup35NM and its derivatives were overexpressed in *E. coli* strain BL21[DE3] upon the addition of the inducer IPTG to the final concentration of 0.8 mM when OD_{600} reached 0.8. Following 3 hr of induction, cells were harvested and lysed in 8 M urea buffer (8 M urea, 20 mM Tris-HCl, pH 8.0). Proteins were purified first on Ni-NTA column (Qiagen Inc.), using 8 M urea buffer containing 20 mM imidazole for washing and 400 mM imidazole for elution. The protein solution eluted from the Ni-NTA column was loaded on DEAE Sephacel column (Pharmacia Biotech Inc.) for another round of purification. The column loaded with the proteins was washed with 8 M urea buffer and eluted with 8 M urea buffer containing 300 mM NaCl. Proteins were methanol precipitated and air dried before they were resuspended in 6 M GuHCl buffer and shaken overnight to disaggregate preformed polymers. The purity of the proteins was verified by SDS-PAGE electrophoresis and MALDI mass spectrometry. Proteins were quantified either by monitoring the UV absorbance at 276 nm or by using the BCA protein assay kit (Pierce Biotechnology).

To initiate fiber formation, protein was diluted by at least 100 times to the Congo red binding buffer (CRBB: 5 mM potassium phosphate, pH 7.4, 150 mM NaCl) to a final concentration of 2.5 μM. The reactions were generally set up in a volume of 1 mL in 2-ml microcentrifuge tubes, which were rotated end-to-end on a roller. The formation of

the fibers was monitored by the Congo red binding assay (Chernoff et al., 2002). At different time points, 1 μM Sup35NM and 10 μM Congo red were mixed at room temperature for 30 min, and then the solution was scanned between 400 and 600 nm on a UV-Vis spectrometer. Sup35NM fiber exhibited a spectra shift in absorbance, with a new peak at 540 nm, compared to unpolymerized protein or Congo red alone. The amount of Congo red bound to Sup35NM was calculated using the following equation:

$$\text{mole Congo red bound/liter solution} = (A_{540}/25295)-(A_{477}/46306)$$

where A_{540} and A_{477} refer to the absorbance at 540 and 477 nm, respectively. In the seeding experiments, preformed fibers were sonicated briefly and added to the unpolymerized protein solution at a final ratio of 5%.

Fibers were negatively stained for electron microscopy (EM) analysis (Chernoff et al., 2002). To clear the undissolved crystals, 2% uranyl acetate solution was centrifuged at 16000 x *g* for 5 mins, and the supernatant was transferred into a new vial. Proteins were applied to a glow-discharged 400 mesh carbon-coated copper grid and then stained with 2% (w/v) aqueous uranyl acetate. Excess liquid was removed from the grid, and the grid was then allowed to dry in a vacuum desiccator. Samples were viewed in a Philips LS-410 transmission electron microscope (TEM), at an accelerating voltage of 80 kV, at the integrated microscopy and microanalytical facility (IM&MF) at Emory University.

Results

As reported previously, the IAPP(8-37) peptide, similar to IAPP, forms aggregates that have the structural characteristics of amyloid fibrils (Abedini and Raleigh, 2006). Therefore, the IAPP(8-37) fragment was selected as an aggregation-prone sequence that could be substituted for the NQ domain of Sup35p. When wild type *SUP35* gene was replaced by the *IAPP-sup35* mutant gene, the yeast strain exhibited prion-like properties, as demonstrated by the appearance of both white and red colonies on YPD medium (Chapter 2). To provide further support that IAPP-Sup35p is able to form a prion, a series of biochemical and genetic analysis were performed on the suppositious prion and non-prion states of *S. cerevisiae* strains containing the modified Sup35p.

The expression of IAPP-GFP-Sup35 fusion protein at different levels and its effect on the characteristics of IAPP-GFP-Sup35 fusion protein.

GFP has been as a powerful tool to study the aggregation of yeast prions, and, when fused to the prion-forming domain, GFP generally exhibits punctate fluorescence in the presence of prions and show diffuse fluorescence in the absence of prions. Song et al. reported the insertion of GFP in between the N and M domains of Sup35p, which associated the fluorescence morphology in cytoplasm directly with the prion phenotypes but did not perceptibly effect either prion formation or propagation (Song et al., 2005). Based on this analogy, we adopted a strategy to study IAPP-substituted Sup35p in which

the IAPP-NR-GFP-M-C fusion protein was employed as the substrate for creation of a prion.

A new cloning method was designed as the plasmid constructed by Song et al (Song et al., 2005) was not compatible with the established modular system employed in this study. Using a multi-step PCR, Sup35N, GFP, and Sup35MC genes were ligated together to make the gene encoding for Sup35N-GFP-SupMC (NGMC), which was verified by DNA sequencing and functional assays. This new construct allowed the subsequent modular exchanges among Sup35 mutants with different aggregation domains at their *Bam*H I/*Pfl*M I sites. The fusion protein NGMC was cloned under the native promoter P_{SUP35} on a single-copy plasmid to mimic the expression level of Sup35p in wild type strains. By plasmid shuffling, NGMC was substituted for wild type Sup35p in strains that were [*PSI*$^{+}$] or [*psi*$^{-}$], which generated the strains exhibiting the same phenotypes as the parent strains. As described previously, the phenotypes were monitored on 1/4YPD medium as the strains contained the *ade1-14* mutation in the chromosome. Therefore, not only did NGMC function properly as a termination factor to maintain the viability of cells, but it was also able to form prions and inherit from the existing Sup35 prions.

The gene encoding for IAPP-NR-GFP-M-C fusion protein (IAPP-GMC) was constructed similarly under the P_{SUP35} promoter on a single-copy plasmid, generating pJET149.IAPP. Strains harboring this plasmid, when growing on 1/4YPD medium, showed an ambiguous color of light pink. The cells were subjected to the GuHCl treatment that was generally able to cure prions efficiently; however, the cells remained

the same color after the GuHCl treatment. An examination of the expression level of IAPP-GMC in these cells by Western blot showed that less protein was expressed compared to NGMC on the same plasmid vector (Figure 4-2). Furthermore, the fluorescence strength of the cells expressing IAPP-GMC, as analyzed by flow cytometry, was also smaller than that of the cells expressing NGMC (Figure 4-2). The low expression level of IAPP-GMC might have resulted in insufficient termination factor activity, which led to the light colors on 1/4YPD medium. In addition, the formation and propagation of prion, which are dependent on the concentration of protein components, might have been affected by the less expression level as well.

To overcome the expression shortage, IAPP-G-MC was subcloned into pRS423, a high-copy number plasmid, to generate pJET150.IAPP. As a result, the expression of IAPP-G-MC was elevated to a level that was comparable to or higher than that of NGMC on the single-copy number plasmid (Figure 4-2). Interestingly, the increased expression level of IAPP-C-MC enabled the host strains to exhibit two phenotypes corresponding to the prion and non-prion states, as described below.

IAPP-substitute GFP-Sup35 fusion protein was able to form prion.

Both white and pink colonies appeared when cells expressing IAPP-G-MC at an elevated level were plated on 1/4YPD medium, which suggested the formation of prions by IAPP-G-MC. Furthermore, the white colonies grew on the minimal medium lacking adenine (SD-Ade), while the pink colonies did not (Figure 4-3). The white and pink

Figure 4-2. The expression level of IAPP-G-MC fusion proteins.

A. Western-blot quantification of fusion proteins expressed on various plasmid vectors. 1, NGMC, *CEN*, [*PRION*$^{+}$]; 2, NGMC, *CEN*, [*prion*$^{-}$]; 3, IAPP-G-MC, *CEN*; 4, IAPP-G-MC, 2μ, [*I-PSI*$^{+}$]; 5, IAPP-G-MC, 2μ, [*i-psi*$^{-}$]. Proteins were detected by anti-GFP monoclonal antibody (BD Bioscience). B. Analysis of fluorescence strength by flow cytometry.

A

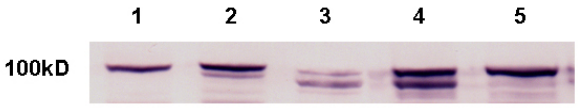

B

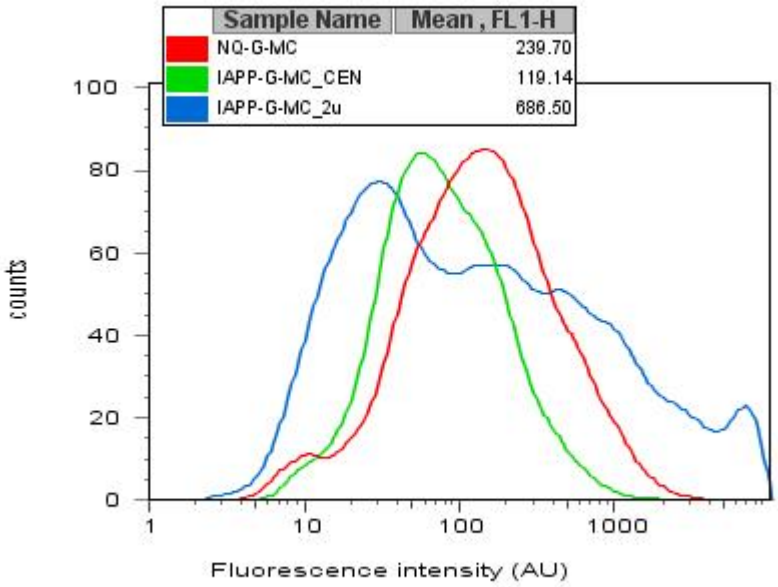

Figure 4-3. The growth of cells expressing IAPP-G-MC on the high-copy number plasmid on 1/4YPD and SD-Ade medium.

Strains growing on each sector were: top left, NGMC, [*PSI*$^{+}$]; bottom left, NGMC, [*psi*$^{-}$]; top right, IAPP-G-MC, [*I-PSI*$^{+}$]; bottom right, IAPP-G-MC, [*i-psi*$^{-}$]. The top plate was 1/4YPD and the bottom one was SD-Ade. Cells expressing NGMC on the single-copy number plasmid were streaked on the media for comparison.

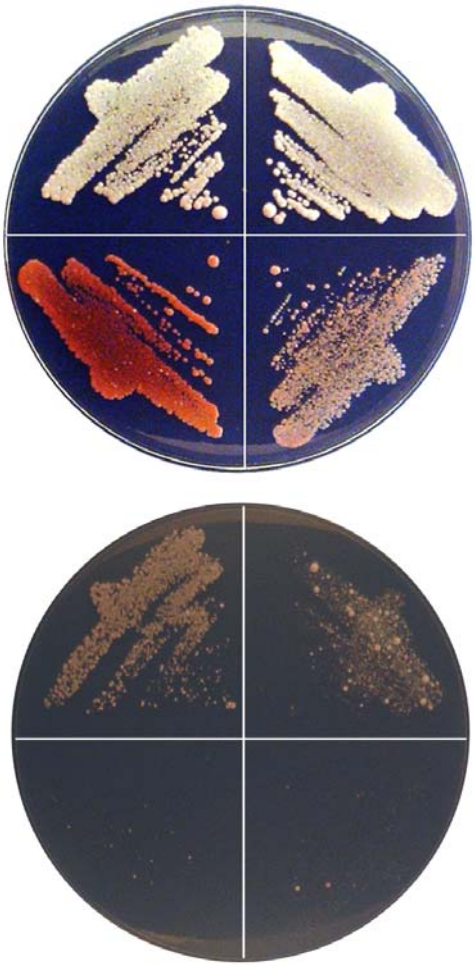

strains were designated as [*I-PSI*$^+$] and [*i-psi*$^-$], respectively, to represent the prion and non-prion states of the strain. It was noticed that, compared to the [*psi*$^-$] colonies of the NGMC control strain, [*i-psi*$^-$] colonies showed a lighter pink color on 1/4YPD. The reason for this phenomenon is unclear and may be that IAPP-G-MC was expressed at a higher level than NGMC. The concentration of IAPP-G-MC that remains soluble in the [*I-PSI*$^+$] cells is relatively high such that the translation of *ade1-14* can be terminated, which causes the color development.

The suggestion that the different phenotypes were caused by the formation of prion was supported by the fluorescence microscopy and protein sedimentation assay (Figure 4-4). Fluorescence foci were observed in [*I-PSI*$^+$] cells, but not in [*i-psi*$^-$] cells. The punctate fluorescence indicated that GFP fusion proteins adopted an aggregated conformation characteristic of prions, while the diffused fluorescence indicated the absence of prions. It was shown by the protein sedimentation assay that the distribution of IAPP-G-MC in the supernatant and pellet portions were different between [*I-PSI*$^+$] and [*i-psi*$^-$] cells. The ratio of the proteins in the pellet portion to those in the supernatant portion was higher in [*I-PSI*$^+$] cells than in [*i-psi*$^-$]. As proteins tend to be centrifuged down when they form prion particles that are large in size, it is plausible that IAPP-G-MC is in the prion conformation in [*I-PSI*$^+$] cells.

Genetic analysis of [*I-PSI*$^+$] prion: cytoduction, mating, and tetrad analysis.

Cytoduction is a useful test for the non-Mendelian inheritance of yeast prions. At a

Figure 4-4. The presence of IAPP-substituted prion as shown by fluorescence microscopy and protein sedimentation experiments.

A. Confocal fluorescence images of yeast cells that are [*I-PSI*$^+$] and [*i-psi*$^-$].

B. The protein sedimentation assay showing the protein distribution in the supernatant (s) and pellet (p) portions. Strains subjected to the assay were: [*I-PSI*$^+$] (white), [*i-psi*$^-$] (pink), [*I-PSI*$^+$] after GuHCl treatment (w-GuHCl), and [*i-psi*$^-$] after GuHCl treatment (p-GuHCl).

A

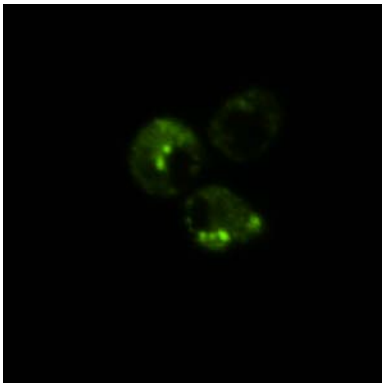

[*I-PSI*$^+$]

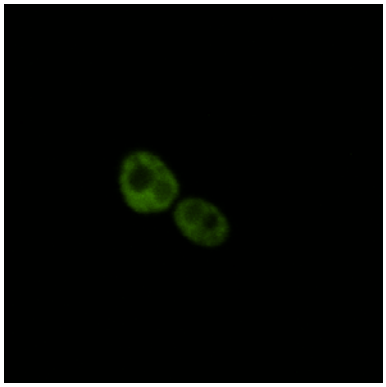

[*i-psi*$^-$]

B

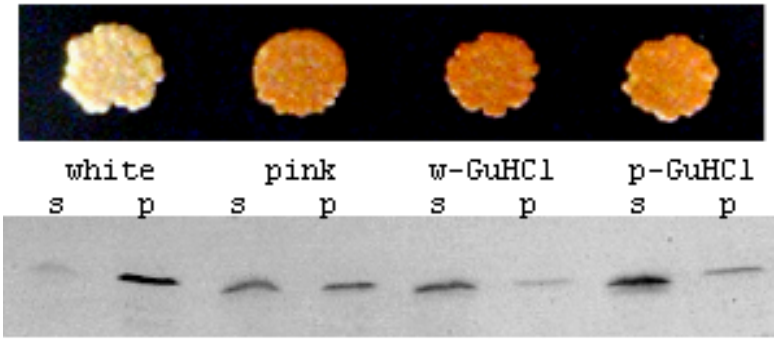

low frequency during mating, nuclei fail to fuse, generating haploid cytoductants that contain the cytoplasmic contents of both parents, but the nuclear content of only one parent. The donor strain, usually the strain to be tested for the presence of a prion, delivers its cytoplasmic materials including prion particles to the recipient strain that does not contain the prion. Prions are usually transferred with high efficiency so essentially all cytoductants should contain a prion.

Yeast strain GT388 (*MATα lys1-1 his3 leu1 ura3 ade2-1 SUQ5 kar1-1 cyh*^{R} [*psi*$^{-}$ *rho*$^{-}$]) was used to construct the recipient strain (Borchsenius et al., 2001). The strain possesses *kar1* mutation, which inhibits the formation of karyogamy, the fusion of nuclei of two cells, and increases the frequency of cytoduction greatly. It is a mitochondrially defective *rho*$^{-}$ derivative that can not grow on minimal media containing glycerol and ethanol as the only carbon sources, so the cytoplasmic mixing can be detected by the transfer of mitochondria from the *rho*$^{+}$ donor, which allows the cytoductants to grow on such media. Furthermore, it has a recessive *cyh*^{R} marker which allows the selection against the donor and rarely occurring diploid cells.

Wild type Sup35 was replaced with IAPP-G-MC to make the recipient strain GT388k[pJET150.IAPP]. Cells were treated with GuHCl to generate [*i-psi*$^{-}$] cells. The cytoduction was conducted using various donor strains and the non-prion recipient strain (Figure 4-5). As determined by the color assay on 1/4YPD medium, the cytoductant from the [*I-PSI*$^{+}$] donor turned [*I-PSI*$^{+}$], while the one from the [*i-psi*$^{-}$] donor remained [*i-psi*$^{-}$]. This indicates that [*I-PSI*$^{+}$] is cytoplasmic inheritable and plausibly a prion. As control

Figure 4-5. Cytoduction of [*I-PSI*$^+$] prion.

A. The scheme that shows the transfer of cytoplasmic materials during cytoduction (Sondheimer and Lindquist, 2000). In cytoduction, a strain containing the desired phenotypic element (the donor) is co-incubated with a strain lacking the element (the recipient). The two cell types fuse cytoplasmic content, but not their nuclei, preventing gene exchange. Haploid buds form from the heterokaryon. Desired offspring buds can be selected using nuclear markers from the recipient and propagated into colonies.

B. The recipient strain was GT388k[pJET150.IAPP], [*i-psi*$^-$]. The donor strains were: a, IAPP-G-MC, [*i-psi*$^-$]; b, IAPP-G-MC, [*I-PSI*$^+$]; c, NGMC, [*psi*$^-$]; d, NGMC, [*PSI*$^+$]. The strains resulted from the cytoduction were tested for the presence of [*I-PSI*$^+$] by the color assay on 1/4YPD medium. [*I-PSI*$^+$] prion particles transmitted during the cytoduction caused the formation of prion, as demonstrated by the phenotype conversion of the recipient strain (line b). However, wild type [*PSI*$^+$] prion particles, which should have been transmitted theoretically, did not induce the formation of [*I-PSI*$^+$] (line d).

A

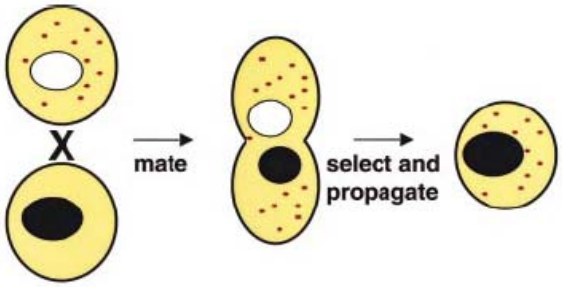

B

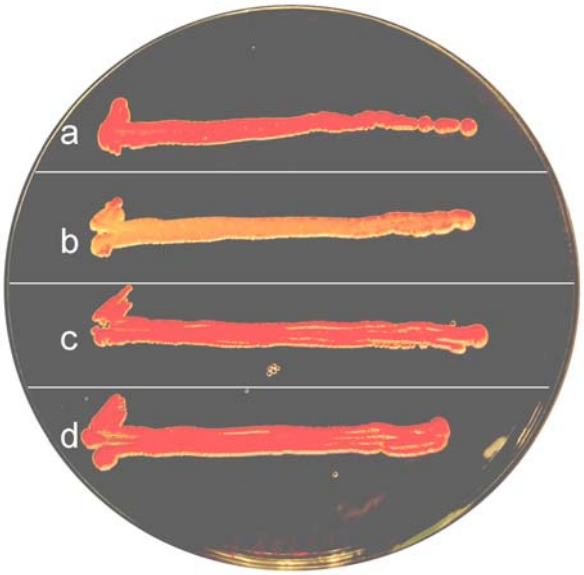

experiments, NGMC strains that are [*I-PSI*$^+$] or [*i-psi*$^-$] were used to cytoduce the recipient strain. Neither of the donor strains was able to turn the recipient strain into [*I-PSI*$^+$]. It is unlikely that prion particles have not been transferred from [*PSI*$^+$] cells to the recipient cells because the transfer is generally very efficient. Actually, it indicates that IAPP-G-MC can not be incorporated onto the template formed by [*PSI*$^+$].

[*I-PSI*$^+$] prion was also subjected to the mating and sporulation experiments. The gene encoding for IAPP-G-MC was cloned to *TRP1*- and *URA3*-marked high-copy number plasmids, which were then transformed into yeast strains with the opposite mating types. The MAT**a** strain harboring the *URA3*-marked plasmid grew on SD-Ura but not on SD-Trp; while the MATα strain harboring the *TRP1*-marked plasmid grew on SD-Trp but not on SD-Ura. From each of the two strains, both [*I-PSI*$^+$] and [*i-psi*$^-$] cells were isolated. The mating was conducted between the cells that were in opposite mating type. Diploids were selected on double-dropout minimal medium SD-Ura-Trp and tested for the phenotype by the color assay on 1/4YPD medium. The diploid formed from two [*i-psi*$^-$] parents were red on 1/4YPD, while the diploids formed from one [*i-psi*$^-$] parent and one [*I-PSI*$^+$] parent, or two [*I-PSI*$^+$] parents, were white or lighter pink (Figure 4-6). This suggests that [*I-PSI*$^+$] prion is dominant. When the diploid formed from one [*i-psi*$^-$] parent and one [*I-PSI*$^+$] parent was subjected to sporulation, all four hyploids grew white on 1/4YPD medium. This suggests that [*I-PSI*$^+$] prion is a non-Mendelian genetic element, which is characteristic of yeast prions.

Figure 4-6. Mating experiment of [*I-PSI*$^{+}$] prion. After mating, diploids were grown on 1/4YPD for the color assay.

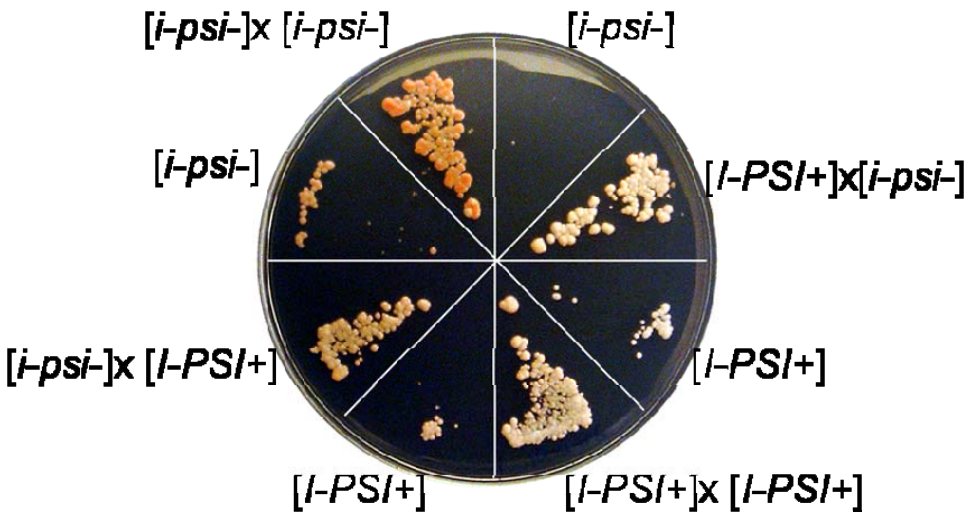

The effect of Hsp104p on [*I-PSI*$^+$] prion.

It was tested whether [*I-PSI*$^+$] prion could be cured by GuHCl, which is characteristic of yeast prions. After [*I-PSI*$^+$] cells were passed on YPD medium containing 5 mM GuHCl for 3 times, they became pink on 1/4YPD medium, which indicated that, like other prions, [*I-PSI*$^+$] prion could be cured by GuHCl. As GuHCl cures prion because of its inhibition to Hsp104p, the deletion of *hsp104* gene in the [*I-PSI*$^+$] strain should also be able to cure [*I-PSI*$^+$] prion. This turned out to be the case, as the chromosomal *hsp104* knockout mutant of [*I-PSI*$^+$] strain was pink when assayed on 1/4YPD medium (Figure 4-7). Furthermore, after the P_{CUP1}-promoted *HSP104* gene was induced in [*I-PSI*$^+$] cells for 1 day, the cells became pink upon the color assay, which indicated overproduced Hsp104p was able to convert [*I-PSI*$^+$] to [*i-psi*$^-$] (Figure 4-7).

Overexpression of IAPP-M-GFP induced the formation of [*I-PSI*$^+$] prion

It is regarded as one of the criteria for a yeast prion that overexpression of the protein increases the frequency of the prion arising. Because the *de novo* generation of the prion is a stochastic process involving nucleus formation, overexpressing the component protein should increase the frequency with which the prion arises. To test whether [*I-PSI*$^+$] prion fulfills this criterion, fusion protein IAPP-NR-M-GFP was constructed and cloned under the P_{CUP1} promoter. This fusion protein contains IAPP-NR, the prion-forming domain in IAPP-GMC, but does not contain Sup35 C domain. The advantage of overexpressing the prion-forming domain only is that the effect of excess

Figure 4-7. The effect of Hsp104p on [*I-PSI*$^+$] prion. Deletion and overexpression of Hsp104 in [*I-PSI*$^+$] strains were assayed on 1/4YPD.

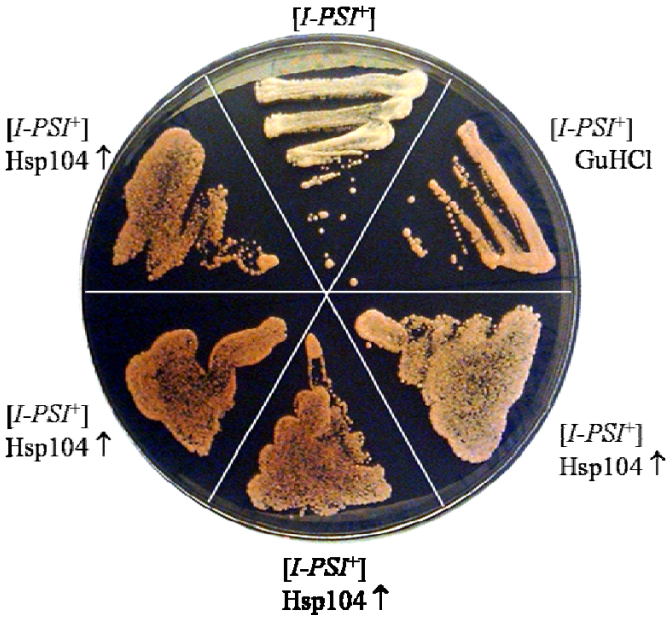

Sup35C on the phenotype can be avoided. When IAPP-M-GFP was overexpressed in [*i-psi*$^-$] cells, it was found that the *de novo* generation rate of [*I-PSI*$^+$] prion increased substantially (Figure 4-8). Even in the absence of the inducer $CuSO_4$, the formation rate still increased greatly due to the leaky expression of IAPP-M-GFP.

IAPP-substituted Sup35NM protein formed amyloid fibers *in vitro*.

The gene encoding for IAPP-NR-M fusion protein (IAPP-NM) was constructed and cloned into vector pET21a (Novagen) for the overexpression in *E. coli*. The gene cloning into the vector allowed a 6xHis tag to be added to the C-terminus of the protein to assist the purification. The C-terminal attachment of the 6xHis tag should not affect the aggregation of IAPP-NM significantly, because the prion-forming domain is located at the N-terminus. Recombinant IAPP-NM was expressed in *E. coli* and purified under denatured condition in order to keep the protein soluble. An affinity column followed by an ion-exchange column was used for the purification, and the purity of the protein was confirmed by SDS-PAGE electrophoresis and MALDI mass spectrometry. Although two bands appeared on the SDS-PAGE gel, there was only one peak on the MALDI spectrum, which suggests that the protein is pure (Figure 4-9). The reason for the appearance of double bands on the gel is unclear. Protein aggregation was initiated by diluting the denatured protein solution into a non-denaturing buffer by at least 100 times. Fully-grown aggregates could bind the diagnostic dye Congo red, as indicated by the spectral shift of the UV absorbance. The aggregates were viewed in a transmission

Figure 4-8. Overexpression of IAPP-GFP fusion protein induced the formation of [*I-PSI*$^+$] prion. IAPP-NR-M-GFP fusion protein, under the P_{CUP1} promoter, was induced by various concentration of $CuSO_4$. Empty pRS426 plasmids were used as negative control. Overexpression caused the phenotype conversion, scored on 1/4YPD medium plates. White colonies were randomly picked and confirmed for the prion status.

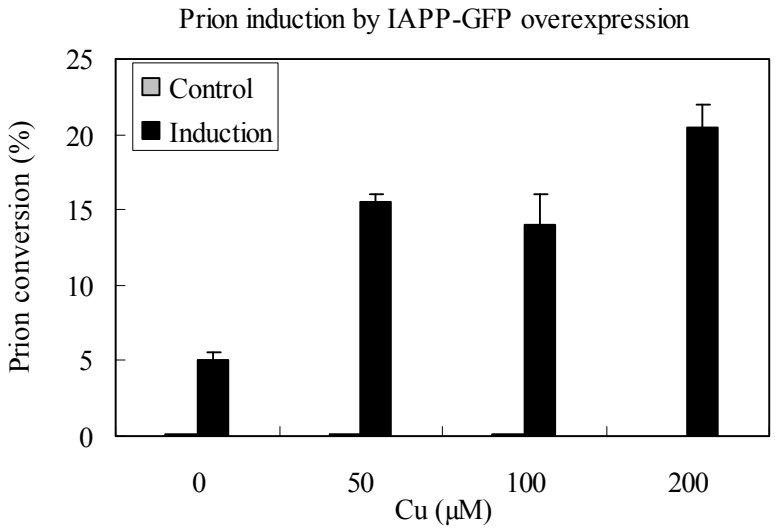

Figure 4-9. MALDI-TOF mass spectrum of purified Sup35NM, IAPP-NM, and ΔNQ-NM proteins. Sup35NM, Cal. MW. 30012 Da, Exp. MW. 29867 Da; IAPP-NM, Cal. MW. 30013 Da, Exp. MW. 29963 Da; ΔNQ-NM, Cal. MW. 26964 Da, Exp. MW. 26805 Da.

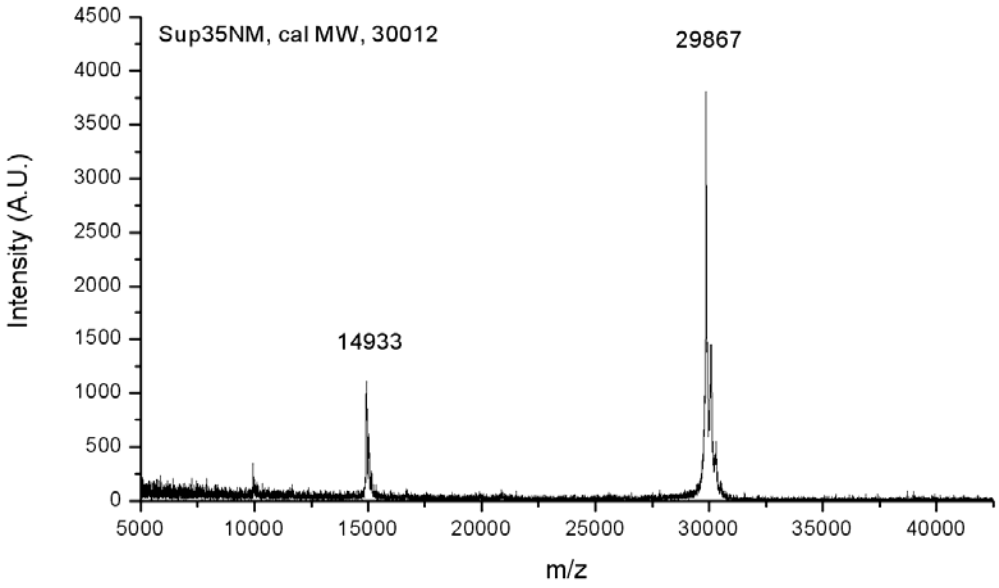

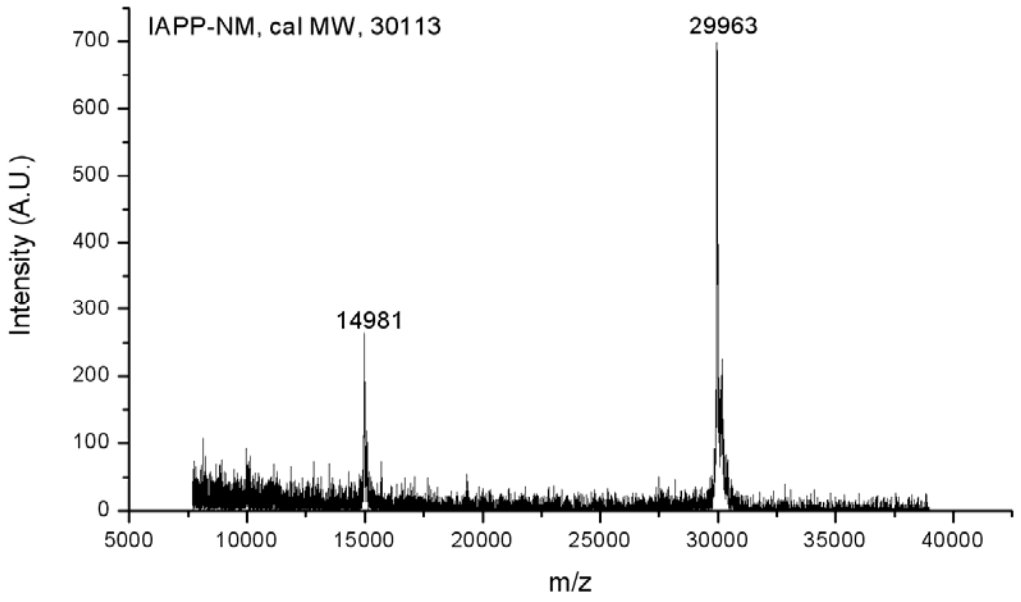
IAPP-NM, cal MW, 30113
29963
14981
Intensity (A.U.)
m/z
0
100
200
300
400
500
600
700
5000
10000
15000
20000
25000
30000
35000
40000

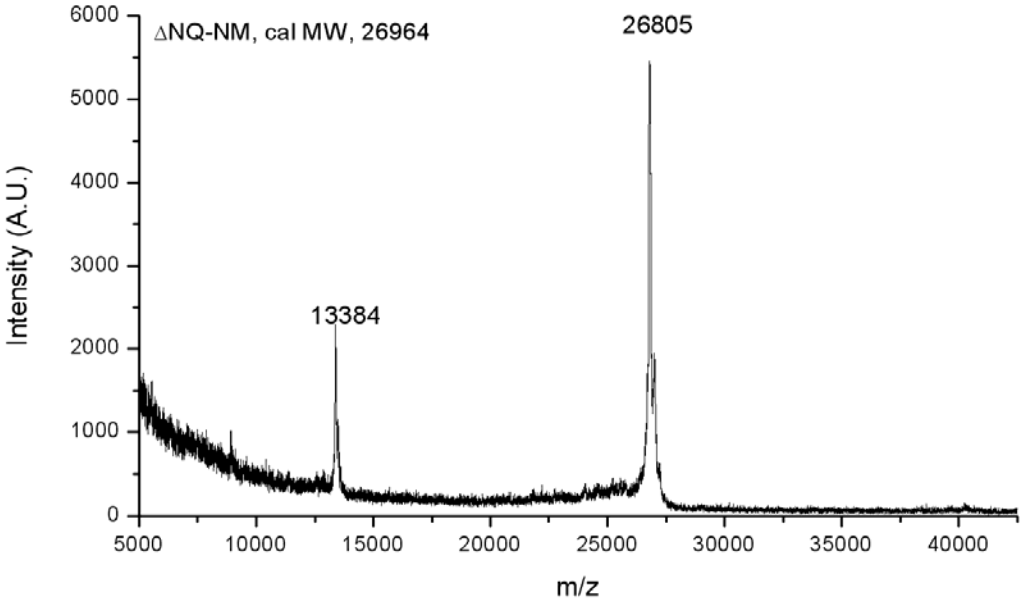
ΔNQ-NM, cal MW, 26964
26805
13384
Intensity (A.U.)
m/z
0
1000
2000
3000
4000
5000
6000
5000
10000
15000
20000
25000
30000
35000
40000

Figure 4-10. Electron microscopy of fibers formed by Sup35NM and its derivatives. Protein samples were prepared for visualization by electron microscopy as described and viewed in a Philips LS-410 transmission electron microscope (TEM) at an accelerating voltage of 80 kV and a magnification of 21,000 x.

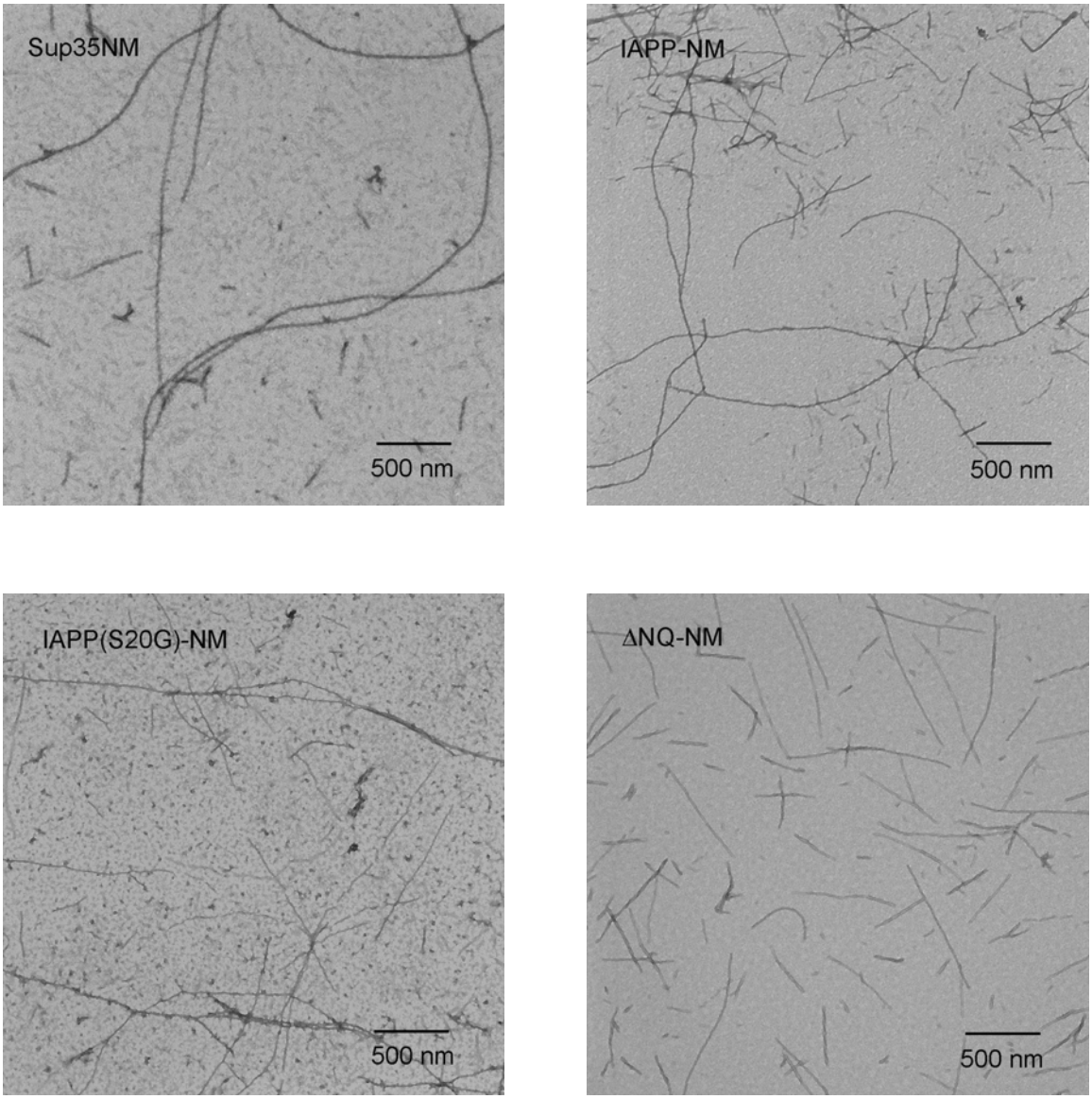

electron microscope (TEM), which revealed the formation of amyloid fibers by IAPP-NM (Figure 4-10). Compared to the fibers formed by wild type Sup35NM, IAPP-MC fibers are similar in morphology but appear to be thinner.

The kinetics of the aggregate formation by IAPP-substituted Sup35NM protein

Like other amyloid fibers, the growth of the aggregates formed by IAPP-NM can be monitored by their ability to bind to the dye Congo red and cause the shift of absorbance in the UV spectrum. The kinetics of the spontaneous amyloid formation exhibits a profile consisting of an initial lag phase followed by a rapid growth phase terminating at a plateau. The sigmoidal profile of the growth curve is typical for nucleation-dependent amyloid formation as observed for many fibrillogenic proteins and peptides, including Sup35NM. When the polymerization reaction is mixed by end-over-end inversion, the lag phase is around 40 minutes; however, when it is mixed by side-to-side rotation, it is still in the lag phase after 3 hours. Therefore, vigorous mixing enhances protein aggregation by shortening the lag phase, possibly because large aggregates are broken into more smaller aggregates that serve as the templates for the addition of monomers.

The addition of SupNM fibers to the aggregation reaction of SupNM monomers leads to the disappearance of the lag phase (Figure 4-11) and (Glover et al., 1997). As predicted, preformed IAPP-NM aggregates also greatly shortened or eliminated the lag phase of the unseeded reaction of IAPP-NM when added at 5 % by weight of total monomeric protein in the reaction. The seeding effect is specific, as preformed

Figure 4-11. Kinetics of aggregation by Sup35NM and IAPP-NM with or without self-seeding.

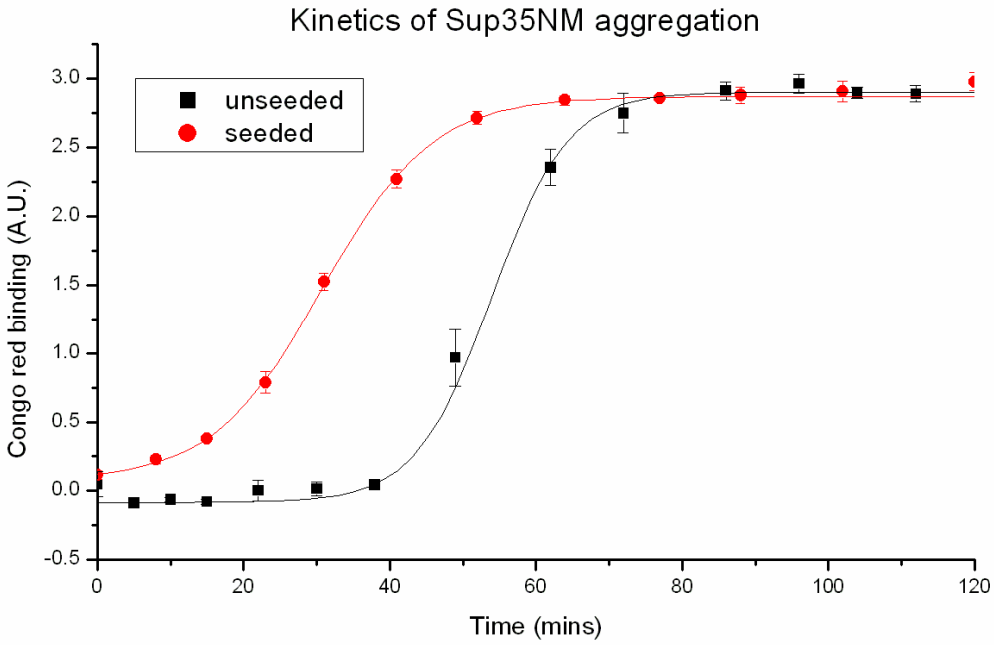

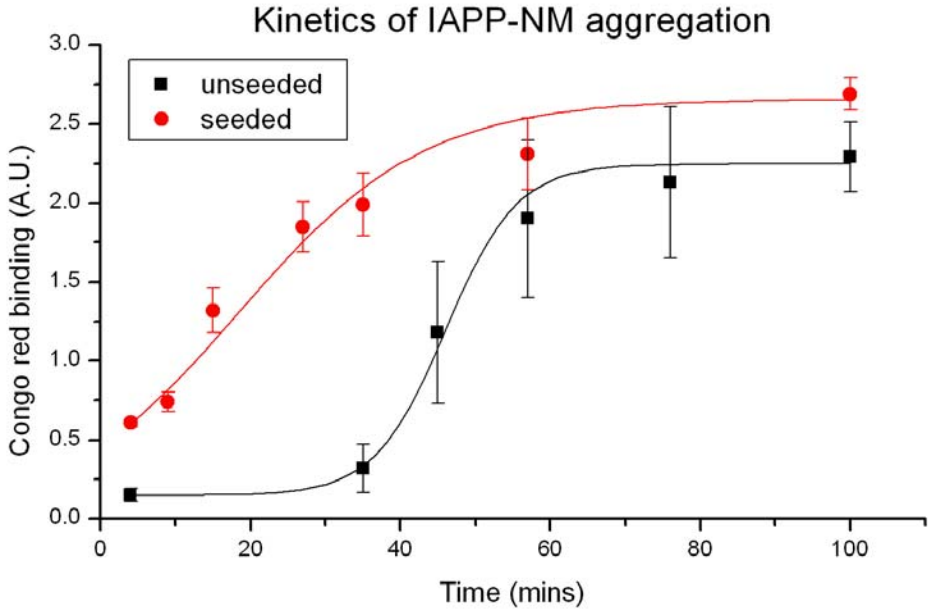

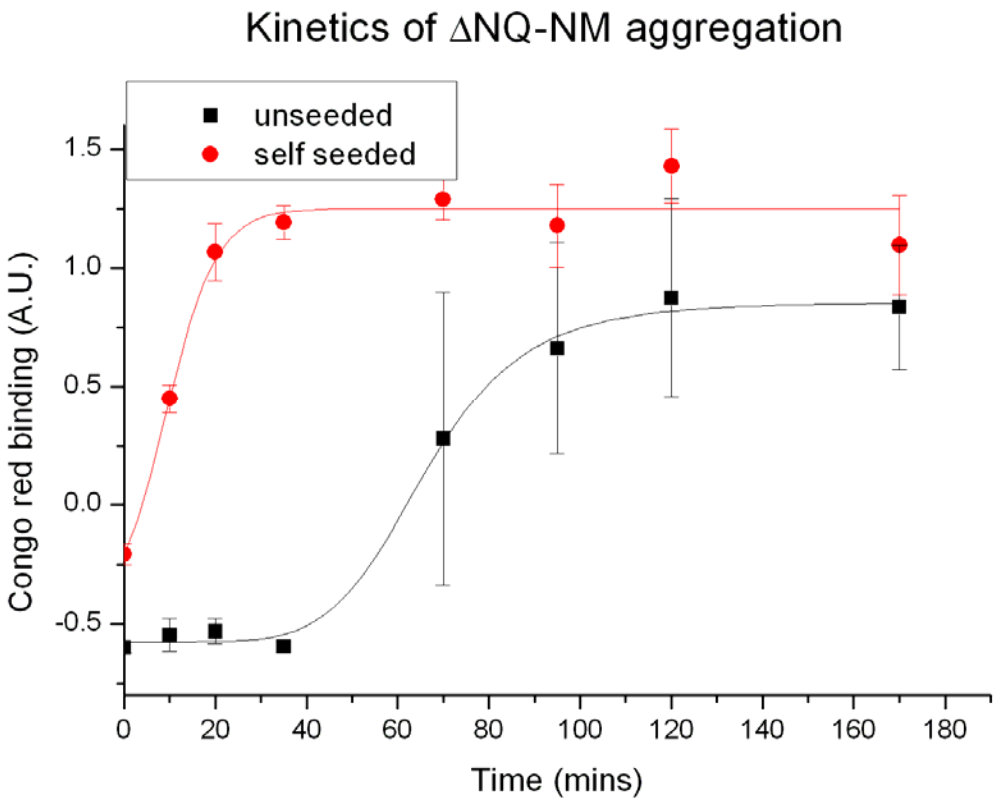
Kinetics of ΔNQ-NM aggregation
unseeded
self seeded
Congo red binding (A.U.)
1.5
1.0
0.5
0.0
-0.5
0
20
40
60
80
100
120
140
160
180
Time (mins)

Figure 4-12. Kinetics of aggregation by Sup35NM and IAPP-NM with heterologous seeding. A. Sup35NM fibers seed IAPP-NM aggregation. B. IAPP-NM fibers seed Sup35NM aggregation.

A.

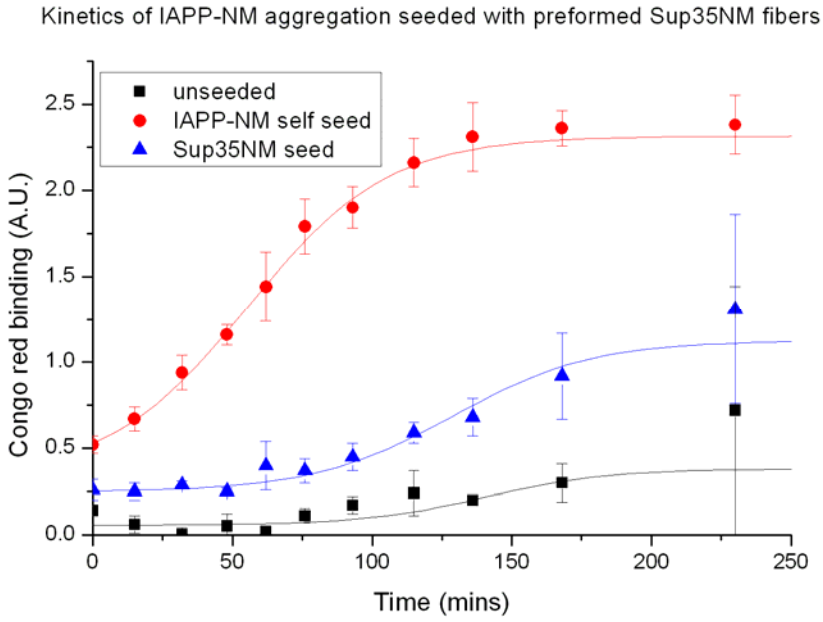

B.

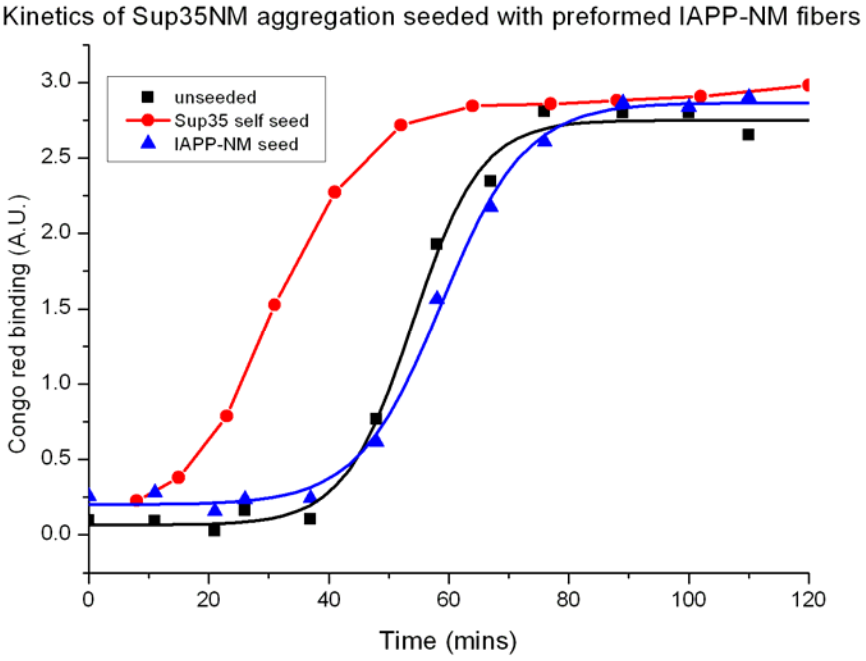

aggregated formed by SupNM did not promote the aggregation of IAPP-NM, and vice versa (Figure 4-12). The assays were conducted by adding the preformed aggregates at a ratio of 5 % ratio to the aggregation reaction of the heterologous protein. Varying the amount of IAPP-NM seeds to 2 % or 10 % of total monomers had no effect on the aggregation of Sup35NM, as compared to the 5 %-seeding experiment.

Mutant protein ΔNQ-NM, which contains only NR and M domain of Sup35p, is also able to form amyloid fibers. Like that of Sup35NM and IAPP-NM, the kinetics of the formation by ΔNQ-NM also shows a sigmoidal curve, suggesting ΔNQ-NM aggregates in a nucleation-dependent feature (Figure 4-13). Preformed fibers by ΔNQ-NM, when added to the aggregation reaction of protein monomers, are able to accelerate the fiber formation by either Sup35NM or IAPP-NM (Figure 4-14). However, neither preformed fibers of Sup35NM nor those of IAPP-NM are able to promote the aggregation of ΔNQ-NM (Figure 4-15).

Introduction of S20G into IAPP and its effect on prion formation

S20G mutation was introduced into IAPP(8-37) by mutagenesis PCR. The strain expressing S20G-modified IAPP-GMC shows prion-like phenotypes, as assayed on 1/4YPD medium. The white and pink colonies, potentially corresponding to the prion and non-prion forms of the protein, are stable on 1/4YPD medium, and the spontaneous conversion between the two prion states rarely occurred. Recombinant IAPP(S20G)-NM protein was expressed in *E. coli* and the purified protein formed amyloid fibers that

Figure 4-13. Kinetics of aggregation by Sup35NM or IAPP-NM with ΔNQ-NM seed.

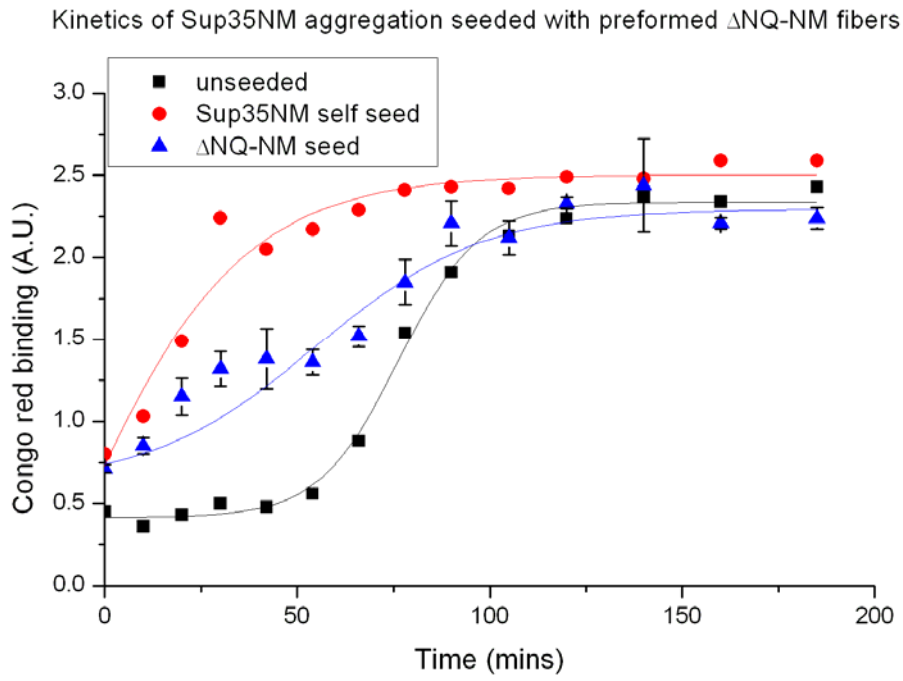

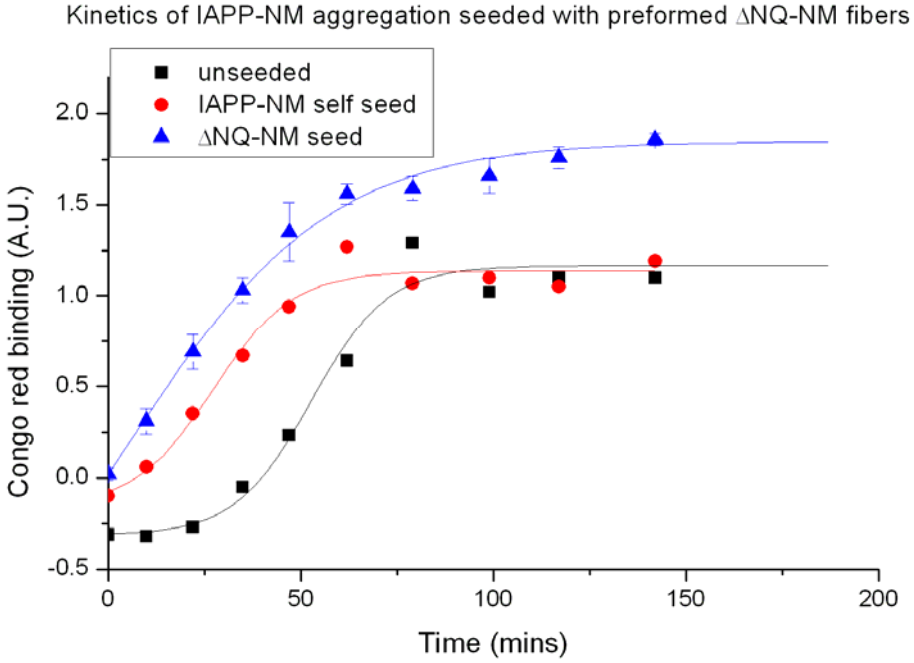

Figure 4-14. Kinetics of aggregation by ΔNQ-NM with Sup35NM or IAPP-NM seed.

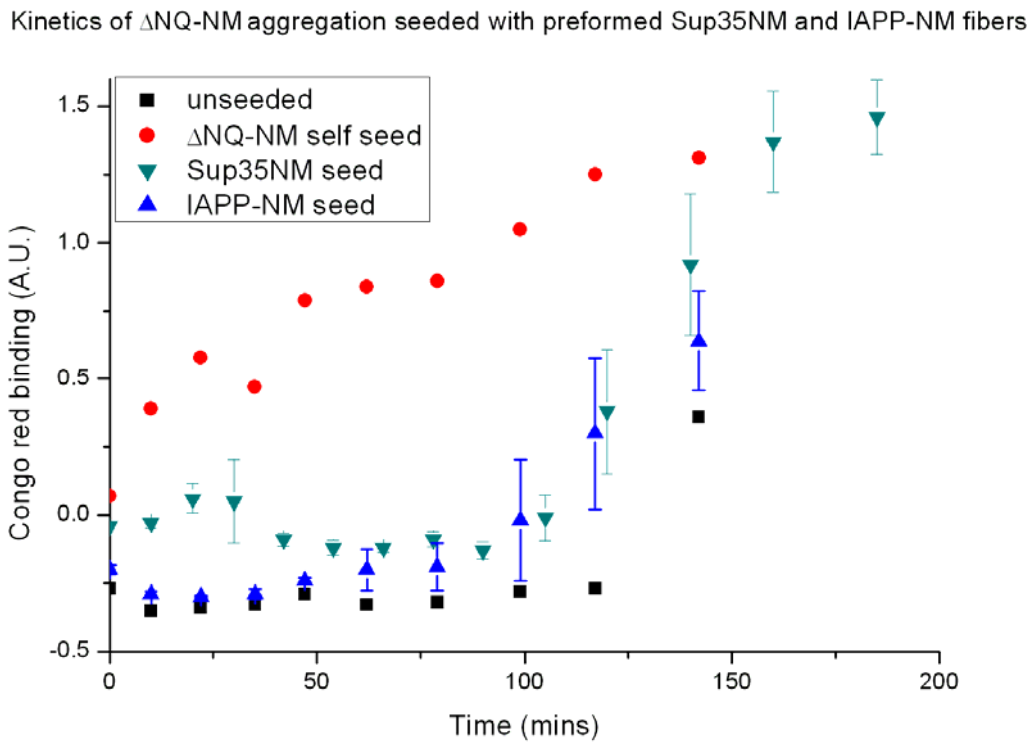

resembled IAPP-NM fibers (Figure 4-10).

Discussion

Researchers have shown that the aggregation domain NQ can be replaced by expanded polyglutamine (Q62) to generate a novel prion (Osherovich et al., 2004). Interestingly, the finding that Sup35p mutants with a shuffled N domain could form prions not only suggested that the primary sequence was not essential for the prion formation, but also emphasized the importance of the Asn/Gln content in the prion-forming domain (Ross et al., 2005). Due to the Asn/Gln-rich feature of the NQ domain, it remained uncertain whether non-Asn/Gln-rich polypeptides could be substituted for the NQ domain. In this study, a non-Asn/Gln-rich polypeptide, IAPP(8-37), was substituted for the NQ domain, and the substitution generated a novel prion.

The expression level of IAPP-GMC is important to its ability to form a prion. When both IAPP-GMC and NGMC were expressed on a single-copy number plasmid, the expression level of IAPP-GMC was lower than that of NGMC, possibly due to the codon usage of IAPP peptides and the slight variation at the starting region of translation introduced during the cloning steps. As a result of different expression levels, only the strains expressing NGMC, but not the ones expressing IAPP-GMC, on the single-copy number plasmid, were able to form prion. Although the IAPP-GMC cells exhibited

prion-like color on 1/4YPD medium, they were not prion because they only exhibit single phenotype and they were not affected by the methods that are typically employed to cure prions. The reason for the light color might be that there was not sufficient translation termination factor function due to a lower effective concentration of the C-terminal domain of Sup35p. When the expression level of IAPP-GMC was increased by using a high-copy number plasmid, the strain expressing IAPP-GMC exhibited two phenotypes, which was subsequently confirmed to be due to prion formation.

Various biochemical and genetic evidences support that [*I-PSI*$^+$] is a prion. [*I-PSI*$^+$] can arise spontaneously from [*i-psi*$^-$] cells; fluorescent foci are present in [*I-PSI*$^+$] cells, but not in [*i-psi*$^-$] cells; more proteins are located in the pellet portion in [*I-PSI*$^+$] cells than in [*i-psi*$^-$] cells; [*I-PSI*$^+$] can be inherited in a non-Mendelian way, as suggested by cytoduction, mating and sporulation; the overexpression of the prion-forming domain, as in IAPP-NR-M-GFP fusion protein, induces the conversion from [*i-psi*$^-$] to [*I-PSI*$^+$]; GuHCl treatment, *hsp104* deletion, and Hsp104p overproduction are capable of curing [*I-PSI*$^+$] prion. Combined together, these evidences indicate that [*I-PSI*$^+$] is a novel yeast prion.

The NQ domain of Sup35p appears to be a critical structural feature that is associated with the specificity of prion inheritance. The inability of isolated fibril preparations of Sup35-NM and IAPP-NM to effectively cross-seed each other suggests a transmissibility barrier between [*I-PSI*$^+$] and [*PSI*$^+$]. The overexpression of IAPP-M-GFP fusion protein failed to induce [*PSI*$^+$] formation, and [*PSI*$^+$] prion could not induce

[*I-PSI*$^{+}$] through cytoduction. These observations are remarkable considering that the only difference between the two proteins is the identity of the N-terminal domain of approximately 40 amino acids. These data support the hypothesis that the NQ domain is the aggregation unit for Sup35p. A recent finding also showed that the main nucleation site of Sup35 is located within the NQ domain (Tessier and Lindquist, 2007). Therefore, yeast prions can be used to study the cross-seeding effect between different proteins as they will not interfere with each other unless they can cross-seed. For instance, the interaction between Aß and IAPP can be studied in the context of yeast prion, as it was shown that Aß and IAPP fibers could seed each other *in vitro* (O'Nuallain et al., 2004). Yeast prions provide excellent model systems to study the cross-seeding activity, because the propagation can be monitored in living cells. Another aspect of the model resulting from this prion dissection is that the NR domain mediates the fragmentation of aggregates (Osherovich et al., 2004). The IAPP fusion proteins contain the intact NR domain; therefore, it is not surprising that the prion particles can be disaggregated by Hsp104 chaperon.

Since a parallel ß-sheet structure was observed in IAPP fibers (Jayasinghe and Langen, 2004), it is plausible that IAPP region of IAPP-Sup35 also adopts parallel packing. If IAPP-NM forms fibers with the IAPP region in the parallel packing, it is likely Sup35NM forms fibers with the NQ domain in the same parallel ß-sheet structure. Other packing structures for Sup35, however, should not be excluded based on this hypothesis, because the structure adopted by IAPP-Sup35 does not necessarily reflect

how the native Sup35p aggregates.

Although the deletion of the NQ domain from Sup35p prevents the protein from forming a prion, the ability of Sup35NM to form amyloid fibers *in vitro* is not abolished by NQ deletion. The results are not contradictory because of the huge difference between the reaction conditions *in vivo* and *in vitro*. Kinetics of the aggregation by ΔNQ-NM showed the same sigmoidal pattern, suggesting a nucleus-dependent growth. Preformed fibers by ΔNQ-NM are able to seed Sup35NM and IAPP-NM aggregation, indicating the aggregation domain in ΔNQ-NM is used in the seeding process. However, there is no seeding effect in the opposite direction, when preformed Sup35NM or IAPP-NM fibers are added to the aggregation of ΔNQ-NM. One explanation is that there are more than one aggregation units, or nucleation regions, in Sup35NM. As shown recently, there are two nucleation region in Sup35NM, the major one around the 20th residue within the NQ domain, and another one around the 100th residue with the NR domain (Tessier and Lindquist, 2007). When Sup35NM and, presumably, IAPP-NM form fibers on their own, they use mainly the NQ domain and IAPP as the nucleation region, respectively. In contrast, ΔNQ-NM forms fibers using the nucleation site in the NR domain because of the lack of the NQ domain. Therefore, when Sup35NM and IAPP-NM form fibers in the presence of ΔNQ-NM seeds, which expose the NR-domain nucleation region, they grow upon the seeds using the same nucleation region. However, ΔNQ-NM can not be recruited onto the fibers formed by Sup35NM and IAPP-NM, because it does not contain the same nucleation region as the ones exposed by the seeds (Figure 4-16).

In summary, the substitution of IAPP for the NQ domain has generated a chimeric Sup35p protein that is able to form prion. The prion status can be easily monitored and inherited with fidelity. Future mutagenesis study on IAPP might help reveal the individual residues that are important for the aggregation. It might also be useful in the screening of the drugs that can specifically inhibit IAPP aggregation. And finally, this study has expanded the possibility of Sup35 prion of serving as a model to study the aggregation of proteins.

Figure 4-15. A model for the specificity in the fiber aggregation. Sup35NM aggregates at the NQ nucleation site, and similarly, IAPP-NM aggregates at the IAPP nucleation site. ΔNQ-NM aggregates at the NR nucleation site, as it lacks the NQ nucleation site. The NQ and IAPP nucleation sites provide the specificity in fiber aggregation and prion propagation. Sup35NM and IAPP-NM can also aggregate at the NR nucleation site in the presence of pre-formed ΔNQ-NM fibers.

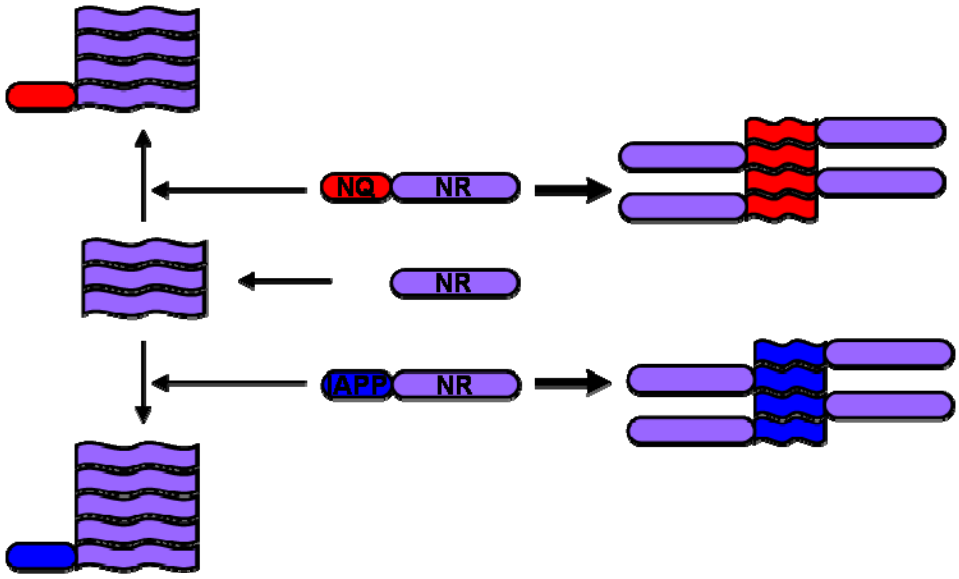

CHAPTER 5

The Substitution of a Bacterial Protein Fragment for the NR Domain of Sup35p Generated Prion-Like Phenotypes

Introduction

The N domain of Sup35p, the main driving force for prion propagation, consists of the Asn/Gln-rich subdomain (NQ) and the imperfect oligopeptide repeat subdomain (NR). While the NQ domain is important in initiating protein aggregation, the NR domain is also required for proper prion propagation. The NR domain consists of five and a half non-perfect repeats of the consensus sequence PQGGYQQ-YN (residues 40–112) (Crist et al., 2003; Liu and Lindquist, 1999; Parham et al., 2001). The length of the oligopeptide repeat is an important factor in determining the stability of Sup35 prion. Increasing the numbers of oligopeptide repeat causes more spontaneous *de novo* appearance of [*PSI*$^+$], while the truncation and deletion of the NR domain cause the destabilization and elimination of [*PSI*$^+$] (Liu and Lindquist, 1999). The minimum length required for stable [*PSI*$^+$] propagation, as suggested by a systematic deletion analysis of the NR domain, is the N-terminal 1-93 residues that consists of the NQ domain and five oligopeptide repeats (Osherovich et al., 2004; Parham et al., 2001). The NR domain is also suggested

to regulate the strain variation of [*PSI*$^{+}$] by its different folding in the aggregates, as different lengths of oligopeptide repeats are required for the maintenance of different strains (Shkundina et al., 2006).

The requirement of the NR domain for the stable inheritance of prion aggregates is proposed to result from its capability of mediating their fragmentation by the chaperone Hsp104p (Osherovich et al., 2004). The proposal is plausible and agrees with experimental results; however, it does not specify how Hsp104 chaperone recognizes and interacts with the NR domain. The repeating pattern of the NR domain suggests that the consensus sequence PQGGYQQ-YN may be recognized by the chaperone. Meanwhile, the content of Asn/Gln residues in the NR domain is abnormally high (~40%), which suggests the high Asn/Gln content to be responsible for the recognition by the chaperone. The latter hypothesis is supported by the finding that variants of Sup35p with randomized amino acid sequences in the N domain are also capable of forming prions in vivo (Ross et al., 2005). It is important to understand how the NR domain contributes to the prion propagation because it will not only help to understand the mechanism involved in other prions, but also provide a guideline in searching for the new proteins that are prone to form prions.

In this study, an approach was taken to further understand whether the consensus sequence or the Asn/Gln content is important in the NR domain. A bacterial peptide fragment that is totally different from the NR domain in primary sequence but similar as NR domain in Asn/Gln content was substituted for the NR domain of Sup35p (Figure

5-1). It was shown that the yeast strains containing the Sup35 mutant showed prion-like phenotypes, which strengthened the importance of the high content of Asn/Gln residues.

Experimental Procedures

Plasmids construction

DNA encoding three bacterial oligopeptide repeats (*bac3*) was generated by annealing together oligonucleotides BACPRION-F and BACPRION-R, and it was cloned into plasmid pZerO2 at *Hin*d III/*Bam*H I sites. Degenerate codons were incorporated in the design of the oligonucleotides in order to randomize the codon usage and diversify the DNA sequences. The generated plasmids were sequenced, and four plasmids with different DNA sequences and same protein sequence were obtained. The plasmids were name as pJET74a, pJET74b, pJET74c, and pJET74d. The previously described seamless strategy was used to multimerize *bac3* gene. The *bac3* cassette was prepared by the digesting pJET74a with *Bbs* I and *Bsm*B I, the *bac3*-flanking type IIs restriction enzymes that were introduced into the oligonucleotides in their design, and the digestion product self-ligated in a head-to-tail fashion to generate *bac6* and *bac9*, which encode for six and nine bacterial oligopeptide repeats, respectively. To construct the adaptor plasmid for the *bac* (*bac3*, *bac6*, and *bac9*) genes, pZerO1+NM was amplified by an inverted PCR, using NM_BAC_ADAPTOR-F and NM_BAC_ADAPTOR-R as primers. The amplification product was digested with *Bgl* II, and then self-ligated to

Figure 5-1. The amino acid sequence of MshL protein in *Magnetococcus sp. MC-1*

(NCBI-GI: 117926538).

```
  1 MNRQEKTMSR QMTIHKYAPC VSWKTGLVLG LVGLLSLSAC QTPSSITPSK QHFLRPTDPP
 61 PGALTTALPP EAQDVVADTG QADMEEGDQI SITVNDTPAR TVLLALARDT KKNLDIHPGI
121 QGNVTISVVN QTLPRVLERI AKQVNMRYEI NGDTIQVYPD KAFLKIYQVD YVNIVRSSKT
181 TNKISTQLDT NSAMDPAMAG KEVPNQSDMT LTTDFKNDFW ASLTANITAI VSQGQASAPE
241 ALPAMANGSL PLPSAAPGGT ASPAKAEPKV TSSGVVSINQ ETGVISIFAT AADHERIGSY
301 LESLMENAHR QVLIESTVVE VTLSDDHQQG VDWASINDDG LSRLSAPFFA NSIGVNGGSR
361 PMALSDLPVF SLPTSINSGF GKITSTVRAL AKFGNTKVLS SPKIMALNNQ TAVLKVVDNT
421 VFFTVEAEAG SSANASGGTD TTALINTRVH TVPVGLVMSV TPQISADDVV TLNVRPTISS
481 VSRWVSDPNP HLNAGVENLI PEIQVKEMES ILRVHSGQIT VMGGLMQDKI SKVDTGLPLI
541 SQVPGIGGLF GYKEKTVSKT ELVIFMRPVV MTHGKPRGVA VANSGSSTNT VITPRTMVAP
601 DPAALSAAEA PVMQPREPQA SSGGYLNFTN GGQASSYAAP AAPVSPSVVM PQAGMRSPSM
661 TPQAENPSAW NGQQQVVPTT YTGGSQQQGY AQPMQQQGYY QPVQQQGYAQ PMQQQGYYQP
721 MQQQGYAQPM QQQGYAQPMQ QQGYAQPMQQ QGYAQPMQQQ GYAQPMQQQG YAQPVAPAAY
781 GMSQGYANPN VALQPSTMGY PVMPNDQQMV AAPDPSMMVQ PVPVSPTATH
```

Repeat 1	**QPMQQQGYY**
Repeat 2	**QPVQQQGYA**
Repeat 3	**QPMQQQGYY**
Repeat 4	**QPMQQQGYA**
Repeat 5	**QPMQQQGYA**
Repeat 6	**QPMQQQGYA**
Repeat 7	**QPMQQQGYA**
Repeat 8	**QPMQQQGYA**
Repeat 9	**QPMQQQGYA**
Consensus sequence	**QPMQQQGYA**

make pJET75. The *bac* gene fragments prepared with *Bbs* I/*Bsm*B I digestion were ligated into pJET75 vector prepared with *Bsm*B I double digestion. For instance, *bac3* was subcloned into pJET75 to make pJET134, and peptide repeats Bac3 was fused in frame with the NQ domain and substituted for the NR domain. Subsequently, NQ-Bac fusions were subcloned into pJET101, the *HIS3*-marked plasmid containing SUP35 (described in previous chapters), at *Bam*H I/*Pfl*M I sites to make the plasmids encoding for NQ-Bac-M-C fusion proteins (Figure 5-2).

To construct the plasmids for the expression of NQ-Bac6-M fusion protein in *E. coli*, pJET137 was PCR amplified using primers colinF/0313R and the product was inserted into pET21a at *Nde* I/*Bam*H I sites. The plasmids and oligonucleotides used in this study are listed in Table 5-1 and 5-2.

Strains

Yeast strain GT17k was engineered from GT17 by knocking out the chromosomal *sup35* gene with *sup35::KanMX* (Chapter 2). The *ade1-14* mutation allows the identification of prion through color assay on YPD medium. The formation of prion leads to the inactivation of Sup35 and the read-through of the stop codon in *ade1*, causing the white color on YPD medium plates; however, cells containing no prion accumulate red pigment due to the truncation of Ade1p, causing the red color on YPD medium plates.

Figure 5-2. Diagrams of the representative plasmids in this study.

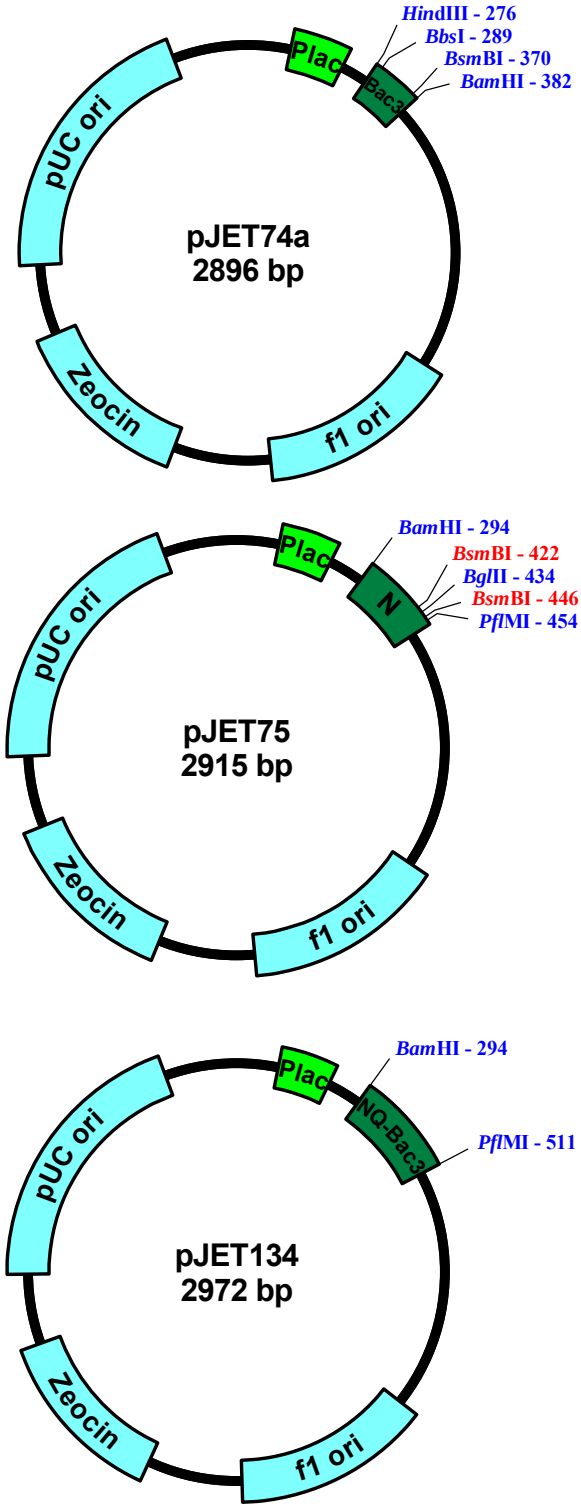

Table 5-1. Plasmids used in this study.

Plasmids	Characteristics	References
pZerO1	Zero background cloning vector	Invitrogen
pZerO2	Zero background cloning vector	Invitrogen
pRS313	Yeast shuttle vector, *CEN, HIS3,* Amp^R	(Sikorski and Hieter, 1989)
pRS426	Yeast shuttle vector, 2μ, *URA3,* Amp^R	(Sikorski and Hieter, 1989)
pJET101	pRS313, P_{SUP35}, *SUP35*	Chapter 2
p316-Sp-Sup35	pRS316, P_{SUP35}, *SUP35*	(DePace et al., 1998)
pZerO1+NM	pZerO1, sup35-NM	Chapter 2
pJET74a	pZerO2, *bac3(a)*	this study
pJET74c	pZerO2, *bac3(c)*	this study
pJET74d	pZerO2, *bac3(d)*	this study
pJET74.da	pZerO2, *bac6*	this study
pJET74.dac	pZerO2, *bac9*	this study
pJET75	pZerO2, *bac adaptor* pZerO1+NM inverse PCR, *Bgl*II, self-ligation	this study
pJET134	pZErO-1, *sup35-NM(Δ40-92::bac3)* pJET75(*Bsm*B I) ← pJET74.a (*Bbs* I/*Bsm*B I)	this study
pJET135	pZErO-1, *sup35-NM(Δ40-92::bac6)* pJET75(*Bsm*B I) ← pJET74.da (*Bbs* I/*Bsm*B I)	this study
pJET76	pZErO-1, *sup35-NM(Δ40-92::bac9)* pJET75(*Bsm*B I) ← pJET74.dac(*Bbs* I/*Bsm*B I)	this study

Plasmids	**Characteristics**	**References**
pJET136	pRS313, P_{SUP35}, *sup35(Δ40-92::bac3)* pJET101 ← pJET134 (*Bam*H I/*Pfl*M I)	this study
pJET137	pRS313, P_{SUP35}, *sup35(Δ40-92::bac6)* pJET101 ← pJET135 (*Bam*H I/*Pfl*M I)	this study
pJET94	pRS313, P_{SUP35}, *sup35(Δ40-92::bac9)*	this study
pJET138	pRS426, P_{CUP1}, *sup35NM(Δ40-92::bac3)-GFP* pJET108 ← pJET134 (*Bam*H I/*Pfl*M I)	this study
pJET139	pRS426, P_{CUP1}, *sup35NM(Δ40-92::bac6)-GFP* pJET108 ← pJET135 (*Bam*H I/*Pfl*M I)	this study
pJET85	pRS316, P_{CUP1}, *sup35NM(Δ40-92::bac9)-GFP*	this study
pJET114	pRS426, P_{CUP1}, *HSP104*	Chapter 3
pJET154.Bac6	pET21a, *sup35-NM(Δ40-92::bac6)-(His)$_6$* pET21a ← Bac6 PCR (*Nde* I/*Bam*H I)	this study

Table 5-2. The oligonucleotides used in this study.

Name	Sequence
BACPRI-F	5’-*AGCTT*GAAGACCAACCAATGCARCAACARGGWTAYGCHCARCCWATGCARCARCAAGGWTAYGCHCARCCWATGCARCAACARGGWTAYGCHCAACCAAGAGACGG-3’
BACPRI-R	5’-*GATCC*CGTCTCTTGGTTGDGCRTAWCCYTGTTGYTGCATWGGYTGDGCRTAWCCTTGYTGYTGCATWGGYTGDGCRTAWCCYTGTTGYTGCATTGGTTGGTCTTCA-3’
NM_BAC_ADAPTOR-F	5’-GCCTTA*AGATCT*CGTCTCAACCACAAGGTGGCCGTGGAAATTAC-3’
NM_BAC_ADAPTOR-R	5’-GGCAT*AGATCT*CGTCTCTTGGTTGGGCTTGAGCATTGTAAGCTTGATAACC-3’
colinF	5’-GCTTA*CATATG*TCGGATTCAAACCAAGGCAAC-3’
0313R	5’-ACT*GGATCC*ATATCGTTAACAACTTCGTC-3’

Gene replacement

Various *bac-sup35* genes with different numbers of repeats were substituted for wild type *SUP35* gene by plasmids shuffling. GT17k harboring *URA3*-marked *SUP35* was transformed with *HIS3*-marked *bac-sup35* plasmids. The transformants were incubated on SD-His medium to allow the loss of the *URA3* plasmids, and the cells abolishing the *URA3* plasmids were selected on SD-His+5-FOA.

***In vitro* characterization of Bac6-NM protein**

Bac6-NM protein was cloned into pET21a to facilitate its overexpression and purification through the attached C-terminal 6 x His tag. The protein was expressed and purified as described previously (Chapter 4). Purified protein was methanol precipitated and resuspended in 6 M GuHCl overnight to disaggregate preformed polymers. To initiate the fiber formation, protein was diluted by 100 times to the Congo red binding buffer (CRBB) to the final concentration of 2.5 μM. Using the method described in Chapter 4, the aggregation was monitored by its ability to bind Congo red and calculated according to the absorbance spectrum shift of the dye upon the formation of the aggregates.

Results

Selection of an NR-like bacterial oligopeptide repeats fragment

In this study, we searched NCBI protein database for a sequence showing similarity in Asn/Gln content to the NR domain of Sup35p, and found a protein containing such oligopeptide repeats region. The protein (NCBI-GI: 117926538) is from strain *Magnetococcus sp. MC-1*, a magnetotactic bacterium that is characterized by its ability to synthesize intracellular magnetite (Meldrum et al., 1993). According to its sequence, the protein is conjectured as a pilus (MSHA type) biogenesis protein MshL, although its detailed function is unclear. The protein is 830 amino acids in length, and located near its C-terminus is a region (aa 692-772) consisting of nine oligopeptide repeats with the consensus sequence QPMQQQGYA (Figure 5-1). The primary sequence of the oligopeptide is different than the consensus sequence of the NR domain of Sup35p, PQGGYQQ-YN; however, their contents of Asn/Gln residues are similar to each other (~44%). Therefore, the oligopeptide was selected to study its ability to replace the NR domain of Sup35p.

The substitution of Bac6 repeats generated prion-like phenotypes.

The original replacement of native oligopeptide repeats by Bac6 generated red colonies on YPD medium, indicating the absence of prion. By streaking the cells out on YPD medium plate and searching for the spontaneous conversion to white color, the *de*

novo formation of prion was discovered (Figure 5-3). The cells were tested for their growth on SD-Ade medium, and the white cells grew while the red cells could not grow (data not shown). The two phenotypes exhibited by the same strain suggested the presence and absence of the prion, and the white prion strain was named as [$BAC6^{+}$] and the red non-prion state was named as [$bac6^{-}$] for simplification.

The effect of Hsp104 chaperone on [*BAC6*$^{+}$] prion.

Growing on low concentration of GuHCl was sufficient for curing the prions. By passing [$BAC6^{+}$] cells on YPD medium containing 5 mM GuHCl for 3 times, all the cells became red on the subsequent YPD medium. In addition, the chromosomal deletion of *hsp104* gene cured [$BAC6^{+}$] prion completely (Figure 5-3). Overexpression of Hsp104p in the presence of inducer $CuSO_4$ converted the [$BAC6^{+}$] strain to its non-prion state. Even in the absence of $CuSO_4$, the leaky expression of Hsp104p from the plasmid, besides the normal expression from the chromosome, was sufficient to cure [$BAC6^{+}$] prion.

Bac6-NM protein aggregated in a nucleation-dependent pattern.

NQ-Bac6-M protein (Bac6-NM) was expressed in *E. coli* with 6xHis tag attached to the C-terminal end, and purified as described. The 6xHis tag is believed not to affect the assembly of the protein, whose aggregation core is located at the N-terminus. The molecular size of the protein was verified with MALDI-MS. The protein formed

Figure 5-3. The growth of cells expressing NQ-Bac6-MC on 1/4YPD medium and the effect of Hsp104 deletion and overexpression on [*BAC6*$^{+}$] prion.

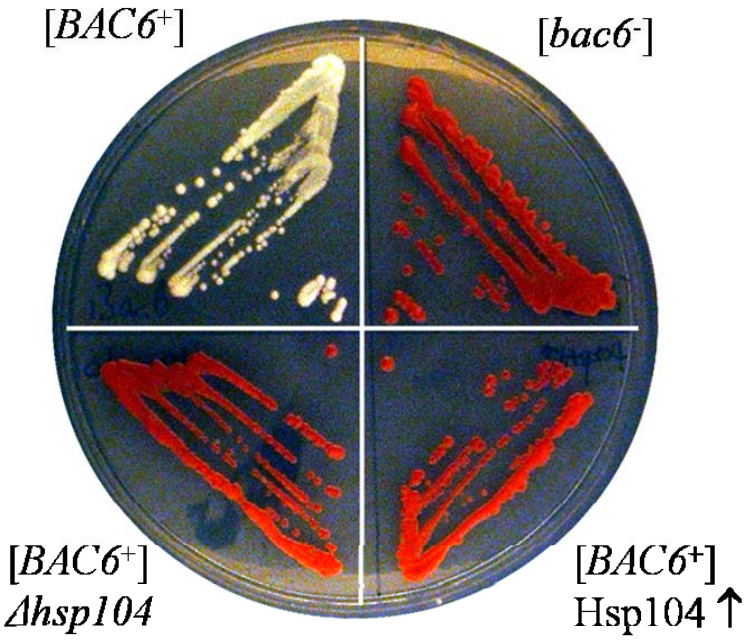

aggregates that bound to the dye Congo red after diluted from the concentrated denaturing buffer into native CRBB buffer at room temperature. The kinetics of the aggregation, monitored by its Congo red binding, showed a sigmoidal growth curve typical for nucleation-dependent fiber growth reactions (Figure 5-4). The lag phase of the aggregation, which is believed to reflect the initial formation of nucleus for the protein assembly, was eliminated by the addition of 5% preformed aggregates.

Discussion

Although progress has been made to illustrate the reason why the oligopeptide repeats region of Sup35p is important for the propagation of the yeast prion [*PSI*$^{+}$], the detailed mechanism still remains unclear. This dissection study of the yeast prion has suggested that the oligopeptide repeats mediate the interaction of the Sup35p aggregate with Hsp104p, a chaperone required for prion division (Osherovich et al., 2004). Although the repeating pattern might seem to be necessary for the recognition by Hsp104p, the amino acid composition within this region has been shown to act as the primary factor assisting prion propagation (Ross et al., 2005). The main requirement for the prion forming domain may not be any particular sequence, but the rich Asn/Gln content (Ross et al., 2005). Meanwhile, additional features including the alteration of polar and hydrophobic stretches have been shown to play important roles for another yeast prion [*PIN*$^{+}$] (Vitrenko et al., 2007).

Figure 5-4. Kinetics of the aggregation by Bac6-NM protein.

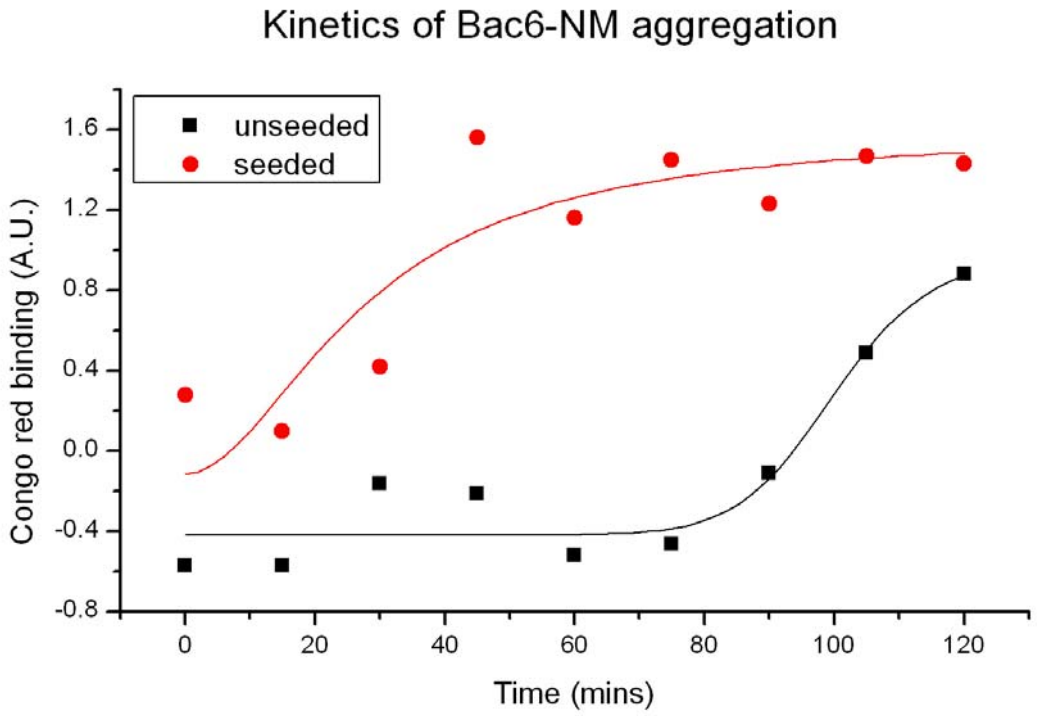

To further study the contribution of Asn/Gln residues to prion propagation, a bacterial protein containing an Asn/Gln-rich oligopeptide repeats stretch is selected from NCBI databank. The stretch consists of solely nine oligopeptide repeats with the consensus sequence QPMQQQGYA, which is similar in Asn/Gln content to the consensus sequence PQGGYQQ-YN of the NR domain. When a shorter version of the bacterial protein fragment, which consists of six oligopeptide repeats, is substituted for NR of Sup35p, the host cells expressing the mutant protein exhibits prion-like phenotypes. The cells in the hypothesized prion state can be cured by GuHCl treatment, *hsp104* deletion, and Hsp104p overproduction. Considering that the NR domain mediates prion propagation through its interaction with Hsp104p chaperone, it is suggested that the bacterial oligopeptide repeats can also be recognized by Hsp104 chaperone. Therefore, it further supports that Asn/Gln content is important and may be the sole requirement to mediate prion propagation.

The importance of the rich Asn/Gln content has resulted in the search for new prions and the discovery of the yeast prion [NU^{+}]. However, it remains a mystery whether prokaryotic prions exist in nature despite the existence of the Asn/Gln-rich amino acid sequences in prokaryotic organisms. The two components of yeast prion proteins, the aggregation domain (NQ) and the propagation domain (NR), likely have their counterparts in bacteria; for example, the protein forming curli fibers in *E. coli* can be regarded as an equivalent to the aggregation domain (Olsen et al., 1989), and the propagation domain may also exist, like reported in this study. As a result, bacterial

prions may be able to form in nature. However, it still depends on the existence of bacterial Hsp104p homologs and how they function. As an advantageous way of regulating cells to adapt to their environments, prions should provide an evolutionary advantage to bacteria as well. It will be interesting to find or generate genuine prokaryotic prions, which will further help investigate the mechanism of prion propagation and study the evolution of prions.

CHAPTER 6

Summary

Researchers have made a great deal of progress in understanding yeast prions since the prion concept was proposed to explain the non-Mendelian inheritance in yeast strains (Wickner, 1994). More yeast prions have been identified, and numerous biochemical and genetic evidences have been found to support the protein-only concept. The studies on yeast prions have revealed the mechanism how prions form and propagate, which provides important clues for studying mammalian prions and other protein aggregates that are often involve in protein misfolding diseases.

It is one of many important findings that the prion forming domain of Sup35p can be further divided into the Asn/Gln-rich domain (NQ) and the oligopeptide repeats domain (NR), which are proposed to be responsible for protein aggregation and prion propagation, respectively (Osherovich et al., 2004). Based on this proposal, the extended polyglutamine sequence was substituted for the NQ domain and a novel prion was created (Osherovich et al., 2004). In this study, in order to generalize this hypothesis, various other aggregation-prone proteins have been selected as the candidates that can potentially replace the NQ domain and generate novel prions. As described in Chapter 2, these proteins function differently as regard to there abilities to maintain cell survival and

exhibit prion-like phenotypes.

In Chapter 3, a detailed examination of Syn1 peptide, an aggregation fragment of α-synuclein, shows that its substitution for the NQ domain enables the host strains to adopt two distinct phenotypes. Although direct evidences are still needed, the results strongly suggest that it is a new prion, [*SYN1*$^{+}$]. It is interesting that [*SYN1*$^{+}$] can be formed from the automatic conversion from its non-prion state, [*syn1*$^{-}$], at a very high frequency. The reason for the abnormally high conversion rate is thought to be associated with the strong tendency of syn1 to aggregate, as the introduction of A76E and A76R mutations, which can increase the lag phase of the aggregation *in vitro*, is able to decrease the rate of *de novo* prion formations. Another reason might be that the prion particles formed by Syn1-substituted Sup35p do not form the deal-end aggregate products easily, and these small prion particles can be disaggregated more efficiently to generate more prion seeds. This hypothesis agrees with the diffuse fluorescence exhibited by Syn1-M-GFP fusion protein even in [*SYN1*$^{+}$] cells.

In Chapter 4, IAPP(8-37) fragment from islet amyloid polypeptide is substituted for the NQ domain of Sup35p. To make a stable prion that can be cured by GuHCl, the expression level is elevated by using a high-copy number plasmid. Therefore, the appropriate level of expression is necessary for the mutant protein to form a prion. The protein forms a prion [*I-PSI*$^{+}$], as supported by various evidences obtained from fluorescence foci detection, protein sedimentation assay, cytoduction, mating and sporulation. The overexpression of IAPP-NR-M-GFP fusion protein induces the de novo

formation of prion from the non-prion cells. In addition, [*I-PSI*$^{+}$] prion can be cured by GuHCl treatment, *hsp104* deletion, and Hsp104p overproduction, suggesting that its propagation involves the interaction between prion particles and Hsp104 chaperone. *In vitro*, IAPP-substituted Sup35NM protein forms amyloid fibers that resemble those formed by native Sup35NM. The kinetics of the spontaneous amyloid formation exhibits a profile consisting of an initial lag phase followed by a rapid growth phase terminating at a plateau, which is typical for nucleation-dependent amyloid formation. The lag phase is eliminated by the addition of preformed IAPP-NM fibers, but not Sup35NM fibers, suggesting that IAPP-NM fibers can specifically promote the aggregation by recruiting soluble monomeric proteins from the solution.

The NR domain of Sup35p, which is proposed to be responsible for prion propagation, consists of five and half imperfect oligopeptide repeats. It remains unclear whether the consensus sequence or the Asn/Gln content is important for the contribution of the NR domain to prion propagation. In Chapter 5, a bacterial protein fragment with different primary sequence but similar Asn/Gln content is substituted for the NR domain of Sup35p. The six-repeat truncation of the protein fragment, which originally consists of nine oligopeptide repeats, appears to be able to replace the NR domain and assist prion propagation. Therefore, it further supports that Asn/Gln content is important and may be the sole requirement to mediate prion propagation.

Based on the above results, some factors in generating novel yeast prions by the substitution for the NQ domain needed to be considered. Firstly, the tendency of the

candidate protein to aggregate should not be too strong, otherwise the mutant proteins would aggregate too much to maintain the cell survival. Furthermore, for better results, the proteins can be expressed at different levels as the expression level is important for prion formation. Last but not least, multiple experimental methods should be utilized to assess prion formation as each individual prion variant may exhibit idiosyncratic phenotypes. For instance, the color development assay can be conducted on either YPD or 1/4YPD, depending on which medium gives better contrast between prion and non-prion strains.

In summary, novel yeast prions have been generated by the substitution of aggregation-prone proteins for the NQ domain of Sup35p. It has been shown that the proteins capable of serving as the aggregation unit are not restricted to Asn/Gln-rich proteins, thus this model system can be used to study more aggregation-prone proteins. In the context of yeast prions, protein aggregation can be investigated *in vivo*. The model can be useful in identifying the factors important for protein aggregation, such as amino acid composition, growing condition, and small molecules. Mutations introduced by site-directed or random mutagenesis can help to locate the critical residues in the aggregation, as a change in the aggregation propensity may be reflected in the stability of the related prion. In addition, the model may provide a tool to screen drugs that can inhibit or counteract the aggregation of certain proteins, ideally in a specific fashion, by screening for small molecules that inhibit the propagation of the corresponding prions.

References

Abedini A. and Raleigh D. P. (2006) Destabilization of human IAPP amyloid fibrils by proline mutations outside of the putative amyloidogenic domain: is there a critical amyloidogenic domain in human IAPP? *Journal of Molecular Biology* **355**, 274-281.

Anfinsen C. and Haber E. (1961) Studies on the reduction and re-formation of protein disulfide bonds. *Journal of Biological Chemistry* **236**, 1361-1363.

Anguiano M., Nowak R. and Lansbury Jr P. (2002) Protofibrillar islet amyloid polypeptide permeabilizes synthetic vesicles by a pore-like mechanism that may be relevant to type II diabetes. *Biochemistry* **41**, 11338-11343.

Aylon Y., Liefshitz B. and Kupiec M. (2004) The CDK regulates repair of double-strand breaks by homologous recombination during the cell cycle. *The EMBO Journal* **23**, 4868-4875.

Bach S., Talarek N., Andrieu T., Vierfond J., Mettey Y., Galons H., Dormont D., Meijer L., Cullin C. and Blondel M. (2003) Isolation of drugs active against mammalian prions using a yeast-based screening assay. *Nature Biotechnology* **21**, 1075-1081.

Balbirnie M., Grothe R. and Eisenberg D. (2001) An amyloid-forming peptide from the yeast prion Sup35 reveals a dehydrated beta-sheet structure for amyloid. *Proceedings of the National Academy of Sciences* **98**, 2375.

Benzinger, T.L.S., Gregory, D.M., Burkoth, T.S., Miller-Auer, H., Lynn, D.G., Botto, R.E. and Meredith, S.C. (1998) Propagating structure of Alzheimer's -amyloid(10-35) is parallel-sheet with residues in exact register. *Proceedings of the National Academy of Sciences* **95**, 13407-13412

Borchsenius A., Wegrzyn R., Newnam G., Inge-Vechtomov S. and Chernoff Y. (2001) Yeast prion protein derivative defective in aggregate shearing and production of new 'seeds'. *EMBO J.* **20**, 6683-6691.

Bueler H. (1993) Mice devoid of PrP are resistant to scrapie. *Cell* **73**, 1339-1347.

Byrne L. J., Cox B. S., Cole D. J., Ridout M. S., Morgan B. J. T. and Tuite M. F. (2007) Cell division is essential for elimination of the yeast [PSI+] prion by guanidine hydrochloride. *PNAS.* **104,** 11688-11693.

Carrell R. W. and Lomas D. A. (1997) Conformational disease. *The Lancet* **350**, 134-138.

Carrell R. W. and Lomas D. A. (2002) Mechanisms of disease. Alpha1-antitrypsin deficiency - a model for conformational diseases. *N. Engl. J. Med.* **346**, 45-53.

Chandra S., Gallardo G., Fernandez-Chacon R., Schluter O. M. and Sudhof T. C. (2005) [alpha]-synuclein cooperates with CSP[alpha] in preventing neurodegeneration. *Cell* **123**, 383-396.

Chernoff Y., Lindquist S., Ono B., Inge-Vechtomov S. and Liebman S. (1995) Role of the chaperone protein Hsp104 in propagation of the yeast prion-like factor [PSI+]. *Science* **268,** 880-884.

Chernoff Y., Uptain S. and Lindquist S. (2002) Analysis of prion factors in yeast. *Methods Enzymol* **351**, 499-538.

Chien P., Weissman J. S. and DePace A. H. (2004) Emerging principles of conformation-based prion inheritance. *Annual Review of Biochemistry* **73**, 617-656.

Clark P. (2004) Protein folding in the cell: reshaping the folding funnel. *Trends Biochem. Sci* **29**, 527-534.

Cohen F. E. and Kelly J. W. (2003) Therapeutic approaches to protein-misfolding diseases. **426**, 905-909.

Conde J. and Fink G. (1976) A Mutant of Saccharomyces cerevisiae Defective for Nuclear Fusion. *Proceedings of the National Academy of Sciences* **73**, 3651-3655.

Coustou V., Deleu C., Saupe S. and Begueret J. (1997) The protein product of the het-s heterokaryon incompatibility gene of the fungus *Podospora anserina* behaves as a prion analog. *Proceedings of the National Academy of Sciences*, **94,** 9773-9778.

Cox B. (1965) [PSI], a cytoplasmic suppressor of super-suppression in yeast. *Heredity* **20,** 505.

Cox B., Ness F. and Tuite M. (2003) Analysis of the generation and segregation of propagons: entities that propagate the [PSI+] prion in yeast. *Genetics* 1**65,** 23-33.

Cox B., Tuite M. and McLaughlin C. (1988) The PSI factor of yeast: a problem in inheritance. Y*east* **4,** 159-178.

Crist C., Nakayashiki T., Kurahashi H. and Nakamura Y. (2003) [PHI+], a novel Sup35-prion variant propagated with non-Gln/Asn oligopeptide repeats in the absence of the chaperone protein Hsp104. G*enes to Cells* **8,** 603-618.

DePace A. and Weissman J. (2002) Origins and kinetic consequences of diversity in Sup35 yeast prion fibers. N*at Struct Biol* **9,** 389-396.

DePace A. H., Santoso A., Hillner P. and Weissman J. S. (1998) A critical role for amino-terminal glutamine/asparagine repeats in the formation and propagation of a yeast prion. **93,** 1241-1252.

Derkatch I. L., Bradley M. E., Hong J. Y. and Liebman S. W. (2001) Prions affect the appearance of other prions: the story of [PIN+]. C*ell* **106,** 171-182.

Derkatch I. L., Bradley M. E., Zhou P., Chernoff Y. O. and Liebman S. W. (1997) Genetic and Environmental Factors Affecting the de novo Appearance of the [PSI(+)] Prion in Saccharomyces cerevisiae. G*enetics* **147,** 507-519.

Derkatch I. L., Chernoff Y. O., Kushnirov V. V., Inge-Vechtomov S. G. and Liebman S. W. (1996) Genesis and variability of [PSI] prion factors in *Saccharomyces cerevisiae*. G*enetics* **144,** 1375-1386.

Dobson C. M. (2003a) Protein folding and disease: a view from the First Horizon Symposium. N*ature Rev. Drug Discov.* **2,** 154-160.

Dobson C. M. (2003b) Protein folding and misfolding. N*ature* **426,** 884-890.

Dobson C. M., Sali A. and Karplus M. (1998) Protein folding: a perspective from theory and experiment. A*ngew. Chem. Int. Ed. Eng.* **37,** 868-893.

Ferreira P., Ness F., Edwards S., Cox B. and Tuite M. (2001) The elimination of the yeast [PSI] prion by guanidine hydrochloride is the result of Hsp104 inactivation. M*ol. Microbiol* **40,** 1357-1369.

Gebre-Medhin S., Olofsson C. and Mulder H. (2000) Islet amyloid polypeptide in the islets of Langerhans: friend or foe? D*iabetologia* **43,** 687-695.

Giaever G., Chu A., Ni L., Connelly C., Riles L., Vonneau S., Dow S., Lucau-Danila A.,

Anderson K. and Andre B. (2002) Functional profiling of the Saccharomyces cerevisiae genome. Nat*ure* **418,** 387-391.

Giasson B., Murray I., Trojanowski J. and Lee V. (2001) A hydrophobic stretch of 12 amino acid residues in the middle of a-synuclein is essential for filament assembly. *Journal of Biological Chemistry* **276,** 2380-2386.

Giasson B. I. (2004) Mitochondrial injury: a hot spot for parkinsonism and parkinson's disease? *Sci. Aging Knowl. Environ.* **2004,** pe42.

Glover J., Kowal A., Schirmer E., Patino M., Liu J. and Lindquist S. (1997) Self-seeded fibers formed by Sup35, the protein determinant of [PSI+], a heritable prion-like factor of *S. cerevisiae. Cell* **89,** 811-819.

Glover J. and Lindquist S. (1998) Hsp104, Hsp70, and Hsp40: a novel chaperone system that rescues previously aggregated proteins. *Cell* **94,** 73-82.

Goedert M. (2001) Alpha-synuclein and neurodegenerative diseases. *Nat Rev Neurosci* **2**, 492-501.

Goldberg A. L. (2003) Protein degradation and protection against misfolded or damaged proteins. *Nature* **426,** 895-899.

Greenbaum E. A., Graves C. L., Mishizen-Eberz A. J., Lupoli M. A., Lynch D. R., Englander S. W., Axelsen P. H. and Giasson B. I. (2005) The E46K mutation in {alpha}-synuclein increases amyloid fibril formation. *J. Biol. Chem.* **280,** 7800-7807.

Gregersen N., Bross P., Vang S. and Christensen J. H. (2006) Protein misfolding and human disease. *Annual Review of Genomics and Human Genetics* **7,** 103-124.

Hara H., Nakayashiki T., Crist C. G. and Nakamura Y. (2003) Prion domain interaction responsible for species discrimination in yeast [PSI+] transmission. *Genes to Cells* **8**, 925-939.

Howard M. and Welch W. J. (2002) Manipulating the folding pathway of [Delta]F508 CFTR using chemical chaperones. *Methods Mol. Med.* **70,** 267-275.

Jaikaran E., Higham C., Serpell L., Zurdo J., Gross M., Clark A. and Fraser P. (2001) Identification of a novel human islet amyloid polypeptide b-sheet domain and factors influencing fibrillogenesis. *J. Mol. Biol* **308,** 515-525.

James T., Liu H., Ulyanov N., Farr-Jones S., Zhang H., Donne D., Kaneko K., Groth D., Mehlhorn I. and Prusiner S. (1997) Solution structure of a 142-residue recombinant prion protein corresponding to the infectious fragment of the scrapie isoform. *Proceedings of the National Academy of Sciences*, **94,** 10086-10091.

Jaroniec C. P., MacPhee C.E., Astrof N.S., Dobson C.M. and Griffin R.G. (2002) Molecular conformation of a peptide fragment of transthyretin in an amyloid fibril. *Proc Natl Acad Sci U S A.* **99,** 16748-16753.

Jayasinghe S. A. and Langen R. (2004) Identifying structural features of fibrillar islet amyloid polypeptide using site-directed spin labeling. *J. Biol. Chem.* **279,** 48420-48425.

Jones G. and Masison D. (2003) Saccharomyces cerevisiae Hsp70 mutations affect [PSI+] prion propagation and cell growth differently and implicate Hsp40 and tetratricopeptide repeat cochaperones in impairment of [PSI+]. *Genetics* **163,** 495-506.

King C.-Y. and Diaz-Avalos R. (2004) Protein-only transmission of three yeast prion strains. *Nature.* **428,** 319-323.

Krishnan R. and Lindquist S. (2005) Structural insights into a yeast prion illuminate nucleation and strain diversity. *Nature* **435,** 765-772.

Kruger R., Kuhn W., Muller T., Woitalla D., Graeber M., Kosel S., Przuntek H., Epplen J. T., Schols L. and Riess O. (1998) Ala30Pro mutation in the gene encoding alpha-synuclein in Parkinson's disease. *Nat. Genet.* **18,** 106-108.

Kryndushkin D., Alexandrov I., Ter-Avanesyan M. and Kushnirov V. (2003) Yeast [PSI+] prion aggregates are formed by small sup35 polymers fragmented by Hsp104p. *Journal of Biological Chemistry* **278,** 49636-49643.

Kushnirov V. and Ter-Avanesyan M. (1998) Structure and replication of yeast prions. *Cell* **94,** 13-16.

Lee S. C., Hashim Y., Li J. K. Y., Ko G. T. C., Critchley J. A. J. H., Cockram C. S. and Chan J. C. N. (2001) The islet amyloid polypeptide (amylin) gene S20G mutation in Chinese subjects: Evidence for associations with type 2 diabetes and cholesterol levels. *Clinical Endocrinology* **54,** 541-546.

Legname G. (2004) Synthetic mammalian prions. *Science* **305,** 673-376.

Li L. and Lindquist S. (2000) Creating a protein-based element of inheritance. *Science* **287,** 661-664.

Liebman S. W. (2005) Structural clues to prion mysteries. *Nat Struct Mol Biol,* **12,** 567-568.

Liu J. and Lindquist S. (1999) Oligopeptide-repeat expansions modulate 'protein-only' inheritance in yeast. *Nature* **400,** 573-576.

Liu J.-J., Sondheimer N. and Lindquist S. L. (2002) Changes in the middle region of Sup35 profoundly alter the nature of epigenetic inheritance for the yeast prion [PSI+] *Proceedings of the National Academy of Sciences* **99**, 16446-16453.

Meldrum F., Mann S., Heywood B., Frankel R. and Bazylinski D. (1993) Electron microscopy study of magnetosomes in a cultured coccoid magnetotactic bacterium. *Proceedings: Biological Sciences* **251,** 231-236.

Moriyama H., Edskes H. and Wickner R. (2000) [URE3] Prion propagation in *Saccharomyces cerevisiae*: Requirement for chaperone Hsp104 and curing by overexpressed chaperone Ydj1p. *Molecular and Cellular Biology* **20**, 8916-8922.

Nakayashiki T., Kurtzman C., Edskes H. and Wickner R. (2005) Yeast prions [URE3] and [PSI+] are diseases. *Proceedings of the National Academy of Sciences* **102,** 10575-10580.

Nelson R., Sawaya M. R., Balbirnie M., Madsen A. O., Riekel C., Grothe R. and Eisenberg D. (2005) Structure of the cross-[beta] spine of amyloid-like fibrils. *Nature* **435,** 773-778.

Ness F., Ferreira P., Cox B. S. and Tuite M. F. (2002) Guanidine hydrochloride inhibits the generation of prion "seeds" but not prion protein aggregation in yeast. *Mol. Cell. Biol.* **22**, 5593-5605.

Olsen A., Jonsson A. and Normark S. (1989) Fibronectin binding mediated by a novel class of surface organelles on *Escherichia coli*. *Nature* **338,** 652-655.

Oma Y., Kino Y., Sasagawa N. and Ishiura S. (2004) Intracellular localization of homopolymeric amino acid-containing proteins expressed in mammalian cells. *J. Biol. Chem.* **279,** 21217-21222.

O'Nuallain B., Williams A., Westermark P. and Wetzel R. (2004) Seeding specificity in

amyloid growth induced by heterologous fibrils. *Journal of Biological Chemistry* ***279*****,** 17490-17499.

Osherovich L. Z., Cox B. S., Tuite M. F. and Weissman J. S. (2004) Dissection and design of yeast prions. *PLoS Biology* **2***,* e86.

Osherovich L. Z. and Weissman J. S. (2002) The utility of prions. *Developmental Cell* **2***,* 143-151.

Outeiro T. F. and Lindquist S. (2003) Yeast cells provide insight into alpha-synuclein biology and pathobiology. *Science* **302,** 1772-1775.

Parham S., Resende C. and Tuite M. (2001) Oligopeptide repeats in the yeast protein Sup35p stabilize intermolecular prion interactions. *The EMBO Journal* **20,** 2111-2119.

Parsell D., Kowal A., Singer M. and Lindquist S. (1994) Protein disaggregation mediated by heat-shock protein Hsp104. *Nature* **372,** 475.

Patel B. K. and Liebman S. W. (2007) "Prion-proof" for [PIN+]: infection with in vitro-made amyloid aggregates of Rnq1p-(132-405) induces [PIN+]. *Journal of Molecular Biology* **365,** 773-782.

Patino M., Liu J., Glover J. and Lindquist S. (1996) Support for the prion hypothesis for inheritance of a phenotypic trait in yeast. *Science* **273,** 622.

Paushkin S., Kushnirov V., Smirnov V. and Ter-Avanesyan M. (1997) Interaction between yeast Sup45p (eRF1) and Sup35p (eRF3) polypeptide chain release factors: implications for prion-dependent regulation. *Molecular and Cellular Biology* **17,** 2798-2805.

Perutz M., Staden R., Moens L. and De Baere I. (1993) Polar zippers. *Curr Biol* **3.** 249-253.

Poirier M.A., Li H., Macosko J., Cai S., Amzel M., Ross C.A. (2002) Huntingtin spheroids and protofibrils as precursors in polyglutamine fibrilization. *J Biol Chem*. **277,** 41032-41037.

Polymeropoulos M. H., Lavedan C., Leroy E., Ide S. E., Dehejia A., Dutra A., Pike B., Root H., Rubenstein J., Boyer R., Stenroos E. S., Chandrasekharappa S., Athanassiadou A., Papapetropoulos T., Johnson W. G., Lazzarini A. M., Duvoisin R.

C., Di Iorio G., Golbe L. I. and Nussbaum R. L. (1997) Mutation in the alpha-synuclein gene identified in families with Parkinson's disease. *Science* **276.** 2045-2047.

Post K. (1998) Rapid acquisition of [beta]-sheet structure in the prion protein prior to multimer formation. *Biol. Chem.* **379.** 1307-1317.

Prusiner S. B. (1982) Novel proteinaceous infectious particles cause scrapie. *Science* **216,** 136-144.

Prusiner S. B. (1991) Molecular biology of prion diseases. *Science* **252,** 1515-1522.

Riek R., Hornemann S., Wider G., Billeter M., Glockshuber R. and Wuethrich K. (1996) NMR structure of the mouse prion protein domain PrP (121?31). *Nature* **382,** 180-182.

Ripaud L., Maillet L. and Cullin C. (2003) The mechanisms of [URE3] prion elimination demonstrate that large aggregates of Ure2p are dead-end products. *The EMBO Journal* **22,** 5251-5259.

Ross E. D., Edskes H. K., Terry M. J. and Wickner R. B. (2005) Primary sequence independence for prion formation. *PNAS* **102,** 12825-12830.

Santoso A., Chien P., Osherovich L. Z. and Weissman J. S. (2000) Molecular basis of a yeast prion species barrier. *Cell* **100,** 277-288.

Schirmer E. and Lindquist S. (1997) Interactions of the chaperone Hsp104 with yeast Sup35 and mammalian PrP. *PNAS.* **94,** 13932-13937.

Serio T., Cashikar A., Kowal A., Sawicki G., Moslehi J., Serpell L., Arnsdorf M. and Lindquist S. (2000) Nucleated conformational conversion and the replication of conformational information by a prion determinant. *Science* **289,** 1317.

Shewmaker F., Wickner R. B. and Tycko R. (2006) Amyloid of the prion domain of Sup35p has an in-register parallel beta-sheet structure. *PNAS* **103**, 19754-19759.

Shkundina I. S., Kushnirov V. V., Tuite M. F. and Ter-Avanesyan M. D. (2006) The role of the N-terminal oligopeptide repeats of the yeast Sup35 prion protein in propagation and transmission of prion variants. *Genetics* **172,** 827-835.

Sikorski R. and Hieter P. (1989) A system of shuttle vectors and yeast host strains

designed for efficient manipulation of DNA in *Saccharomyces cerevisiae*. *Genetics* **122**, 19-27.

Singleton A. B., Farrer M., Johnson J., Singleton A., Hague S., Kachergus J., Hulihan M., Peuralinna T., Dutra A., Nussbaum R., Lincoln S., Crawley A., Hanson M., Maraganore D., Adler C., Cookson M. R., Muenter M., Baptista M., Miller D., Blancato J., Hardy J. and Gwinn-Hardy K. (2003) alpha-synuclein locus triplication causes parkinson's disease. *Science* **302**, 841.

Sondheimer N. and Lindquist S. (2000) Rnq1: an epigenetic modifier of protein function in yeast. *Mol. Cell.* **5***,* 163-172.

Song Y., Wu Y.-x., Jung G., Tutar Y., Eisenberg E., Greene L. E. and Masison D. C. (2005) Role for Hsp70 chaperone in *Saccharomyces cerevisiae* prion seed replication. *Eukaryotic Cell* **4***, 2*89-297.

Tanaka M., Chien P., Naber N., Cooke R. and Weissman J. S. (2004) Conformational variations in an infectious protein determine prion strain differences. *Nature* **428,** 323-328.

Tessier P. and Lindquist S. (2007) Prion recognition elements govern nucleation, strain specificity and species barriers. *Nature* **447,** 556-561.

Tribouillard D., Bach S., Gug F., Desban N., Beringue V., Andrieu T., Dormont D., Galons H., Laude H. and Vilette D. (2006) Using budding yeast to screen for anti-prion drugs. *Biotechnol. J.* **1,** *5*8-67.

True H. L. and Lindquist S. L. (2000) A yeast prion provides a mechanism for genetic variation and phenotypic diversity. *Nature* **407,** 477-483.

Uptain S. M. and Lindquist S. (2002) Prions as protein-based genetic elements. *Annual Review of Microbiology* **56,** 703-741.

Vitrenko Y., Pavon M., Stone S. and Liebman S. (2007) Propagation of the [PIN+] prion by fragments of Rnq1 fused to GFP. *Current Genetics* **51,** *3*09-319.

Wegrzyn R., Bapat K., Newnam G., Zink A. and Chernoff Y. (2001) Mechanism of prion loss after Hsp104 inactivation in yeast. *Mol. Cell Biol.* **21,** 4656.

Weissmann C. (2004) The state of the prion. *Nature Reviews Microbiology* **2,** 861**-**871.

Westermark P., Engstrom U., Johnson K., Westermark G. and Betsholtz C. (1990) Islet amyloid polypeptide: pinpointing amino acid residues linked to amyloid fibril formation. *PNAS* **87,** *5*036-5040.

Wickner R. B. (1994) [URE3] as an altered URE2 protein: evidence for a prion analog in Saccharomyces cerevisiae. *Science* **264,** 566-569.

Wickner R. B., Edskes H. K. and Shewmaker F. (2006) How to find a prion: [URE3], [PSI+] and [[beta]]. *Methods* **39,** 3-8**.**

Wu Y.-X., Greene L. E., Masison D. C. and Eisenberg E. (2005) Curing of yeast [PSI+] prion by guanidine inactivation of Hsp104 does not require cell division. *PNAS* **102,** 12789-12794.

Zarranz J. J., Javier Alegre, Juan C. Guez-Esteban, Elena Lezcano et al. (2004) The new mutation, E46K, of alpha-synuclein causes parkinson and Lewy body dementia. *Annals of Neurology* **55,** 164-173.

Zhang S., Holmes T., Lockshin C. and Rich A. (1993) Spontaneous assembly of a self-complementary oligopeptide to form a stable macroscopic membrane. *Proceedings of the National Academy of Sciences* **90,** 3334-3338**.**